Analysis of environmental changes with respect to groundwater resources – globally and for karst regions

Zur Erlangung des akademischen Grades eines
DOKTORS DER NATURWISSENSCHAFTEN
(Dr. rer. nat.)

von der KIT-Fakultät für
Bauingenieur-, Geo- und Umweltwissenschaften
des Karlsruher Instituts für Technologie (KIT)
genehmigte

DISSERTATION

von
M. Sc. Jiawen Zhang

Tag der mündlichen Prüfung: 10. Februar 2025

Referent. Prof. Dr. Nico Goldscheider

Korreferent. Prof. Dr. Andreas Hartmann

Karlsruhe 2025

Abstract

Groundwater is a vital resource for drinking water and is crucial for maintaining healthy ecosystems, particularly in regions with limited water availability. Karst areas, known for their distinctive geological formations, host some of the world's most valuable groundwater resources and are characterized by high levels of biodiversity. With global warming and intensified human activities, there are significant effects on hydrological cycles, natural ecosystems, and socio-economic development, which have also led to changes in the spatial and temporal patterns of global groundwater resources. At the same time, karst region is highly susceptible to the impacts of climate change and human activities. Nevertheless, most existing studies have focused on analyzing the effects of environmental changes on groundwater at the basin or regional scales, lacking a comprehensive global perspective on groundwater characteristics and spatial distribution. The advancement of satellite remote sensing technology in recent years has enabled large-scale, long-term monitoring of hydrological processes. This thesis investigates the complex relationship between groundwater resources and the overarching influence of global environmental changes, with a particular focus on karst regions and trends in global groundwater storage.

To clarify the impact of environmental changes on global groundwater storage and the driving forces behind these changes, and land-use changes in global karst regions. This study focuses on the following aspects: First, the study utilizes GRACE data from 2003 to 2022, combined with ERA5-Land dataset, to derive global groundwater storage trends, and analyzes the spatial and temporal distribution characteristics and patterns of global groundwater storage changes over the past 20 years. Next, by integrating meteorological data and human activity data, the study discusses the driving forces behind specific regions with significant changes in groundwater storage. Finally, using Climate Change Initiative-Land Cover (CCI-LC) and World Karst Aquifer Map (WOKAM) datasets, it examines the current status and spatial changes of land use in global karst regions over multiple years. It also proposes factors that can quantitatively assess global karst land-use changes in spatial terms. Based on this analysis, three karst regions with high land-use change intensity are identified. The main conclusions of this study are as follows:

(1) The study's results indicate that global groundwater storage between 2003 and 2022 has shown spatial heterogeneity, with most depletion occurring in the Earth's mid-latitudes. Notably, regions such as northern India, eastern Brazil, and areas around the Caspian Sea experienced significant declines in groundwater storage, exceeding 20 mm/a. It is estimated that around 3.4 billion people live in areas where groundwater storage has substantially decreased over the past two decades.

(2) Spatial analysis revealed that the most significant groundwater declines occurred in arid and semi-arid regions, particularly where the aridity index (AI) ranges from 0.1 to 0.5, peaking at 0.1 to 0.2. Contrary to common belief, although there is a correlation between precipitation and groundwater storage, changes in precipitation do often not directly affect groundwater storage. Compared to precipitation, changes in the Standardized Precipitation-Evapotranspiration Index (SPEI) have a more significant spatial impact on groundwater storage.

(3) Human activities, particularly irrigation and excessive groundwater abstraction, are the major drivers of groundwater storage decline. Among human activities, agricultural activities have a more significant impact on groundwater storage than population density. There are two main causes of groundwater rise: wetter climate conditions and dam construction.

(4) The analysis of land use in global karst regions in 2020 reveals that forests constitute the largest land-use type, covering 31.78% of these areas, followed by bare areas (27.58%), cropland (19.02%), grassland (10.87%), shrubland (7.21%), wetlands (1.67%), ice and snow (1.16%), and urban areas (0.71%). From 1992 to 2020, the total change in land use in global karst regions is estimated to be 1.30 million km², accounting for approximately 4.85% of the global karst surface.

(5) The primary trend identified is afforestation, which is supplemented by localized urbanization and agricultural reclamation, particularly in regions with tropical climates where land-use change intensity is higher. Furthermore, areas undergoing agricultural reclamation are closely aligned with regions of high population density, indicating the significant role of human activities in driving these changes.

This thesis emphasizes the urgent need for long-term dynamic observation and the development of sustainable groundwater management policies. Such policies are crucial for regions facing severe groundwater depletion, as they aim to ensure the long-term sustainability of freshwater resources, which are essential for both human survival and ecological health.

Key words

Land-use change, Karst, Groundwater storage change, Climate change, Agricultural irrigation, Global groundwater resources analysis

KURZFASSUNG

Grundwasser ist eine wesentliche Ressource für Trinkwasser und entscheidend für die Erhaltung gesunder Ökosysteme, insbesondere in Regionen mit begrenzter Wasserverfügbarkeit. Karstgebiete, bekannt für ihre charakteristischen geologischen Formationen, beherbergen einige der wertvollsten Grundwasserressourcen der Welt und zeichnen sich durch hohe Biodiversität aus. Mit der globalen Erwärmung und intensivierten menschlichen Aktivitäten gibt es erhebliche Auswirkungen auf hydrologische Kreisläufe, natürliche Ökosysteme und die sozioökonomische Entwicklung, was auch zu Veränderungen in den räumlichen und zeitlichen Mustern globaler Grundwasserressourcen geführt hat. Gleichzeitig sind Karstregionen besonders anfällig für die Auswirkungen des Klimawandels und menschlicher Aktivitäten. Dennoch konzentrieren sich die meisten bestehenden Studien auf die Analyse der Auswirkungen von Umweltveränderungen auf das Grundwasser auf Becken- oder regionaler Ebene und es fehlt eine umfassende globale Perspektive auf die Eigenschaften und die räumliche Verteilung des Grundwassers. Der Fortschritt der Satellitenfernerkundungstechnologie in den letzten Jahren hat die großflächige, langfristige Überwachung hydrologischer Prozesse ermöglicht. Diese Arbeit untersucht die komplexe Beziehung zwischen Grundwasserressourcen und dem übergeordneten Einfluss globaler Umweltveränderungen, mit einem besonderen Fokus auf Karstregionen und Trends in der globalen Grundwasserspeicherung.

Um den Einfluss von Umweltveränderungen auf die globale Grundwasserspeicherung sowie die treibenden Kräfte hinter diesen Veränderungen und Landnutzungsänderungen in globalen Karstregionen zu klären, konzentriert sich diese Studie auf die folgenden Aspekte: Erstens nutzt die Studie GRACE-Daten von 2003 bis 2022, kombiniert mit dem ERA5-Land-Datensatz, um globale Trends in der Grundwasserspeicherung abzuleiten und analysiert die räumlichen und zeitlichen Verteilungseigenschaften und Muster der globalen Grundwasserspeicherveränderungen der letzten 20 Jahre. Als nächstes werden durch die Integration von meteorologischen Daten und Daten menschlicher Aktivitäten die treibenden Kräfte hinter bestimmten Regionen mit signifikanten Veränderungen in der

Grundwasserspeicherung diskutiert. Schließlich untersucht die Studie mithilfe der Datensätze Climate Change Initiative-Land Cover (CCI-LC) und World Karst Aquifer Map (WOKAM) den aktuellen Status und die räumlichen Veränderungen der Landnutzung in globalen Karstregionen über mehrere Jahre hinweg. Es werden auch Faktoren vorgeschlagen, die globale Landnutzungsänderungen in Karstregionen räumlich quantitativ bewerten können. Basierend auf dieser Analyse werden drei Karstregionen mit hoher Intensität von Landnutzungsänderungen identifiziert. Die Hauptschlüsse dieser Studie lauten wie folgt:

(1) Die Ergebnisse der Studie zeigen, dass die globale Grundwasserspeicherung zwischen 2003 und 2022 eine räumliche Heterogenität aufweist, wobei der meiste Verlust in den mittleren Breiten der Erde auftritt. Bemerkenswerte Rückgänge der Grundwasserspeicherung, die 20 mm/a überschreiten, wurden in Regionen wie Nordindien, Ostbrasilien, dem Nahen Osten und Gebieten um das Kaspische Meer beobachtet. Es wird geschätzt, dass etwa 3,2 Milliarden Menschen in Gebieten leben, in denen die Grundwasserspeicherung in den letzten zwei Jahrzehnten erheblich abgenommen hat.

(2) Die räumliche Analyse ergab, dass die bedeutendsten Grundwasserabnahmen in ariden und semiariden Regionen auftraten, insbesondere dort, wo der Aridităsindex (AI) zwischen 0,1 und 0,5 liegt, mit einem Spitzenwert zwischen 0,1 und 0,2. Entgegen der landläufigen Meinung besteht zwar eine Korrelation zwischen Niederschlag und Grundwasserspeicherung, jedoch wirken sich Änderungen im Niederschlag oft nicht direkt auf die Grundwasserspeicherung aus. Im Vergleich zum Niederschlag haben Änderungen des standardisierten Niederschlags-Evapotranspirations-Index (SPEI) einen stärkeren räumlichen Einfluss auf die Grundwasserspeicherung.

(3) Menschliche Aktivitäten, insbesondere Bewässerung und übermäßige Grundwasserentnahme, sind die Haupttreiber des Rückgangs der Grundwasserspeicherung. Unter den menschlichen Aktivitäten haben landwirtschaftliche Tätigkeiten einen größeren Einfluss auf die Grundwasserspeicherung als die Bevölkerungsdichte. Zwei Hauptursachen für den Anstieg des Grundwassers sind feuchtere Klimabedingungen und der Bau von Staudämmen.

(4) Die Analyse der Landnutzung in globalen Karstregionen im Jahr 2020 zeigt, dass Wälder den größten Landnutzungstyp darstellen und 31,78 % dieser Gebiete bedecken, gefolgt von kahlen Flächen (27,58 %), Ackerland (19,02 %), Grasland (10,87 %), Buschland (7,21 %), Feuchtgebieten (1,67 %), Eis und Schnee (1,16 %) sowie städtischen Gebieten (0,71 %). Von 1992 bis 2020 wird die gesamte Landnutzungsänderung in globalen Karstregionen auf 1,30 Millionen km² geschätzt, was etwa 4,85 % der globalen Karstfläche entspricht.

(5) Der Haupttrend, der identifiziert wurde, ist die Aufforstung, die durch lokale Urbanisierung und landwirtschaftliche Rekultivierung ergänzt wird, insbesondere in Regionen mit tropischem Klima, wo die Intensität der Landnutzungsänderungen höher ist. Darüber hinaus stimmen Gebiete, die landwirtschaftlicher Rekultivierung unterliegen, eng mit Regionen hoher Bevölkerungsdichte überein, was auf die bedeutende Rolle menschlicher Aktivitäten bei diesen Veränderungen hinweist.

Diese Arbeit betont die dringende Notwendigkeit langfristiger dynamischer Beobachtungen und die Entwicklung nachhaltiger Grundwassermanagementpolitiken. Solche Politiken sind entscheidend für Regionen mit schwerwiegender Grundwassererschöpfung, da sie darauf abzielen, die langfristige Nachhaltigkeit der Süßwasserressourcen zu gewährleisten, die sowohl für das menschliche Überleben als auch für die ökologische Gesundheit unerlässlich sind.

Schlüsselwörter

Landnutzungsänderungen, Karst, Änderung der Grundwasserspeicherung, Klimawandel, landwirtschaftliche Bewässerung, Analyse globaler Grundwasserressourcen

Acknowledgments

This work would not have been possible without the support of all the people who helped me in various ways, and I am grateful to everyone who has accompanied me along this journey.

First and foremost, I express my deepest gratitude to my supervisor – Prof. Dr. Nico Goldscheider for his invaluable guidance, unwavering support, and continuous encouragement throughout my research. Thank Nico for taking care of my work and life in Germany. He teaches me be patient and precise for what I am doing. The scientific freedom enables me to find collaborations and learn to be an independent Ph.D. student. His diligence and rigours scholarship inspired me to go forward, especially rich knowledge in karst. Thank the encouragement and tolerance for my PhD! Thanks for the countless greeting during my “dark time”.

I also wish to extend my sincere thanks to Dr. Tanja Liesch for her expertise, critical insights, and invaluable suggestions that greatly contributed to its refinement and improvement. She introduced me to the Python world, significantly boosting my research efficiency. She taught me a lot of professional knowledge about satellite data and analysis at global scale, and contribute so much to my thesis. She always really kind and giving me so much useful information. I particularly admire her carefree lifestyle and her serious approach to research. Her mentorship and thoughtful input have been essential to this research.

I am very grateful to my PhD committee for their willingness and time.

I want to thank Dr. Zhao Chen and Dr. Andreas Hartmann for their scientific support and help during the past years. Their suggestions have been very helpful and important for me to complete my studies.

Thank the Chinese Scholarship Council (CSC) for giving me scholarships to study in Karlsruhe Institute of Technique (KIT), Germany. It is a wonderful and worthful experience to study in Karlsruhe. I never dreamed I could go abroad before I getting scholarship.

I would also like to thank Yanina Müller, Xinyang Fan, Alexander Kaltenbrunn, Marc Ohmer, Diep Anh Tran, and all my other colleagues in the Hydrogeology and Engineering Geology Departments for the great times and conversations. My appreciation goes to Christine Mackert for their great help in all organizational matters.

At the same time, I would like to thank many of my Chinese friends in Germany, Benchun Zhou, Meijun Zhou, and Hongyan Wang. Their constant support, helpful discussions, and willingness to share their knowledge have been instrumental in my academic and personal growth.

Finally, I would like to thank my parents for their endless encouragement, patience, and belief in me throughout this endeavor. You always give me support and encouragement.

I would like to thank my boyfriend Zhen for accompanying me on our trip from Changchun to Beijing to Karlsruhe. We have had, and will continue to have, wonderful times together.

This is an unforgettable experience, marking my first time traveling and studying abroad. Time has flown by so quickly. I've come a long way from where I began. I hope to see you again! Thank you all for your invaluable support.

Jiawen Zhang 张佳文

Karlsruhe, 2024

Table of Contents

List of Figures

List of Tables

Table

List of Abbreviations

AI	Aridity Index
ANN	Artificial Neural Network
C3S	Copernicus Climate Change Service
CCI-LC	Climate Change Initiative – Land Cover dataset
CRU	Climatic Research Unit
CWS	Canopy water storage
ERA5	Fifth generation ECMWF atmospheric reanalysis
ESA	European Space Agency
ET	Evapotranspiration
ENSO	El Niño–Southern Oscillation
FAO	The Food and Agriculture Organization
FROM-GLC	Global Land Cover Change Monitoring Platform
GIS	Geographic information system
GLDAS	Global Land Data Assimilation System
GLiM	Global Githological Map
GMIA	Global Map of Irrigation Areas
GLC2000	Global Land Cover 2000
GLCNMO	GLOBCOVER and Global Map-Global LC dataset
GMIA	Global Map of Irrigation Areas
GRACE	Gravity Recovery and Climate Experiment
GRACE-FO	GRACE Follow-On
GWS	Groundwater storage
GWSA	Groundwater storage anomalies
IAH	International Association of Hydrogeologists
ICESat	Ice, Cloud, and land Elevation Satellite
IDO	Indian Ocean Dipole

IGBP DISCover	International Geosphere Biosphere Programme's Data and Information System land use cover
KROW	Karst Regions of the World
LAI	Leaf Area Index
LCCS	Land Cover Classification System
LUCC	Land use and land cover change
MCD12	Moderate Resolution Imaging Spectroradiometer LAND-COVER (LC) dataset
MJO	Madden-Julian Oscillation
MODIS	Moderate Resolution Imaging Spectroradiometer
NAO	North Atlantic Oscillation
PCR-GLOBWB	PCRaster Global Water Balance
PDO	Pacific Decadal Oscillation
RS	Remote sensing
SM	Soil moisture
SMAP	Soil Moisture Active Passive
SMOS	Soil Moisture and Ocean Salinity
SPEI	Standardized Precipitation-Evapotranspiration Index
SWA	Surface water
SWE	Snow water equivalent
USGS	United States Geological Survey
WGHM	WaterGAP Global Hydrology Model
WOKAM	World Karst Aquifer Mapping

Chapter 1
1 Introduction

1.1 Background

Groundwater, stored beneath the Earth's surface in soil and porous rock aquifers, is a vital resource, accounting for approximately 33% of total global water withdrawals. It provides drinking water to over two billion people (Morris et al. 2003) and supplies about 40% of the world's irrigation needs (Siebert et al. 2010), underscoring its importance to human populations, economies, and the environment (Wada et al. 2010; Famiglietti 2014). Notably, groundwater from karst aquifers serves as a major source of freshwater for drinking and agricultural irrigation in many countries and regions worldwide. Goldscheider et al. (2020) estimated that 15.2% of the global ice-free continental surface consists of karstifiable carbonate rock, with approximately 1.3 billion people living in these karst regions.

Over the past few decades, the global climate has been experiencing continuous and intense changes. These changes, driven by both climate variability and increased human activity, have significantly altered the global hydrological cycle of groundwater. Consequently, the spatial and temporal distribution of global groundwater has been affected, posing a threat to local ecosystems and the sustainable use of water resources by populations (Vicente-Serrano et al. 2020; Azadi et al. 2018; IPCC, 2013). In recent years, the over-extraction of groundwater has become increasingly severe, leading to various environmental and geological problems, such as seawater intrusion (Tomaszkiewicz et al. 2014), groundwater salinization (Panagiotou et al. 2022), land subsidence and ground collapse. Monitoring and managing groundwater resources is challenging due to the vast and unseen nature of aquifers. Additionally, aquifers respond slowly to atmospheric precipitation, which hinders our understanding of the distribution of groundwater resources and their response to changing environmental. Traditional groundwater monitoring methods are often restricted by high costs, limited

coverage, and lack of comprehensive long-term data series (Tiwari et al. 2009), limiting their application to catchment or regional scales. However, the advent of remote sensing technology offers a new approach to groundwater monitoring. Its advantages of large-scale coverage, periodic data collection, and low-cost address many of the limitations of traditional methods (Nguyen et al. 2021).

The Gravity Recovery and Climate Experiment (GRACE) satellite is a remote sensing satellite capable of quantitatively detecting changes in the Earth's gravitational field. In the short term, these changes in the Earth's gravitational field are primarily caused by variations in terrestrial water storage or the redistribution of mass within the Earth. By integrating data from the GRACE satellite with hydrometeorological observations data, researchers can uncover the driving forces behind the hydrological cycle. This has applications such as assessing water resources in river basins (Sinha et al. 2019), monitoring glacier mass dynamics (Eicker et al. 2016), and predicting flood and drought events (Li et al. 2019). The reasons for groundwater storage changes vary widely. Overextraction of groundwater for irrigation is a significant factor contributing to the regional groundwater declination, as observed in California's Central Valley (Famiglietti et al. 2011), the North China Plain (Feng et al. 2017, 2013), India (Asoka et al. 2017; Rodell et al. 2009), and the Middle East (Voss et al. 2013). Severe droughts have also led to substantial reductions in groundwater storage, such as in southern and northern Africa (Rodell et al. 2018). The aforementioned studies, conducted across various regions worldwide, have demonstrated the feasibility of using GRACE data to estimate groundwater storage changes by comparing measured groundwater storage with GRACE data. Consequently, the observations from the GRACE satellite can serve as a critical validation tool for traditional terrestrial hydrological models and an effective supplement to surface hydrological observation techniques. In recent years, it has been increasingly applied in hydrological and geoscientific research.

Land-use change play a critical role in the interaction between human and Earth systems (Turner et al. 2013). Land-use change is closely associated with various regional and

global phenomena, including ecosystem dynamics, climate change (Dong et al. 2019), biodiversity (Chaudhary et al. 2018), energy balance (Duveiller et al. 2018), carbon cycling (Eitelberg et al. 2016; Hong et al. 2021), and extreme weather events (Hirsch et al. 2018; Sy & Quesada 2020). The unique dualistic hydrogeological structure of limestone regions makes karst areas particularly sensitive to climate change and anthropogenic factors (Zhao et al. 2020). These regions often exhibit severe soil erosion and fragile vegetation, leading to inadequate soil and water conservation and vegetation restoration capabilities (Monroe et al. 2020). Consequently, this sensitivity has significant impacts on environmental and socio-economic domains, including ecology, soil health, carbon-water cycles (Kang et al. 2020), geological hazards, and economic productivity (Jiang et al. 2014).

Currently, numerous international remote sensing products are available to assess land-use change across various temporal and spatial scales, include the International Geosphere-Biosphere Programme's Data and Information System Land Use Cover (IGBP DISCover; Loveland et al. 2000), Global Land Cover 2000 (GLC2000; Bartholome & Belward 2005), Moderate Resolution Imaging Spectroradiometer LAND-COVER dataset (MCD12; Friedl et al. 2010), GLOBCOVER and Global Map-Global LC dataset (GLCNMO; Tateishi et al. 2011), Global Land Cover Change Monitoring Platform (FROM-GLC; Gong et al. 2013), GlobalLand 30 (Chen et al. 2015), and Climate Change Initiative – Land Cover dataset (CCI-LC; Bontemps et al. 2015). Additionally, high-resolution satellite imagery from Landsat, GF-2, Sentinel, and IKONOS is frequently used for detailed regional land use mapping (Feng & Fan 2021). Among these, the European Space Agency's CCI-LC global land cover product, with a spatial resolution of 300 m and covering the period from 1992 to 2020, is notable. This dataset has an overall accuracy of 74.10% and is selected for this study due to its temporal continuity, high resolution, and consistent classification standards.

Based on the aforementioned research, this thesis examines the impact of environmental changes on groundwater at global scale. We utilize GRACE data and ERA5

data from 2003 to 2022 to model global groundwater storage changes over the past two decades, and then we integrate meteorological data and human activity data to investigate the driven force behind groundwater storage change. Utilizing ESA CCI-LC data and WOKAM data, the study initially analyzes the general land-use distribution in global karst regions. Subsequently, we investigate land-use change patterns from 1992 to 2020 and identifies spatial dynamics characters of land-use changes within global scale. Understanding the impact of various changing factors on global groundwater is crucial for managing and utilizing groundwater resources effectively. This analysis aims to enhance groundwater resource use efficiency and provide a scientific basis for the sustainable management and planning of groundwater resources.

1.2 Methods for groundwater storage

1.2.1 Traditional method

Traditional methods for monitoring groundwater resources primarily rely on various ground-based dynamic monitoring networks, such as the establishment of groundwater observation wells. These wells help assess changes in groundwater levels by measuring flow rates within the wells, providing critical data for the study of groundwater variations in specific regions (Ohmer et al. 2019). The data for traditional monitoring approaches mainly comes from meteorological and hydrological stations. These methods are relatively simple and technologically mature, which has led to their widespread application in assessing groundwater storage changes.

To effectively collect information on key hydrological elements and to evaluate groundwater resource status, many studies use data from observation wells as a crucial information. For example, Russo et al. (2017) analyzed the impact of precipitation and water withdrawal on groundwater resources across different regions of the United States from 15,148 groundwater observation wells. They also explored the relationship between the El Niño–Southern Oscillation (ENSO) and groundwater levels, concluding that interannual variations in deep groundwater levels are closely related to changes in climate indices. Similarly, Perez-Valdivia et al. (2012) utilized water level data from 21

groundwater observation wells in the Canadian Prairies and two climate indices—ENSO and the Pacific Decadal Oscillation (PDO)—to find a significant negative correlation between shallow groundwater variations and the two climate indices.

Hydrological observations obtained from ground-based monitoring not only offer high temporal resolution (usually at daily or hourly scales) but also provide high data reliability. However, these methods have certain limitations, such as relatively limited coverage and uneven spatial distribution of monitoring wells. Monitoring regions typically cover only a few square kilometers, which can introduce significant uncertainties when estimating groundwater resources on larger scales. Although some researchers have attempted to implement long-term, continuous monitoring of groundwater storage changes by constructing dense networks of observation stations, the high costs of construction and the time-consuming and labor-intensive nature of maintenance pose significant challenges.

1.2.2 Hydrological Model

Hydrological models provide an abstract or generalized description of hydrological processes in different regions, enabling the study of the effects of climate change and human activities on these processes. These models are also used to analyze and predict future trends in water resources. Common global hydrological models include the WaterGAP Global Hydrology Model (WGHM; Herbert & Döll 2019; Veldkamp et al. 2017) and the PCRaster Global Water Balance (PCR-GLOBWB; Wada et al. 2014; Samaniego et al. 2018). These models use observational data from hydrometeorological stations as input to drive both land surface models and global hydrological models. Based on various assumptions about hydrological processes, they simulate different components of water storage, such as soil water, surface water, and groundwater, to describe changes in water storage under the influences of climate change and human activities. For example, Doll et al. (2014) utilized observational data from 1,319 runoff hydrological stations worldwide to simulate and invert global-scale runoff, groundwater storage, and terrestrial water storage using the WaterGAP model. They found that the model can

estimate not only long-term trends in water resource changes but also the seasonal variations in runoff.

Overall, while hydrological models can effectively simulate water storage changes in different regions and have produced significant research outcomes, they share limitations similar to ground-based monitoring methods. For instance, during the simulation of water storage, some hydrological elements may be missing. Common land surface hydrological models, such as the Noah and VIC models (Syed et al. 2008), do not account for changes in groundwater. Furthermore, hydrological model simulations require substantial hydrological observations as input parameters, and variations in input parameters can lead to significant uncertainties simulated results for water storage analysis (Qi et al. 2018).

1.2.3 Remote sensing technology

With the emergence of remote sensing technologies in recent years, various satellite data have been applied to research areas such as precipitation, evapotranspiration (ET), soil moisture, glacier snow thickness, and water storage. This has made it possible to conduct large-scale, long-term hydrological forecasting and global hydrological cycle studies. For example, Moderate Resolution Imaging Spectroradiometer (MODIS) and Landsat satellites are used for regional evapotranspiration monitoring (Kiptala et al. 2013), while the Soil Moisture and Ocean Salinity (SMOS) and Soil Moisture Active Passive (SMAP) satellites can accurately retrieve soil moisture (Ridler et al. 2014; Collow et al. 2012). Additionally, the Ice, Cloud, and land Elevation Satellite (ICESat) satellite effectively measures glacier thickness and surface water levels (O'Loughlin et al. 2016).

The advent of satellite gravimetry technology has provided new perspectives for monitoring terrestrial water storage. In particular, the successful launch of the GRACE satellite (as shown in Fig. 1-1) has enabled hydrologists to continuously and effectively monitor large-scale changes in water storage, thereby improving the current global hydrological monitoring system. It is important to note that water storage changes

estimated from gravitational fields represent anomalies over a period of time (Rodell & Famiglietti 1999).

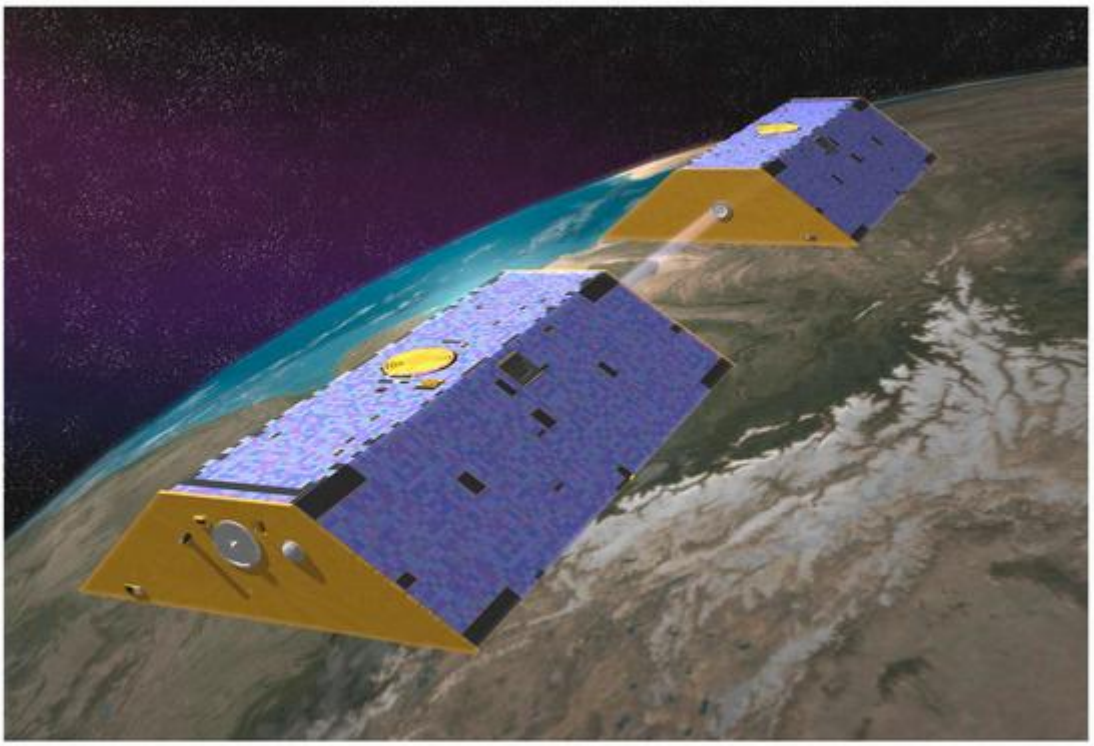

Fig. 1-1 Artist view of the Gravity Recovery and Climate Experiment (GRACE) mission. Source: NASA JPL Space images. Available online: https://www.jpl.nasa.gov/spaceimages/images/largesize/PIA04235_hires.jpg (access 01/08/2024)

Global terrestrial water storage is primarily composed of four components: surface water, soil moisture, groundwater, and glacial meltwater (Richey et al. 2015; Getirana et al. 2017; Xanke & Liesch 2022). The groundwater storage change can be determined by excluding surface water, soil moisture, and glacial meltwater from total terrestrial water storage. Numerous studies have validated the use of GRACE satellite data for estimating groundwater storage changes. These studies generally find that groundwater storage changes derived from GRACE data align well with in situ measurements. For example, Rodell et al. (2018) utilized GRACE data from 2002 to 2016 to analysis freshwater available across 34 major global regions. After calculating water storage trends, they

conducted an attribution analysis considering interannual variability, groundwater over-extraction, and the combined effects of climate change. Similarly, Katpatal et al. (2018) examined the spatiotemporal variations of groundwater storage anomalies (GWSA) in the India by monthly GRACE, GLDAS and field data from 2002 to 2015. Their study demonstrated that GRACE performs well in areas with simple aquifer systems but is less effective in regions with complex aquifer systems. Li et al. (2019) used the Visual MODFLOW model to simulate the groundwater cycle in the peatlands of the Zoigê Plateau, revealing a continuous loss of groundwater stored in the peat. The advent of artificial neural networks (ANN) has improved the reliability of groundwater storage predictions. For instance, Pragnaditya et al. (2021) applied a machine learning approach—support vector machines—to validate the feasibility of using GRACE satellite data for predicting groundwater storage changes.

Compared to ground-based measurements and hydrological models, gravity satellite data offers unique advantages for large-scale groundwater storage monitoring. GRACE data provides global-scale temporal and spatial variations in groundwater storage, enabling continuous and large-scale observations of regional water resource dynamics. Additionally, the cost of conducting groundwater storage studies based on gravity satellite data is relatively low, and the data are timely and relatively easy to obtain. However, there are limitations to using gravity satellite data, such as low spatial resolution, making it most suitable for regions larger than 200,000 km^2, and low temporal resolution (monthly scale).

1.3 Climate change and human activities on groundwater storage change analysis

The United States Geological Survey (USGS) released an updated diagram of the water cycle after 20 years, incorporating human activities for the first time (as illustrated in Fig. 1-2). In addition to natural processes such as precipitation, evaporation, runoff, and lakes, the new diagram also includes human activities like agricultural and industrial

water use, urban runoff, and reservoirs. This updated representation highlights the forms and roles of human influence throughout the water cycle.

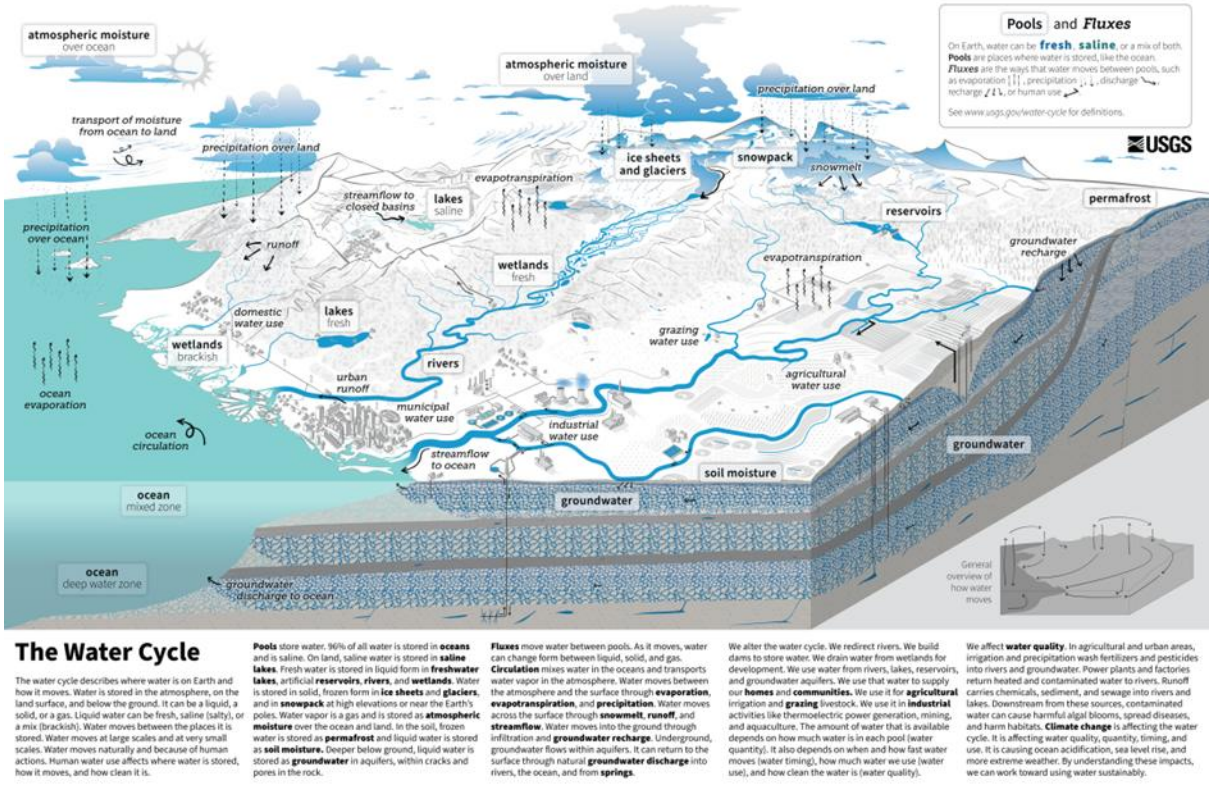

Fig. 1-2 The Water Cycle, source: Hayley Corson-Dosch/USGS Viz Lab

The impact of climate change and human activities on groundwater storage has been a major focus of global hydrological research. As the global average temperature continues to rise significantly, it has had a profound impact on the global ecological environment (Phillips & Gleckler 2006; Rocha et al. 2007). In addition to these effects, various human activities associated have significantly impacted hydrological processes and water resources, like over-extraction for irrigation, water redistribution due to dam construction. However, there remains a lack of consensus on how exactly human activities influence changes in groundwater storage.

Climate change causes a series of alterations in rainfall, evapotranspiration, groundwater, soil moisture, surface runoff, and glacial snow cover through changes in

temperature, atmospheric circulation, and ice-snow conditions (Anghileri et al. 2018; Setegn et al. 2011), leading to significant changes in the hydrological cycle. Consequently, the substantial changes in the quantity and spatial-temporal distribution of hydrometeorological factors such as precipitation and evapotranspiration inevitably affect groundwater storage. For example, Anyah et al. (2018) analyzed the correlation between five global climate teleconnection indices, including the El Niño–Southern Oscillation (ENSO), North Atlantic Oscillation (NAO), and Madden-Julian Oscillation (MJO), and water storage changes in Africa from 2003 to 2012. García-García et al. (2011) examined the water storage decline in central and southern Australia from 2006 to 2008, attributing it to three consecutive Indian Ocean Dipole (IOD) events.

The expansion of urbanization and agricultural areas has led to an imbalance in the supply-demand relationship for global groundwater resources, resulting in regional water shortages (Feng et al. 2017; Asoka et al. 2017). In some regions, human activities are considered the primary drivers of changes in groundwater storage. Groundwater depletion caused by human activities is mainly due to the excessive extraction of groundwater for agricultural irrigation. For instance, Joodaki et al. (2014) estimated groundwater storage in the Middle East from 2003 to 2012 using GRACE satellite data and the CLM4.5 land surface hydrological model. They found a significant downward trend in water storage, with an annual depletion rate of 25 ± 3 Gt/yr during the study period. Over half of this groundwater reduction (14 ± 3 Gt/yr) was attributed to various human activities during the same period. Similarly, Rodell et al. (2009) used GRACE data and hydrological modeling to estimate a groundwater depletion rate of 4.0 ± 1.0 cm/yr in northwest India. During this period, precipitation was near the long-term average, and other components of terrestrial water storage, such as soil water, surface water, snow, glaciers, and biomass, contributed minimally to the total water storage changes, suggesting that groundwater depletion was mainly due to excessive groundwater use for irrigation and other human activities.

Human activities can also lead to an increase in groundwater storage, primarily through inter-basin water transfer and the dam construction that create reservoirs. This has

been observed in several regions. For example, the construction of the Three Gorges Dam in Eastern Central China has led to an increase in groundwater levels (Chao et al. 2020). Similarly, the management of large lakes and dam construction in the Nile headwaters region could contribute to changes in groundwater storage (Ahmed et al. 2014; Kebede et al. 2017). The indirect impact of human activities on groundwater storage is mainly reflected in changes in land use and vegetation cover, which in turn affect runoff, groundwater recharge, and related processes. For example, urbanization and afforestation projects can significantly alter land use types and vegetation percentage, influencing vegetation evapotranspiration processes and the infiltration of precipitation into soil aquifers (Bai et al. 2019; Gao et al. 2020).

Multiple studies (Zou et al. 2020; Zhang et al. 2020; Shen et al. 2018) indicate that climate change and human activities are two key drivers of changes in the hydrological cycle and groundwater resource dynamics. For instance, Thomas & Famiglietti (2019) analyzed groundwater storage changes in the United States and found that groundwater storage changes are directly influenced by climate change, with the effects of groundwater recharge and precipitation being more significant than groundwater extraction.

In summary, changes in groundwater storage are the result of the combined effects of climate change and human activities. However, there is still a lack of effective research methods to accurately quantify and distinguish the contributions of climate change and human activities to changes in groundwater storage. Thus, distinguishing and quantifying their respective impacts on groundwater storage changes remains a challenging issue.

1.4 Karst observation data and changing environments

Hollingsworth (2009) compiled a comprehensive map and data book titled Karst Regions of the World (KROW), which provides a better understanding of the current state of karst landscapes and their ecological conservation worldwide. Building on this foundation, Hartmann and Moosdorf (2012) released the Global Lithological Map (GLiM),

a digital representation of global rock types. Following this, the Karst Commission of the International Association of Hydrogeologists (IAH) launched the World Karst Aquifer Mapping (WOKAM) project in 2012 to address issues related to the protection and management of groundwater resources in karst aquifers. In 2017, the project further digitized continuous and discontinuous carbonate rocks and karst aquifers (Chen et al. 2017). The World Karst Aquifer Map represents the first detailed and comprehensive global geological database, providing an essential scientific foundation for further research on global karst ecosystems and water resources (Goldscheider et al. 2020).

Early research on karst ecosystems primarily focused on the mechanistic processes of karst hydrogeology (LeGrand 1973), including geological and hydrological hazards (Gutiérrez et al. 2014), porosity and aquifer structure (Fu et al. 2016), and soil erosion and water loss (Dai et al. 2017). As rock desertification has intensified in recent decades, some researchers have increasingly recognized the importance of managing and conserving karst ecosystems (Ravbar & Šebela 2015). Consequently, there is a growing focus on the impact of both natural factors and human activities on soil erosion and degradation in karst regions (Valjavec et al. 2018).

In recent years, a general greening trend has been observed globally (Keenan & Riley 2018; Song et al. 2018). However, rapid industrialization and significant changes in land use have inevitably caused severe disturbances and posed substantial risks to the fragile ecosystems in karst regions (Lang et al. 2018). These changes have exacerbated critical issues such as land degradation and desertification (Shukla et al. 2019). Population growth has led to unsustainable and over-dense land use activities (Li et al. 2009; Wang et al. 2004), contributing to severe rocky desertification and soil degradation in vulnerable karst environments (Bai et al. 2013).

Research on the mechanistic processes of karst and rock desertification has provided a scientific foundation for understanding geological conditions and vegetation dynamics in karst regions. However, previous studies on the dynamic changes and responses of human activities and land use in karst areas have mainly focused on watershed or

national scales. There is still a lack of comprehensive research on karst region changes at the global scale.

1.5 Land-use change and its driving mechanisms

Land-use and land-cover change (LUCC) is a key driver of global environmental change (Prestele et al. 2017) and results from the combined effects of natural and human activities. It serves as a crucial source of information for understanding the complex interactions between human activities and global changes (Lambin et al. 2006). With the advancement of high-resolution remote sensing (RS) and geographic information system (GIS) technologies, remote sensing now provides an effective means to monitor dynamic changes in land use on a large scale (Nguyen et al. 2021). Compared to traditional manual land-use change monitoring, the integration of high-resolution RS imagery with GIS offers more accurate, extensive, timely, and up-to-date datasets (Rogan & Chen 2004).

Satellite imagery has been widely used by researchers to study land-use change at various scales and yield significant results. For example, Schweizer and Matlack (2014) used aerial photographs to analyze land-use change in the Mississippi coastal plain over six periods from 1938 to 2010, concluding that urban expansion was the main driver of these changes. Similarly, Gebrelibanos and Assen (2015) combined aerial photographs from 1964 and 1994 with high-resolution SPOT 5 satellite imagery from 2006 to analyze the spatiotemporal changes in cropland, forest, grassland, settlements, and lakes in the Northern Ethiopia. In recent years, some researchers integrate remote sensing data with historical data to study land-use change. For instance, Matasov et al. (2019) used historical maps, statistical data, and satellite imagery to reconstruct land-use change in the European Russia from 1770 to 2010, finding significant influences from political and economic factors. Additionally, the development of radar remote sensing has enriched the data sources available for land-use change analysis, offering enhanced capabilities for analyzing terrain and specific land-use types. For example, Rangzan et al. (2019) used

a supervised cross-fusion method to improve the classification accuracy of residential areas, wastelands, and rivers in thermal, radar, and visible light images.

The drivers of land-use change can be broadly categorized into natural and socio-economic factors. Natural factors mainly include environmental conditions and climate change. For example, Chiu et al. (2019) found that regional carbon balance significantly impacts land-use change, while Leh et al. (2013) used a soil erosion model to analyze land-use change in the White River watershed in northwest Arkansas, USA. Biazin and Sterk (2013) identified recurrent drought as a key driver of land-use change in the arid regions of the East African Rift Valley in Ethiopia. Socio-economic factors include economic development, population growth, policy management, and agricultural practices. For instance, López-Carr et al. (2012) and Newman et al. (2014) found that high rural population growth and deforestation were the primary causes of declining forest cover and land-use change in Guatemala and the Cockpit region of Jamaica. Mansour et al. (2020) highlighted the interaction between mountainous terrain and urban expansion, noting that excessive urban growth encroaches on arable land in valleys and flat areas. Guida-Johnson and Zuleta (2013) demonstrated that the expansion of cropland and the conversion of wetlands to pasture were the main drivers of land-use change in the Espinal ecoregion of Argentina.

In conclusion, the methodologies for analysis land-use change have become relatively mature, providing valuable information for land-use planning and management for stakeholders with diverse interests. The technical framework for land-use change research has become an essential tool for analyzing the spatiotemporal processes of land-use and land-cover changes.

1.6 Research content

This thesis examines the impact of environmental changes on groundwater by data from GRACE, WOKAM, land use, meteorology, and human activity. It develops a global-scale research methodology to analyze the relationship between groundwater and changing environmental conditions. This approach aims to enhance our understanding of global

groundwater dynamics and distribution, providing a scientific basis for the evaluation, management, and sustainable availability of groundwater resources worldwide. Additionally, it investigates the spatiotemporal characteristics of these changes and performs attribution analyses in selected case studies to identify the factors influencing groundwater.

The research addresses the following key questions:

RQ 1: How is the global groundwater storage trends over the past 20 years? Where are the major regions with significant groundwater storage decline? How many people live in areas experiencing with groundwater storage decline?

RQ 2: Which meteorological factors and human factors most significantly impact changes on groundwater storage?

RQ 3: In regions with significant changes in global groundwater storage over the past 20 years, what are the specific characteristic observed? How is the human activity and climate change in these regions? What are the driving forces behind the changes in groundwater storage?

RQ 4: What is the current status of land use in global karst regions?

RQ 5: What are the patterns of land-use area changes and land-use transitions in global karst regions from 1992 to 2020? What are the characteristics of these land-use changes?

RQ 6: In high land-use intensity areas within global karst regions, what are the causes of these changes? and what is their spatial distribution?

This thesis is structured cumulatively and comprises two studies, presented in Chapters 2 and 3. Chapter 2 is currently under review, whereas Chapter 3 has been published in peer-reviewed journals.

Chapter 2: Impacts of climate change and human activities on global groundwater storage from 2003-2022

This chapter estimates and analyzes global groundwater storage trends from 2003 to 2022 using GRACE and ERA5 data. It examines the spatiotemporal distribution and patterns of groundwater storage changes on a global scale, focusing on the influences of climate factors and human activities, such as precipitation, drought indices, population density, aridity index etc. The study identifies 23 regions where groundwater storage has significantly changed over the past 20 years and provides a comprehensive analysis of the driving forces behind these changes by integrating hydrometeorological data and factors related to human activity.

Chapter 3: Global analysis of land-use changes in karst areas and the implications for water resources

This chapter utilizes the CCI-LC and WOKAM datasets to analyze the current state and spatial distribution of land use in global karst regions. Based on data from 1992 to 2020, a quantitative assessment of global land-use area changes and transitions is conducted, with a focus on spatial distribution patterns and dynamic characteristics of land use. The study employs the proportion of land-use change and the dominant type of land-use change to identify spatial change characteristics. Three karst regions with significant changes are selected for detailed case studies to explore the mechanisms and driving forces of land-use change.

Chapter 2
2 Climate change and human activities on groundwater storage

Reproduced from: Zhang, J., Liesch, T., & Goldscheider, N. Impacts of climate change and human activities on global groundwater storage from 2003-2022. submitted

Abstract

Groundwater is integral to land surface processes, significantly influencing water and energy cycles, and it is an important resource for drinking water and ecosystems. Climate change and anthropogenic impacts have an ever-increasing influence on the water cycle and groundwater storage in recent decades. This study leverages GRACE and ERA5-Land data to analyze groundwater storage variability from 2003 to 2022, with a 1° spatial resolution. Approximately 81% of global regions have shown significant groundwater storage changes, with 48% experiencing declines and 52% observing increases. Approximately 3.4 billion people live in regions where groundwater has significantly declined over the past 20 years. Findings indicate considerable global groundwater changes, with depletion hotspots (>20 mm/year) in northern India, the North China Plain, eastern Brazil, and around the Caspian Sea. SPEI trends exhibit a stronger influnce on groundwater storage change than precipitation trends, highlighting the critical role of evapotranspiration. Groundwater depletion is driven primarily by agricultural irrigation and over-abstraction, with population density playing a relatively smaller role. GRACE data facilitates global monitoring, underscoring the need for long-term dynamic observation to inform sustainable groundwater management policies crucial for regions facing groundwater depletion to ensure long-term freshwater resource sustainability.

2.1 Introduction

Groundwater resources play a crucial role in environmental processes, serving as the primary source of drinking water for 50% of the world's urban population and around 25% of all water withdrawn for irrigation (Connor & Miletto 2022). Findings reveal that rapid declines in groundwater levels, more than 0.5 meters per year, are common in the 21st century, especially in dry areas with extensive cropland (Jasechko et al. 2024). Groundwater depletion due to irrigation is evident in many key agricultural regions (Rodell et al. 2009, 2018; Famiglietti et al. 2011; Voss et al. 2013). Human activities, particularly irrigation, which accounts for 70% of global water withdrawals and 90% of water consumption, have a direct impact on these resources (Siebert et al. 2010). Furthermore, 4 billion people face severe water shortages for at least one month each year (Mekonnen & Hoekstra, 2016). This pattern threatens the long-term sustainability of groundwater extraction (Brauman et al. 2016; Wada et al. 2014). Furthermore, excessive groundwater extraction, coupled with irrigation and climate change, could lead to wells running dry (Gleeson et al. 2012; Jasechko & Perrone 2021). Therefore, analyzing groundwater storage and its fluctuations is crucial to comprehending the effects of climate change and interactions between land and atmosphere.

Groundwater is influenced by both climatic and human activities and exhibits different behaviors in various regions (Amanambu et al. 2020; Padrón et al. 2020; Scanlon et al. 2023). Climate change further stresses groundwater systems through its impacts on precipitation rates and intensity, evapotranspiration (ET), water demand, soil moisture, surface runoff, and glacial conditions, significantly affecting the terrestrial hydrological cycle (Fan et al. 2020; Tabari 2020; Williams et al. 2020; Condon et al. 2020). These changes result in the redistribution of water resources across spatial and temporal scales, resulting in more frequent and severe agricultural and ecological droughts (Anghileri et al. 2018; Setegn et al. 2011; IPCC, 2021). Changes in vegetation alter land use, subsequently affecting the distribution of precipitation among evapotranspiration, surface runoff, and groundwater recharge. Human activities significantly impact groundwater storage through various means, such as the regulation of reservoirs or dams, agricultural irrigation, and industrial and domestic water use. Urbanization and

agricultural irrigation further exacerbate regional imbalances in groundwater supply and demand, resulting in water scarcity and notable changes in the spatial and temporal distribution of hydrological processes and water balance elements (Taylor et al. 2013; Joodaki et al. 2014). Understanding the long-term spatiotemporal patterns of groundwater storage changes in response to climate change and human activities is essential for informed groundwater management and protection decisions.

Monitoring and managing groundwater is challenging due to the vast size and hidden nature of aquifers, which are difficult to observe directly, though some remote sensing techniques can provide insights. Typically, local and regional groundwater conditions are assessed through in situ measurements of groundwater levels or water balance estimates (Bhanja et al. 2020). However, comprehensive large-scale data have historically been limited, and direct observations of groundwater level and storage changes have often been constrained by the high cost of data collection and restrictive data policies (Jasechko et al. 2024). In addition to being monitored by in situ well observations, groundwater storage can be simulated by hydrological models. Hydrological models provide an abstract or generalized description of hydrological processes in different regions, enabling the study of the effects of climate change and human activities on these processes. Common global hydrological models include the WaterGAP Global Hydrology Model (WGHM; Herbert & Döll 2019; Veldkamp et al. 2017) and the PCRaster Global Water Balance (PCR-GLOBWB; Wada et al. 2014; Samaniego et al. 2018). Hydrological model simulations require extensive observational data for input parameters. Variability in these parameters can lead to significant uncertainties in simulated water storage analyses (Qi et al., 2018). Furthermore, limited understanding of groundwater recharge and abstraction processes, coupled with the scarcity of independent ground-based observations for model calibration, further exacerbates these uncertainties (Döll et al. 2014).In recent years, this large-scale information gap has been bridged by utilizing data from the Gravity Recovery and Climate Experiment (GRACE) and its successor, the GRACE Follow-On (GRACE-FO) satellite missions. The advent of the GRACE satellites has substantially improved our understanding of global

groundwater storage changes through remote sensing technology at the global scale (Scanlon et al. 2023). Since their launch in 2003, numerous studies have addressed changes in groundwater storage (GWS) derived from GRACE data (Richey et al. 2015; Bhanja et al. 2016; Scanlon et al. 2018; Rateb et al. 2020; Li et al. 2024). However, the use of gravity satellite data has limitations, including low spatial resolution, making it most suitable for regions larger than 200,000 km², and low temporal resolution at a monthly scale. Additionally, it is important to address challenges such as difficulties in selecting data from multiple sources (Gao et al. 2023), data gaps (Wang & Zhang, 2024), and low spatiotemporal resolution (Yin et al. 2022).

The reasons for groundwater storage changes vary widely. Overextraction of groundwater for irrigation is a significant factor contributing to the regional groundwater declination, as observed in California's Central Valley (Famiglietti et al. 2011), the North China Plain (Feng et al. 2017, 2013), India (Asoka et al. 2017; Rodell et al. 2009), and the Middle East (Voss et al. 2013). Severe droughts have also led to substantial reductions in groundwater storage, such as in southern and northern Africa (Rodell et al. 2018). The conclusions derived from GRACE regarding changes in groundwater storage mainly focus on individual aquifers or at catchments scale (Joodaki et al. 2014; Chen et al. 2010; Rateb et al. 2020), as well as large global aquifer systems (Thomas et al. 2017; Shamsudduha et al. 2020, Xanke & Liesch 2022). However, there has been no recent global-scale study examining the characteristics of groundwater storage changes over the past two decades. Furthermore, there is a lack of global-scale analysis to assess the extent to which human activities and climate change affect groundwater storage across specific regions, such as arid zones, or agricultural areas. Additionally, the driving forces behind changes in regional groundwater storage, as well as their implications at a global scale, remain insufficiently discussed. The main objectives of this study are:

1. Investigating global trends in groundwater storage at high spatial resolution from 2003-2022.

2. Examining the relationship between groundwater storage change with climatic characteristics and human activities, and analyzing the driving mechanisms behind groundwater storage changes.

3. Discussing significant changes in groundwater storage over the past 20 years across selected regions worldwide, attributing these changes to climate change factors and human activities.

2.2 Data and Methods

2.2.1 Data on groundwater storage data

The data retrieved from the GRACE/GRACE-FO RL06 Mascon solutions (Save et al. 2016; Save 2020) provided by the Center for Space Research (CSR) for the period January 2003 to December 2022 were used to isolate gridded groundwater storage changes. The data were resampled from a spatial resolution of 0.25° to 1°. Groundwater storage anomalies were estimated using a mass balance approach, which allows for the isolation of a groundwater storage signal from terrestrial water storage. This approach assumes that groundwater storage (ΔGW) can be computed by subtracting soil moisture (ΔSM), snow water equivalent (ΔSWE), surface water (ΔSWA), canopy water storage (ΔCWS) from total water storage (ΔTWS), as shown in Equation 1:

$$\Delta GW = \Delta TWS - \Delta SM - \Delta SWE - \Delta SWA - \Delta CWS \quad (1)$$

Soil moisture (ΔSM), snow water equivalent (ΔSWE), surface water (ΔSWA), and canopy water storage (ΔCWS) data were all taken from the ERA5-Land dataset (Muñoz Sabater 2019; Muñoz Sabater 2021). ERA5-Land data were used on a monthly time resolution and resampled from 0.1° to 1° to match the CSR GRACE Mascon data.

This study examines the impact of environmental changes on global groundwater storage using eight key indicators, encompassing climate factors, human activities, and other relevant variables (see Table 1). These selected indicators are representative factors that capture the multidimensional interactions of environmental changes,

allowing for a comprehensive analysis of their relationship with global groundwater storage.

2.2.2 Data on Climate factors

Monthly gridded precipitation data were obtained from the Climatic Research Unit (CRU) (Harris et al. 2020). The aridity index (AI), proposed by Middleton and Thomas (1997), quantifies climatic dryness and is defined as the ratio of annual precipitation (P) to annual potential evapotranspiration (PET). The PET data used in this study are derived from the Global Land Evaporation Amsterdam Model (GLEAM) (Martens et al. 2017; Miralles et al. 2011). According to the AI index, regions are classified into hyperarid ($AI < 0.05$), arid ($0.05 \leq AI < 0.2$), semiarid ($0.2 \leq AI < 0.5$), and dry subhumid ($0.5 \leq AI < 0.65$) subtypes. The Standardised Precipitation-Evapotranspiration Index (SPEI) is a meteorological drought index used to quantify the severity of drought or wetness in a region. It integrates data on precipitation and potential evapotranspiration (Vicente-Serrano et al. 2010). According to SPEI index, regions are classified into Extremely Wet ($SPEI > 2.0$), Very Wet ($1.5 \leq SPEI \leq 1.99$), Moderate Wet ($1.0 \leq SPEI \leq 1.49$), Normal ($-0.99 \leq SPEI \leq 0.99$), Moderate Dry ($-1.0 \leq SPEI \leq -1.49$), Very Dry ($-1.5 \leq SPEI \leq -1.99$), and Extremely Dry ($SPEI < -2.0$). Global maps of monthly Standardised Precipitation-Evapotranspiration Index (SPEI) for the period January 1901 to December 2022 with monthly resolution are available (Beguería et al. 2023). The climate factors cover the period from 2003 to 2022, and the resolution of these datasets has been standardized to 1°×1° using bilinear interpolation to match the resolution of the GRACE data.

2.2.3 Data on Human factors

Annual population data were collected from WorldPop (WorldPop 2018) spanning the years 2003 to 2020, produced at a 100m spatial resolution. Gridded groundwater extraction estimates were characterized using groundwater abstraction data reported by WaterGAP (Müller Schmied et al. 2021). For this study, monthly net groundwater abstraction data covering the period from 2003 to 2019 were selected for analysis, standardized to units of mm/month. Irrigation data were sourced from the Global Map

of Irrigation Areas (GMIA) (Siebert et al. 2013), produced at a 5 arc-minute spatial resolution around the year 2005. This dataset consists of two components: area actually irrigated and areas equipped for irrigation with groundwater. It provides the percentage of irrigation, derived by integrating subnational statistics with geospatial data on the location and extent of irrigation schemes. The data mentioned above are not available for the entire study period from 2003 to 2022. Therefore, the data used in this study are selected to align as closely as possible with this timeframe. Furthermore, the resolution of these datasets has been standardized to 1°×1° through bilinear interpolation to align with the resolution of the GRACE data.

2.2.4 Data on other factors

Data representing vegetation cover were selected using the monthly Leaf Area Index (LAI) sourced from MOD15A2H (Myneni et al. 2021), spanning the period from 2003 to 2022. These data were included to analyze whether large scale changes in vegetation, especially from deforestation of rainforests, have any influence on GWS.

Table 2-1 Datasets of environmental changes affecting global groundwater storage.

Factor	Time span	Unit	Source
Climate factors			
Precipitation	2003-2022, monthly	mm/a	Harris et al. 2020
Annual potential evapotranspiration	2003-2022, monthly	mm/a	Martens et al. 2017; Miralles et al. 2011
Standardised Precipitation-Evapotranspiration Index (SPEI)	2003-2022, monthly	unitless	Vicente-Serrano et al. 2010
Human factors			
Population	2003 – 2020, yearly	Number of people	WorldPop 2018
Groundwater abstraction data	2003 – 2019, monthly	mm/a	Müller Schmied et al. 2021
Area actually irrigated	2005	%	Siebert et al. 2013
Areas equipped for Irrigation with	2005	%	Siebert et al. 2013

groundwater			
Other factors			
Leaf Area Index (LAI)	2003 to 2022, monthly	%	Myneni et al. 2021

2.2.5 Method on Trend Analysis

Gridded groundwater trends in magnitude and significance were assessed using the Seasonal Mann-Kendall trend test (Hirsch et al. 1982) and the Sen Slope estimator (Sen, 1968). These methods were chosen to mitigate the influence of non-normally distributed variables, particularly those prone to seasonal fluctuations and outliers. The Seasonal Mann-Kendall test evaluates the significance of monotonic trends based on the null hypothesis, distinguishing between significant ($p \leq 0.05$) and non-significant ($p > 0.05$) trends.

2.2.6 Method on Driving Force Analysis

Attribution studies aim to identify the primary factors influencing changes in groundwater storage. Multiple linear regression (MLR) is a widely-used statistical method in hydrology and climate sciences for modeling relationships between dependent and independent variables, helping to explain links between key variables (Seidou et al. 2007; Tibshirani 1996; Zou & Hastie 2005; Hoerl & Kennard 1970). The general purpose of MLR is to learn more about the relationship between several independent or predictor variables and a dependent or criterion variable (Yilmaz and Yuksek 2008), as shown in Equation 2:

$$Y=a + b1 \times x1+ b2 \times x2+b3 \times x3+\cdots\ bn \times xn + \in \quad (2)$$

Where Y is the dependent variable, x1, x2, …xn are the independent variables, b1, b2, … bn are regression coefficient. The regression coefficients represent the independent contributions of each independent variable to the prediction of the dependent variable. In this study, MLR is applied to analyze groundwater storage responses to climatic factors and human activities, including trends in precipitation, drought, population

density, irrigation conditions, and groundwater abstraction, to identify the main drivers of groundwater storage changes. The ultimate goal is to determine whether observed trends are primarily due to climate impacts, human impact, or a combination of both. Additionally, trends for specific factors were calculated and compared mathematically, with detailed analysis conducted on specific regions.

2.3 Results and discussion

2.3.1 Trends in groundwater storage

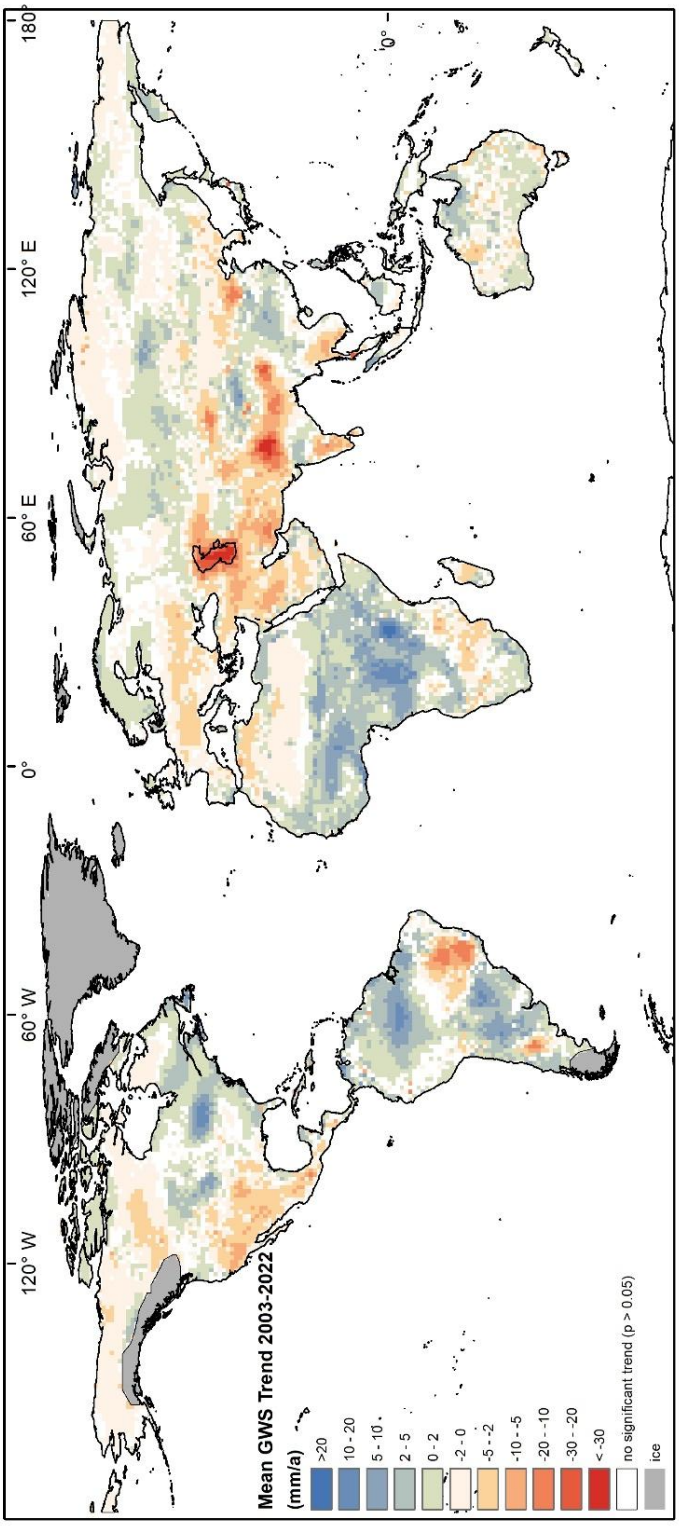

Fig. 2-1 Mean annual trends of GRACE-derived global GWS for the period of 2003–2022 (mm/a) , all calculations were conducted at the original 1° resolution of the dataset. The colored areas in the figure indicate significant trends at the 95% confidence level.

Fig. 2-1 illustrates the spatial distribution of the mean annual groundwater storage change trend from 2003 to 2022. The following regions were excluded: Antarctica, Greenland, the Gulf of Alaska coast, the Canadian Archipelago, and the Patagonian ice fields. The primary reason is that changes in water storage in these regions are mainly due to ice-sheet and glacier ablation caused by a warming climate, rather than changes in groundwater reserves (Rodell et al. 2018; Velicogna et al. 2014).

Over the past two decades, groundwater storage has exhibited spatial heterogeneity, with most depletion occurring within the Earth's mid-latitudes. With a 95% confidence level, approximately 81% of global regions, excluding ice melt regions, have experienced a significant trend in groundwater storage. Of these regions, 48% have witnessed a decline in groundwater levels, whereas 52% have experienced an increase. Approximately 3.4 billion people live in regions where groundwater levels have significantly declined over the past 20 years. Notably, a significant decline in groundwater storage (>20 mm/a) was observed in northern India, eastern Brazil, and areas surrounding the Caspian Sea. Among these, the most severe groundwater depletion occurred in the regions around the Aral, the Caspian Sea and northern India, with an average annual decline exceeding 30 mm over the past 20 years. These areas are characterized by sparse vegetation and fragile ecological environments. Examples of areas with rising groundwater storage (GWS) trends include West and Central Africa, the Amazon rainforest, the Great Lakes region and the area west of the Great Lakes, with groundwater increases exceeding 20 mm annually. This significant increase in groundwater storage is likely due to high average precipitation, dense surface vegetation, and prevailing wetting climate trends (Green et al, 2011; Amanambu et al. 2020). Additionally, groundwater depletion is more pronounced in areas where water tables are already deep (Fan et al. 2013). In such regions, further depletion can exacerbate the challenge of accessing groundwater, potentially requiring the construction of deeper wells, which increases costs (Jasechko & Perrone 2021).

2.3.2 GWS and climate

Precipitation

The correlation between precipitation and groundwater storage has been confirmed in multiple studies (Thomas & Famiglietti, 2019; Russo & Lall, 2017). As shown in Fig. 2-2, precipitation trends exhibit an uneven spatial distribution. The most significant increases in precipitation are observed in the eastern United States, northern Russia, central Africa, and southern China, while marked decreases are primarily concentrated in South America. Despite the notable reduction in precipitation in South America, most regions do not show a corresponding decline in groundwater storage. For instance, in the Amazon rainforest, even though precipitation is decreasing, high average temperatures and high average precipitation have not prevented the trend of rising groundwater storage (Heerspink et al. 2020). Although changes in precipitation can affect groundwater recharge, variations in groundwater storage do not always directly correspond to changes in precipitation. Fig. 2-3 shows the global distribution of multi-year average precipitation. Compared to precipitation trend maps, the average precipitation map is more spatially correlated with the groundwater storage distribution map. Therefore, the increase or decrease in precipitation is not the sole factor influencing groundwater storage, emphasizes the impact of evapotranspiration on groundwater storage. Long-term precipitation changes may impact global groundwater storage due to the slow response to recharge, and many regions experience groundwater decline due to excessive extraction (Herrera-Pantoja & Hiscock 2008; Thomas & Famiglietti 2019). Increased evapotranspiration due to climate change may prevent groundwater reserves from being replenished by precipitation, even if precipitation increases (Green et al. 2011).

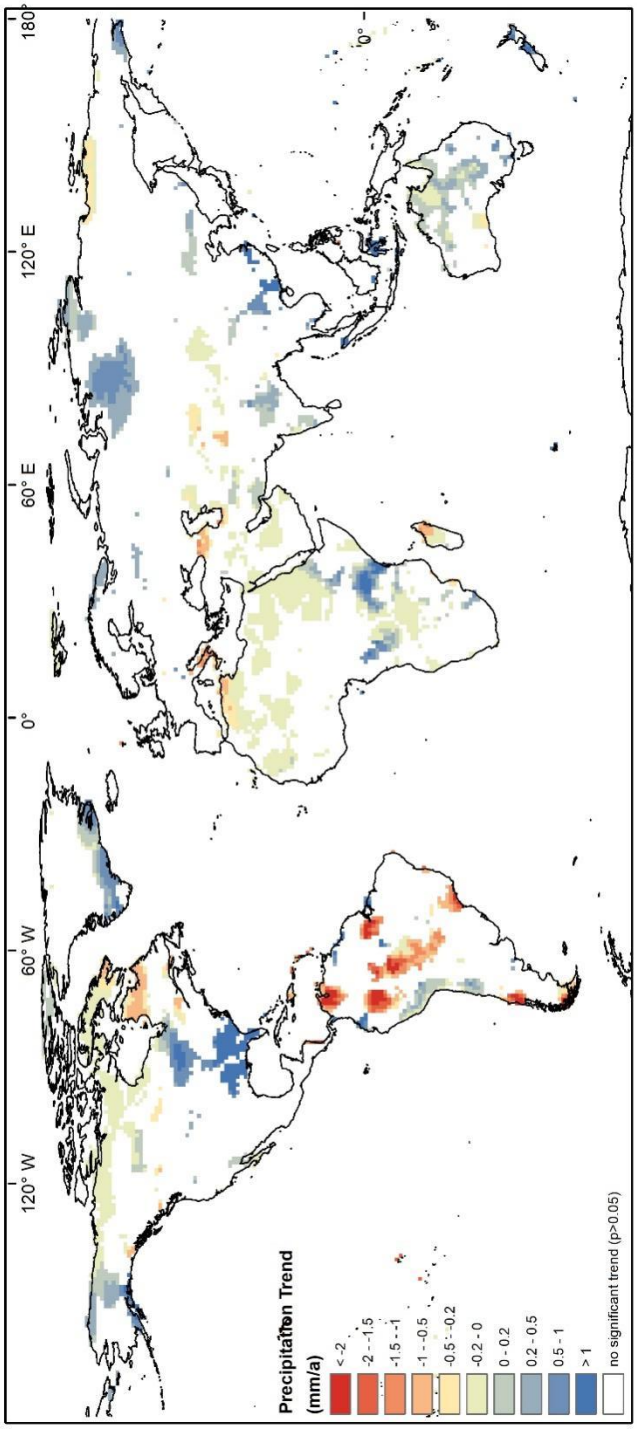

Fig. 2-2 Mean annual trend of precipitation for the period of 2003–2022 (mm/a), the colored areas in the figure indicate significant trends at the 95% confidence level.

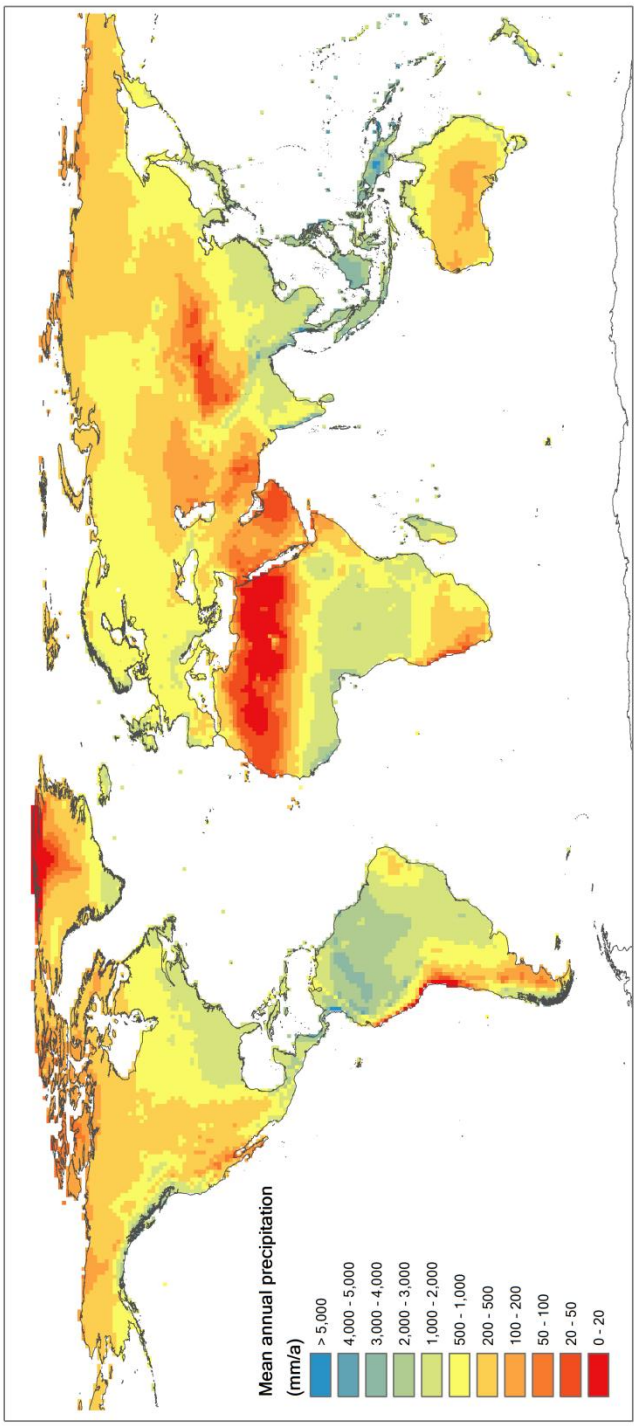

Fig. 2-3 Mean annual precipitation for the period of 2003–2022 (mm/a)

SPEI Drought index

The spatial distribution of the trend of the global SPEI trend over the past 20 years is shown in Fig. 2-4. The climatological mean Standardized Precipitation-Evapotranspiration Index (SPEI), representing meteorological drought conditions for the period from 2003 to 2022, is shown in the Fig. 2-5.Compared to the precipitation trends shown in Fig. 2-2, changes in groundwater storage are more closely aligned with the spatial distribution of the SPEI trend. This relationship has also been observed by Dai (2013) and Wang et al. (2014). The likely reason is that SPEI accounts for multiple factors, including precipitation, temperature, evapotranspiration, and other climatic conditions. Therefore, it highlights the significant role of evapotranspiration in influencing groundwater storage. Van Loon (2015) noted that groundwater storage fluctuates in response to meteorological trends, increasing during wetter periods and decreasing during drier periods. However, not every meteorological drought leads to a decline in groundwater levels. This is mainly because short-term meteorological droughts do not impact groundwater, and only prolonged droughts cause significant changes in groundwater storage (Li & Rodell 2015; Barichivich et al. 2022). Additionally, groundwater droughts exhibit a delayed effect compared to meteorological droughts, as it takes time for precipitation to recharge groundwater, and a reduction in precipitation leading to meteorological drought does not immediately cause groundwater depletion (Han et al. 2019; Gates et al. 2011).

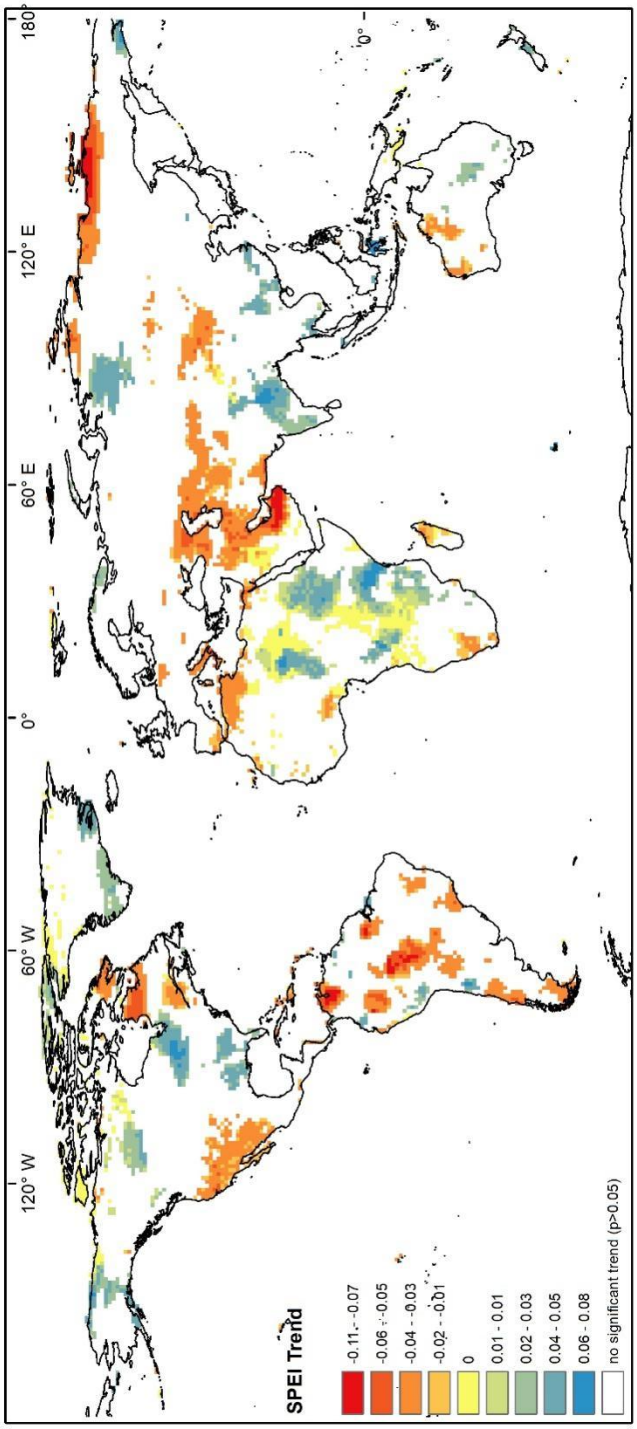

Fig. 2-4 Mean annual trend of Standardised Precipitation-Evapotranspiration Index (SPEI) for the period of 2003–2022, the colored areas in the figure indicate significant trends at the 95% confidence level.

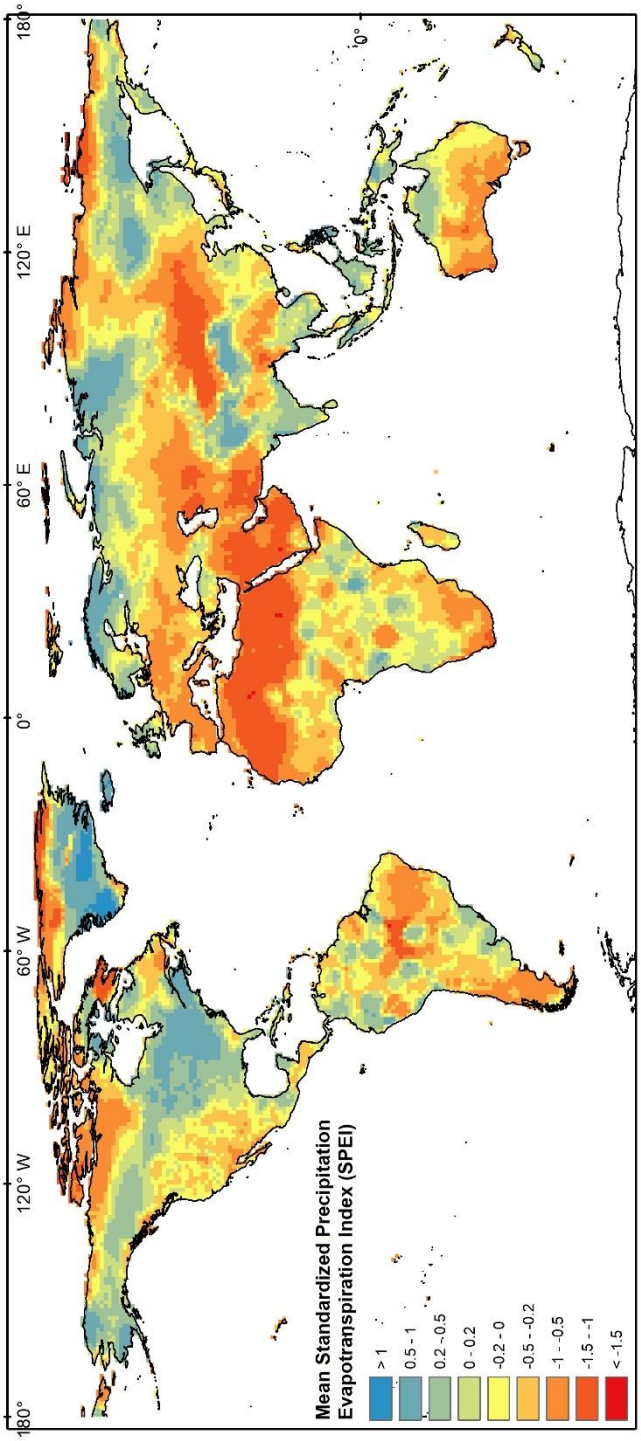

Fig. 2-5 Mean annual standardized precipitation evapotranspiration index (SPEI) for the period of 2003–2022

Aridity index

The climatological mean Aridity index (AI), representing the climatological state for the period from 2003 to 2022, is shown in Fig. 2-6. Since groundwater storage largely depends on both climatic conditions and topography, we focus on the long-term perspective, where climate exerts a stronger influence. Therefore, the regionally averaged groundwater storage trend, plotted against the climatological mean aridity index, is presented in Fig. 2-7. The analysis shows that the most significant groundwater decline occurred within the AI range of 0.1 to 0.5, peaking at 0.1 to 0.2. This indicates that arid and semi-arid areas (see Methods), rather than hyper-arid region, are experiencing the greatest depletion, a fact that has also been found by Scanlon et al. (2023).

The Sahara Desert, which has an AI below 0.1 and lacks vegetation, is not typically dependent on groundwater, and thus does not significantly contribute to this extreme phenomenon (Rohde et al. 2024). Excluding the Sahara Desert from the analysis did not substantially alter the groundwater storage trends, suggesting it is not a primary factor in substantial groundwater depletion, a fact that has also been found by Cuthbert et al. (2019). In arid and semi-arid regions, more than 60% of areas showed groundwater decline trends, indicating that these regions play a dominant role in both the area and intensity of groundwater depletion.

Overall, the observed groundwater distribution trends indicate that groundwater storage are declining in arid and semi-arid regions, while increasing in humid regions (AI ≥ 0.8). This disparity may lead to a more uneven distribution of groundwater.

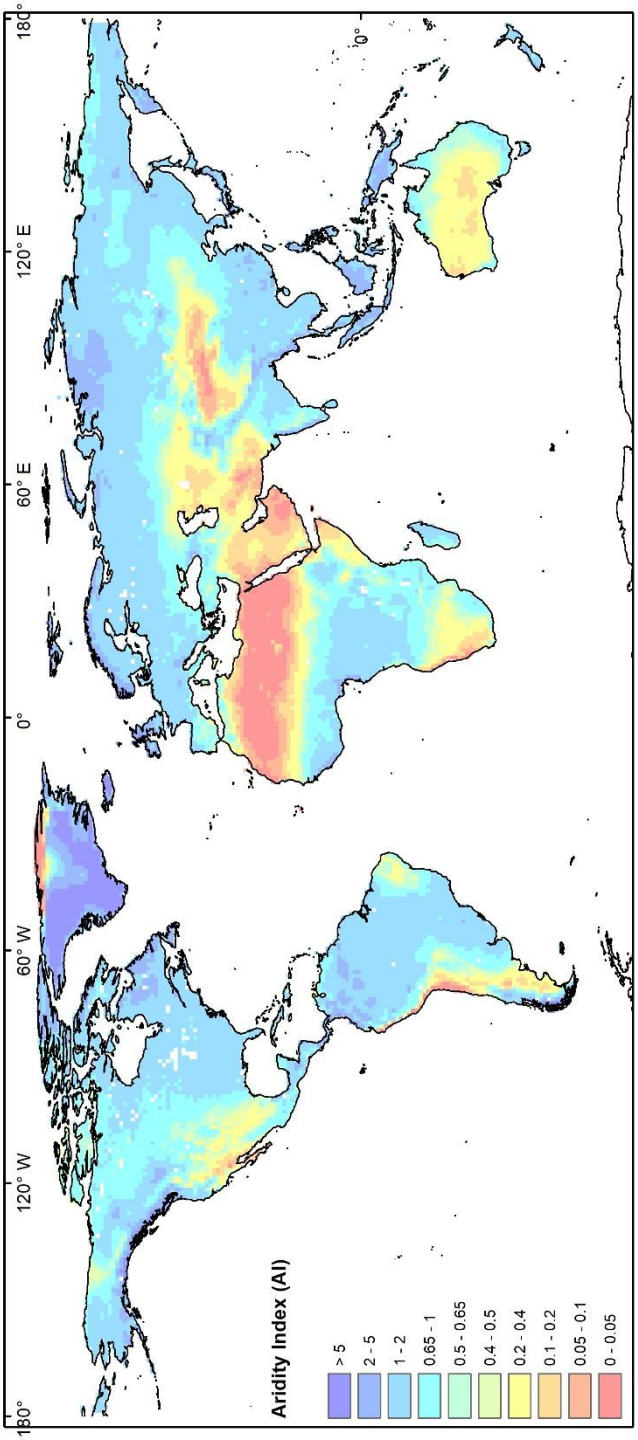

Fig. 2-6 Global Aridity Index (AI) for the period of 2003–2022

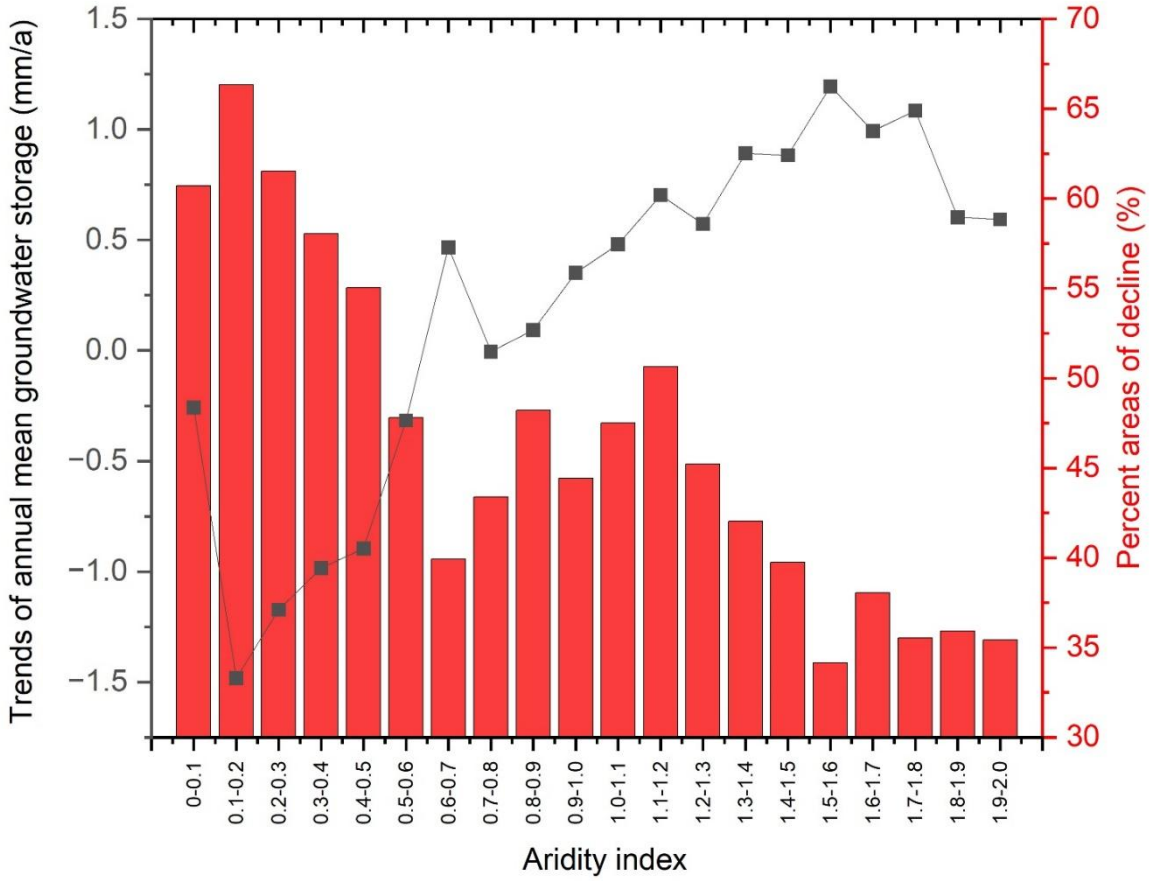

Fig. 2-7 Trends of annual groundwater storage (black line) and percent areas of different Aridity indices (bars) plotted against the climatological mean AI (except the ice melt regions). The climatological mean AI on the x axis is the annual mean AI for the period from 2003 to 2022.

2.3.3 GWS and human factors

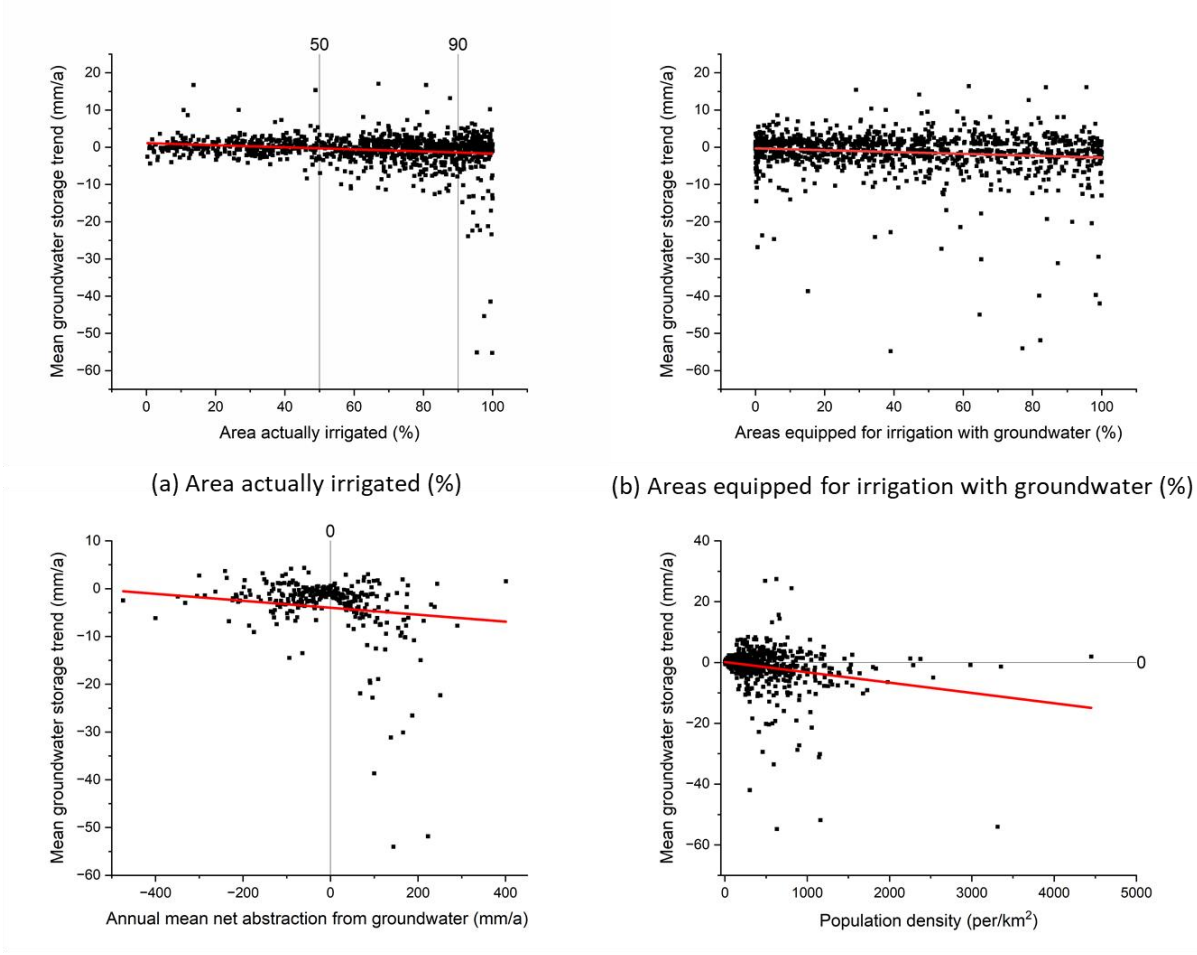

Fig. 2-8 Mean GWS plotted against four possible factors of human impact, (a) area actually irrigated (%), (b) areas equipped for irrigation with groundwater (%), (c) annual mean net abstraction from groundwater (mm/a), and (d) population density (per/km^2).

Regarding the impact of human activity on groundwater storage trends, we examined four human activity related factors as illustrated in Fig. 2-8. These factors are: (a) area actually irrigated (%), (b) areas equipped for irrigation with groundwater (%), (c) annual mean net abstraction from groundwater (mm/a), and (d) population density (per/km^2). For Fig. 2-8(a), when the proportion of the actually irrigated area is below 50%, the trend in groundwater storage is not conspicuous. However, as the proportion increases from 50% to 90%, a discernible decline in groundwater levels becomes evident in more and more areas, with many of them experiencing a decrease of approximately 10 mm per year. Upon surpassing the 90% threshold, more areas exhibit a pronounced

downward trend in groundwater levels, with many regions experiencing declines exceeding 10 mm per year. This also includes the regions with the most pronounced declines of more than 20 up to 50 mm/a. Fig. 2-8(b) shows that many regions with varying proportions of irrigation using groundwater all exhibit significant areas with declines in groundwater storage, most of them in regions with 20% or more area equipped for irrigation with groundwater, while there are also some regions with high declines and no or little irrigation with groundwater. This may be related to regional recharge and discharge rates, making the relationship between areas equipped for irrigation with groundwater and groundwater storage not so clear. For Fig. 2-8(c), the data indicate that net recharge to groundwater (negative values of net abstraction, caused by irrigation return flow in areas irrigated by surface water) does not necessarily lead to an increase in groundwater storage, but excessive groundwater abstraction most often results in a decrease in groundwater storage. Different to irrigation and abstraction factors, population density (Fig. 2-8 (d)) does not have a direct relationship with groundwater storage. Thus, high population density does not necessarily lead to reduced groundwater storage. This confirms that abstractions connected with high population density, e.g. for drinking water or industrial purposes, have a minor effect on GWS, compared to agriculture, which is the cause for the majority of abstracted groundwater and is more likely to be found in less populated regions.

2.3.4 GWS and Vegetation Cover

To analyze the potential impacts of vegetation cover and its changes, particularly due to rainforest deforestation, on groundwater storage (GWS), we compared GWS trends with the mean leaf area index (LAI) (Fig. 2-9) and LAI trends from 2003 to 2022 (Fig. 2-10). In recent years, researchers have observed a global greening trend in vegetation using earth observation technologies and remote sensing imagery (Keenan & Riley 2018; Song et al. 2018), similar to the greening trend observed in the LAI trend discussed in this paper. However, on a global scale, these patterns are not immediately apparent. Regions exhibiting increasing or decreasing GWS trends are found in areas with both

high and low LAI, as well as in regions with both increasing and decreasing LAI trends (Tao et al. 2020). Therefore, we discuss the potential influences in selected regions below.

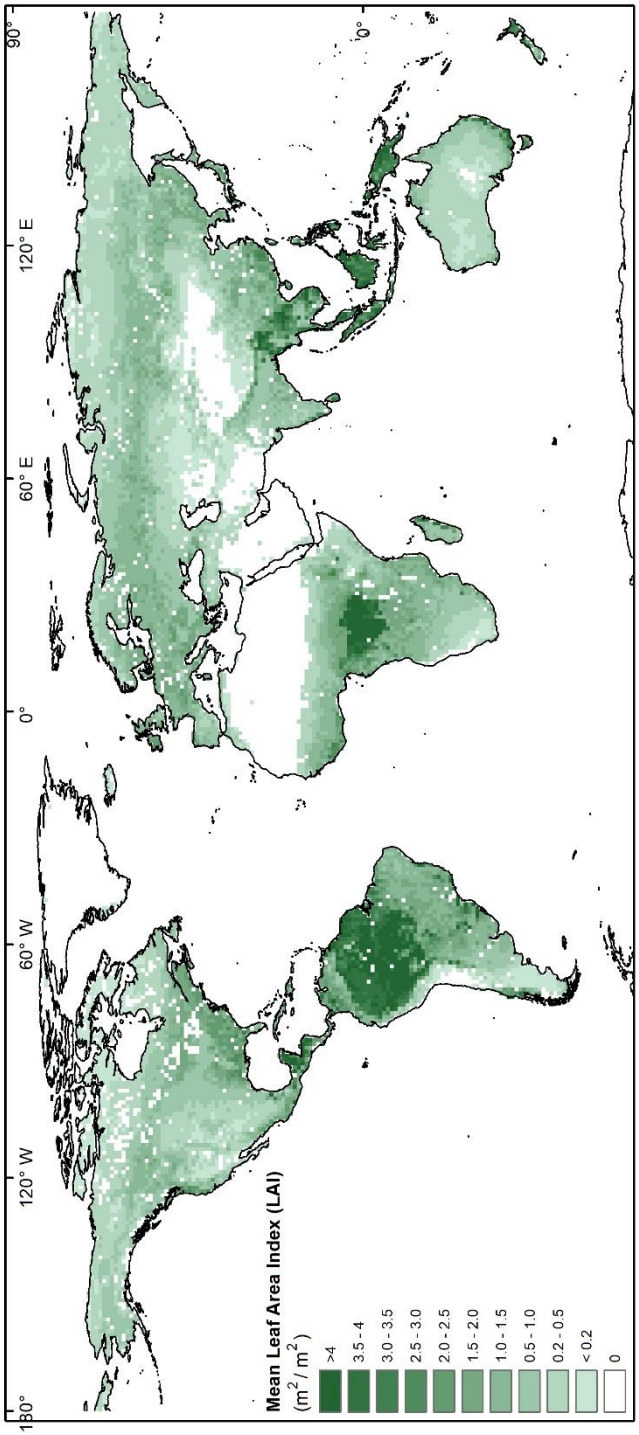

Fig. 2-9 Mean annual leaf area index (LAI) for the period of 2003–2022 (m^2/m^2)

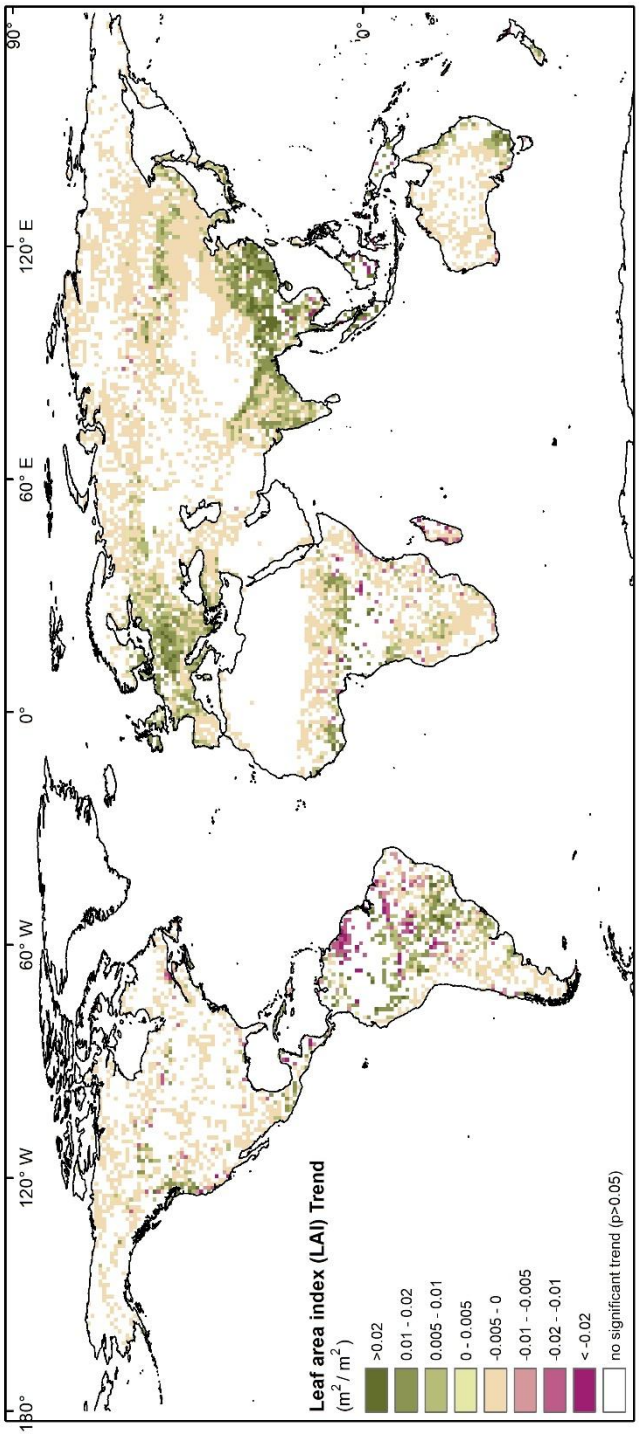

Fig. 2-10 Mean annual trend of leaf area index (LAI) for the period of 2003–2022(m^2/m^2), the colored areas in the figure indicate significant trends at the 95% confidence level.

2.3.5 Regional groundwater storage changes and attributions

To better understand the drivers of regional groundwater storage (GWS) changes, we applied the Hot Spot Analysis method. This spatial statistical technique identifies statistically significant clusters of high values and low values based on the spatial distribution of the data. In this study, areas in the GWS map where absolute changes exceeded 5 mm/year were first selected. Subsequently, regions with adjacent areas showing similar trends were grouped together, resulting in the identification of 23 distinct regions. To investigate the causes behind these changes, we compiled several potential influencing factors, as detailed in Table 2. Trends and extreme values in groundwater storage were calculated using area-weighted mean values and extremes for each region (maximum values for regions with rising groundwater and minimum values for those with declining groundwater). The proportion of irrigated land was calculated by area-weighting pixel values of irrigation intensity across each study region. Spatial variation maps for these factors include precipitation trends in Fig. 2-2, annual mean precipitation in Fig. 2-3, SPEI trends in Fig. 2-4, mean leaf area index (LAI) and its trends in Fig. 2-9 and 2-10, annual mean population density in Fig. 2-11, and annual mean net groundwater extraction in Fig. 2-12. To evaluate the impact of each factor on GWS, we conducted a regression analysis to calculate the coefficients, where larger absolute values denote stronger influence. Positive coefficients indicate positive effects, while negative coefficients indicate negative effects (see Fig. 2-13). Based on these results, we attributed groundwater storage trends to “mainly climate impact,” “potential human impact,” or a “combination of both.” Fig. 2-14 illustrates the global distribution of 23 regions where significant changes in groundwater storage were observed from 2003 to 2022. The main drivers of these changes were inferred from the specific conditions of each region and the outcomes of regression analysis.

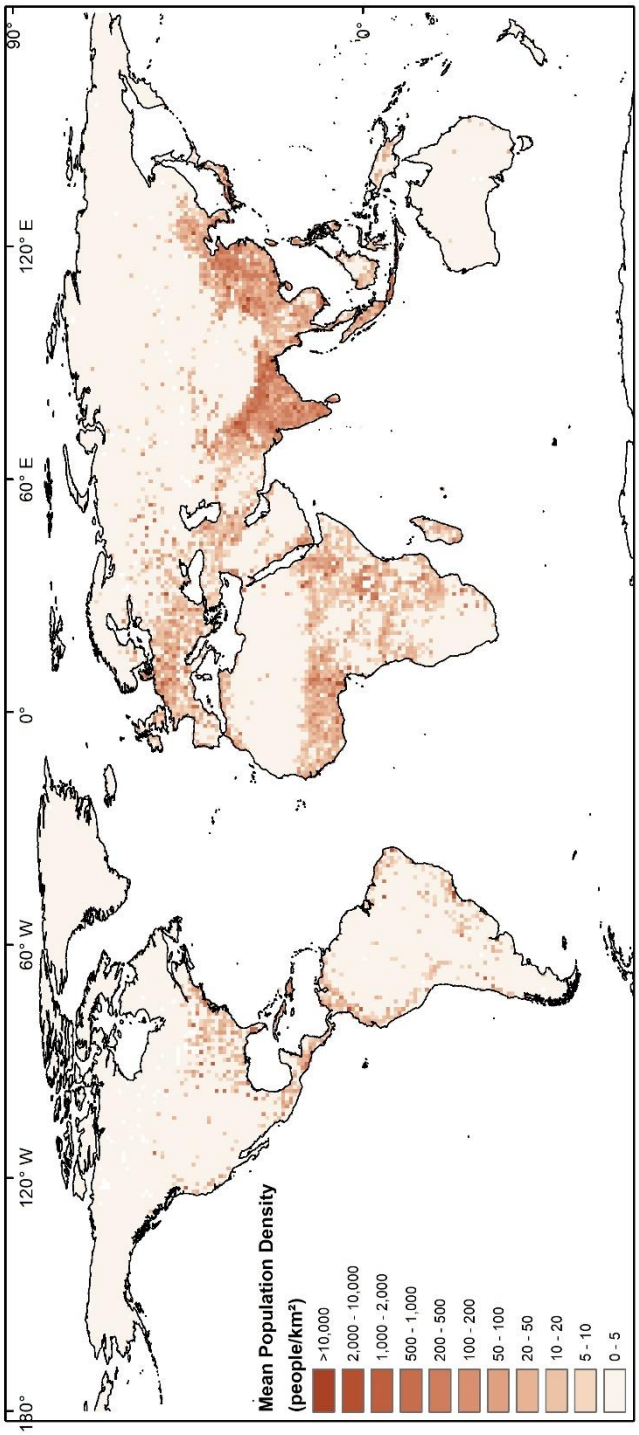

Fig. 2-11 Mean annual population density for the period of 2003–2020 (people/km2)

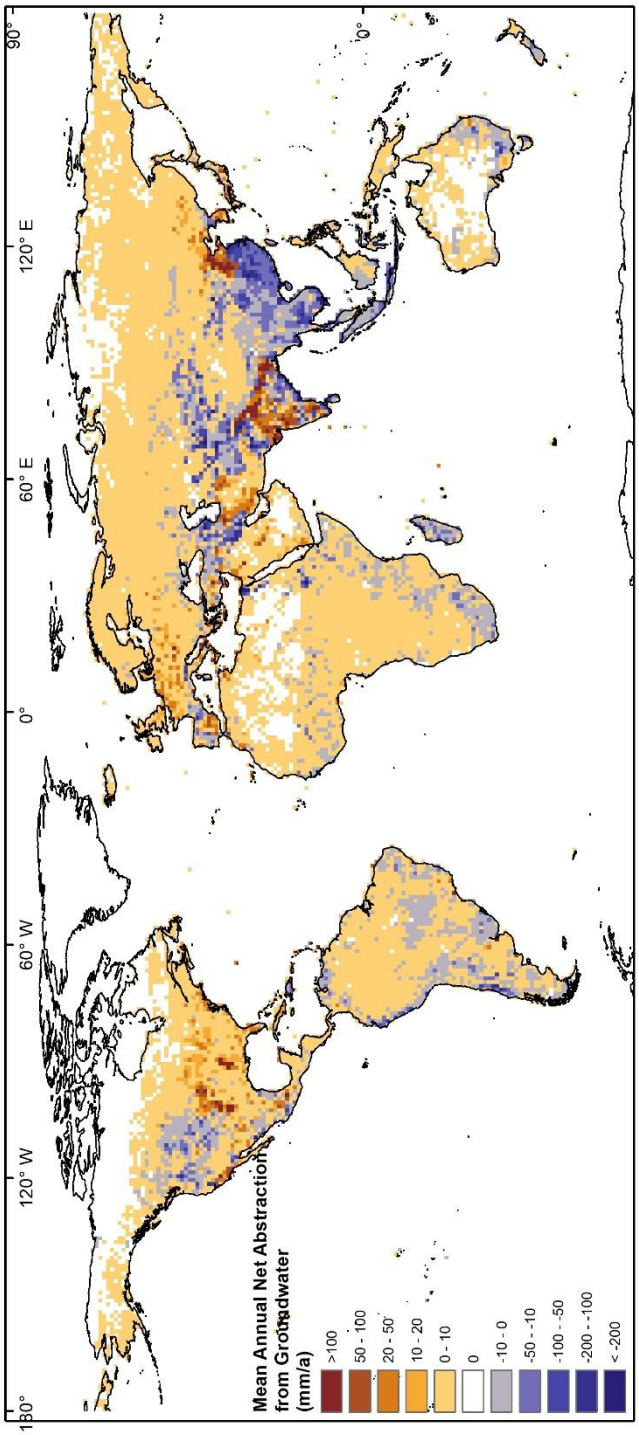

Fig. 2-12 Mean annual net abstraction from groundwater for the period of 2003–2020 (mm/a)

Table 2-2 Statistics of groundwater storage trends and possible influencing factors for the selected regions in Fig. 2-14. Supposed main driving forces are not directly concluded from the statistics but discussed in the text.

Region No.	Location	Area (km^2)	Mean GWS trend (mm/a)	GWS trend extreme value (mm/a)	Mean Precipitation trend (mm/a)	Annual Mean Precipitation (mm/a)	SPEI trend	Areas equipped for irrigation (%)	Area equipped for irrigation with groundwater (%)	Population density (people/km^2)	Annual net abstraction from groundwater max value (mm/a)	Supposed main driving force
1	Western America	4,241,546	-3.0	-12.7	0.00	574	-0.017	49.7	30.2	63	177.2	climate +human impact
2	Central Canada	1,525,571	-1.9	-6.3	-0.03	436	0.008	3.7	0.1	2	3.2	mainly climate impact
3	Eastern United States	906,647	5.4	16.4	0.46	996	0.013	37.9	32.5	94	35.4	mainly climate impact
4	Amazon	2,716,443	4.7	14.1	-0.53	2361	-0.013	12.0	4.2	7	3.9	mainly climate impact
5	Eastern Brazil	1,831,986	-5.2	-17.9	-0.15	1374	-0.016	87.5	18.9	23	32.2	climate +human impact
6	Southern Brazil-Paraguay region	1,553,784	5.0	12.3	-0.17	1059	-0.010	42.0	13.3	20	24.6	mainly climate impact
7	Central Argentina	369,510	-3.5	-11.4	0.01	328	-0.009	12.6	1.6	8	0.5	human impact
8	Central Europe	3,711,950	-1.9	-5.0	0.00	704	-0.013	23.4	16.5	119	244.4	mainly climate impact
9	Northern Africa	2,273,262	-1.6	-7.3	-0.08	95	-0.011	9.4	6.2	21	139.9	climate +human impact
10	Western Africa	2,477,929	4.9	14.8	-0.01	1374	0.003	4.0	0.9	80	22.4	mainly climate impact

11	Nile headwaters	3,451,624	6.9	28.2	0.20	1368	0.012	2.8	0.3	78	3.3	climate +human impact
12	Southeastern Africa	1,802,587	-2.1	-7.2	0.00	649	0.005	7.8	0.6	32	2.4	human impact
13	Aral Sea and Caspian Sea	5,708,583	-5.8	-40.4	-0.09	308	-0.025	22.4	13.3	65	101.9	climate +human impact
14	Northwestern China	898,833	-3.0	-14.7	-0.06	195	-0.020	20.5	4.4	20	19.8	climate +human impact
15	Tibetan Plateau	230,001	5.5	10.7	0.00	154	0.001	0.0	0.0	1	0.0	mainly climate impact
16	North China Plain	1,004,133	-3.4	-16.3	0.02	397	-0.008	43.7	30.2	208	290.3	human impact
17	Northeast China	966,799	-1.7	-5.0	0.12	635	0.009	61.1	36.4	141	68.8	human impact
18	Arabian Peninsula	1,754,517	-2.9	-9.3	0.00	113	-0.017	7.4	9.2	62	169.3	climate +human impact
19	Northern India	1,532,713	-9.9	-54.8	0.08	602	0.012	59.8	36.5	363	251.6	human impact
20	Southern India	434,225	-4.8	-11.7	0.08	1100	0.017	77.1	57.9	447	173.9	human impact
21	South Asia	1,198,228	-5.6	-25.2	-0.02	1200	0.012	49.5	19.9	399	238.4	mainly climate impact
22	Eastern Central China	461,212	3.6	5.4	0.47	1202	0.023	71.3	0.1	295	-0.1	mainly climate impact
23	Mainland Southeast Asia	710,066	-3.3	-9.7	0.18	1846	0.012	49.8	3.0	145	0.5	climate +human impact

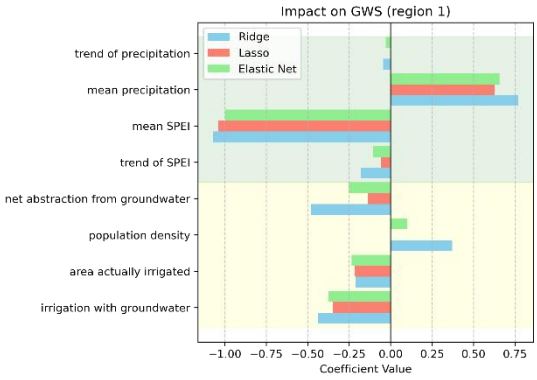
Impact on GWS (region 1)
Ridge
Lasso
Elastic Net
trend of precipitation
mean precipitation
mean SPEI
trend of SPEI
net abstraction from groundwater
population density
area actually irrigated
irrigation with groundwater
−1.00 −0.75 −0.50 −0.25 0.00 0.25 0.50 0.75
Coefficient Value

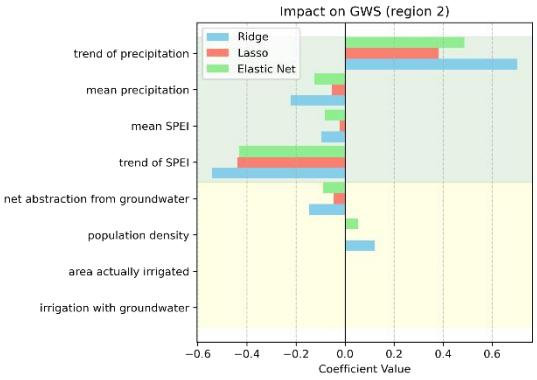
Impact on GWS (region 2)
Ridge
Lasso
Elastic Net
trend of precipitation
mean precipitation
mean SPEI
trend of SPEI
net abstraction from groundwater
population density
area actually irrigated
irrigation with groundwater
−0.6 −0.4 −0.2 0.0 0.2 0.4 0.6
Coefficient Value

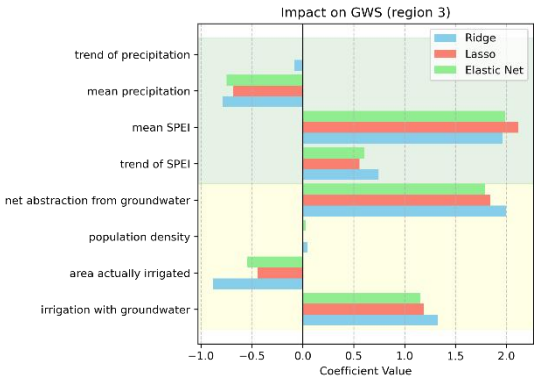
Impact on GWS (region 3)
Ridge
Lasso
Elastic Net
trend of precipitation
mean precipitation
mean SPEI
trend of SPEI
net abstraction from groundwater
population density
area actually irrigated
irrigation with groundwater
−1.0 −0.5 0.0 0.5 1.0 1.5 2.0
Coefficient Value

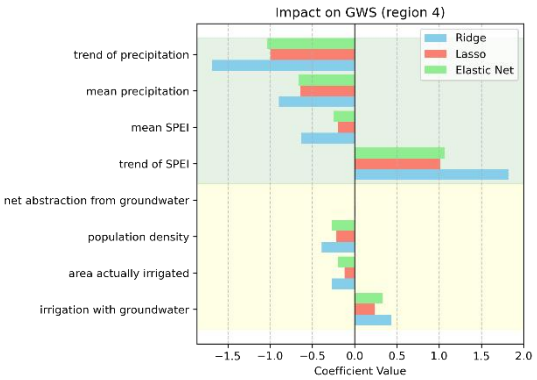
Impact on GWS (region 4)
Ridge
Lasso
Elastic Net
trend of precipitation
mean precipitation
mean SPEI
trend of SPEI
net abstraction from groundwater
population density
area actually irrigated
irrigation with groundwater
−1.5 −1.0 −0.5 0.0 0.5 1.0 1.5 2.0
Coefficient Value

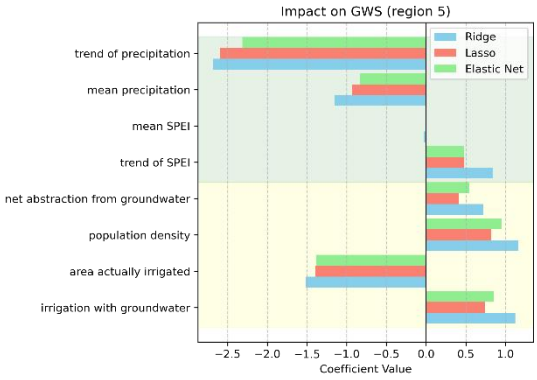
Impact on GWS (region 5)
Ridge
Lasso
Elastic Net
trend of precipitation
mean precipitation
mean SPEI
trend of SPEI
net abstraction from groundwater
population density
area actually irrigated
irrigation with groundwater
−2.5 −2.0 −1.5 −1.0 −0.5 0.0 0.5 1.0
Coefficient Value

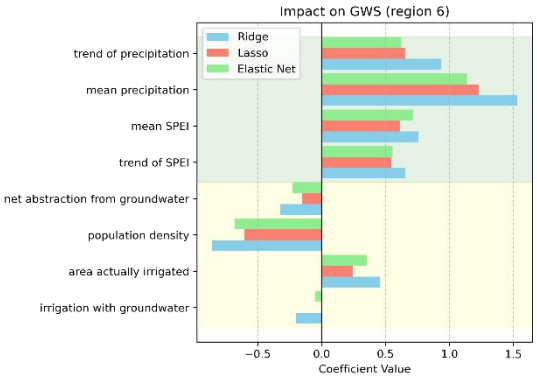
Impact on GWS (region 6)
Ridge
Lasso
Elastic Net
trend of precipitation
mean precipitation
mean SPEI
trend of SPEI
net abstraction from groundwater
population density
area actually irrigated
irrigation with groundwater
−0.5 0.0 0.5 1.0 1.5
Coefficient Value

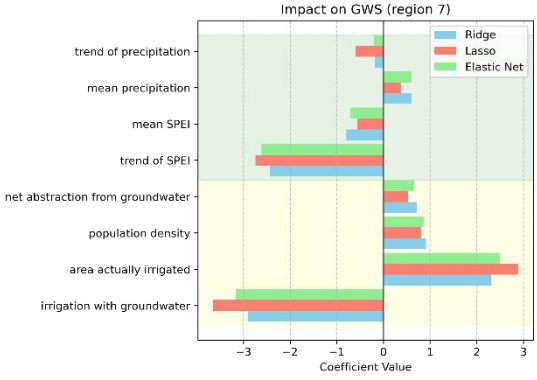
Impact on GWS (region 7)
Ridge
Lasso
Elastic Net
trend of precipitation
mean precipitation
mean SPEI
trend of SPEI
net abstraction from groundwater
population density
area actually irrigated
irrigation with groundwater
−3 −2 −1 0 1 2 3
Coefficient Value

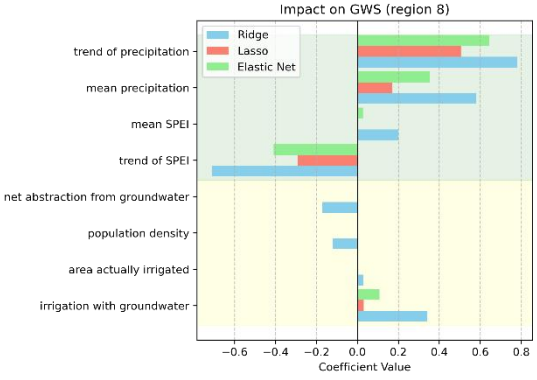
Impact on GWS (region 8)
Ridge
Lasso
Elastic Net
trend of precipitation
mean precipitation
mean SPEI
trend of SPEI
net abstraction from groundwater
population density
area actually irrigated
irrigation with groundwater
−0.6 −0.4 −0.2 0.0 0.2 0.4 0.6 0.8
Coefficient Value

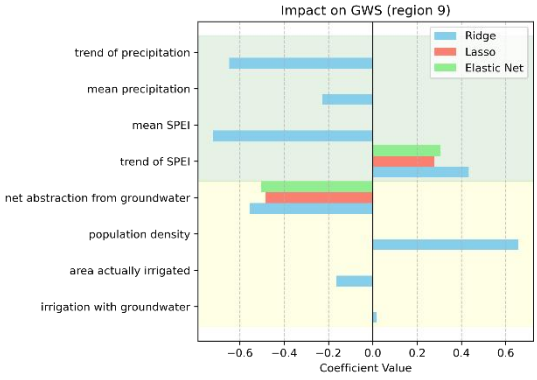
Impact on GWS (region 9)
trend of precipitation
mean precipitation
mean SPEI
trend of SPEI
net abstraction from groundwater
population density
area actually irrigated
irrigation with groundwater
Ridge
Lasso
Elastic Net
−0.6 −0.4 −0.2 0.0 0.2 0.4 0.6
Coefficient Value

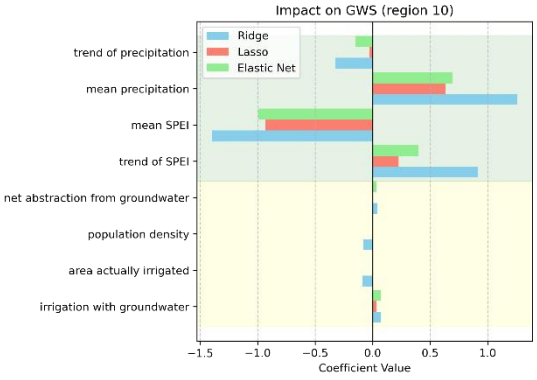
Impact on GWS (region 10)
trend of precipitation
mean precipitation
mean SPEI
trend of SPEI
net abstraction from groundwater
population density
area actually irrigated
irrigation with groundwater
Ridge
Lasso
Elastic Net
−1.5 −1.0 −0.5 0.0 0.5 1.0
Coefficient Value

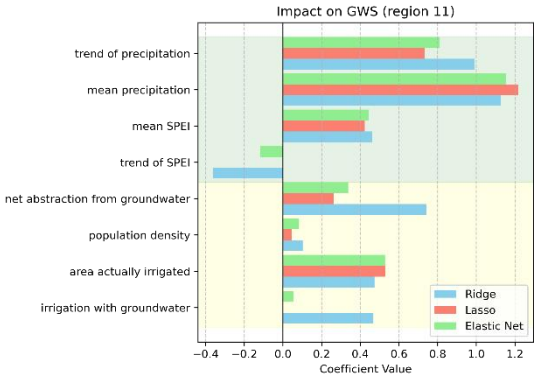
Impact on GWS (region 11)
trend of precipitation
mean precipitation
mean SPEI
trend of SPEI
net abstraction from groundwater
population density
area actually irrigated
irrigation with groundwater
Ridge
Lasso
Elastic Net
−0.4 −0.2 0.0 0.2 0.4 0.6 0.8 1.0 1.2
Coefficient Value

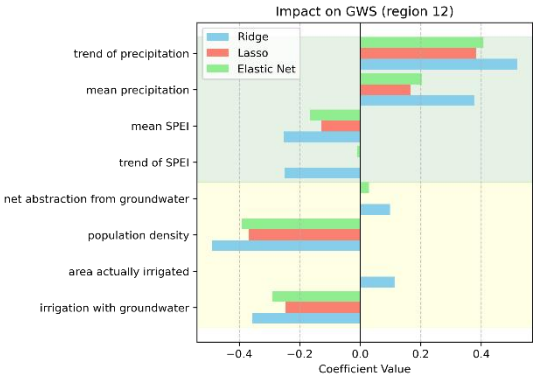
Impact on GWS (region 12)
trend of precipitation
mean precipitation
mean SPEI
trend of SPEI
net abstraction from groundwater
population density
area actually irrigated
irrigation with groundwater
Ridge
Lasso
Elastic Net
−0.4 −0.2 0.0 0.2 0.4
Coefficient Value

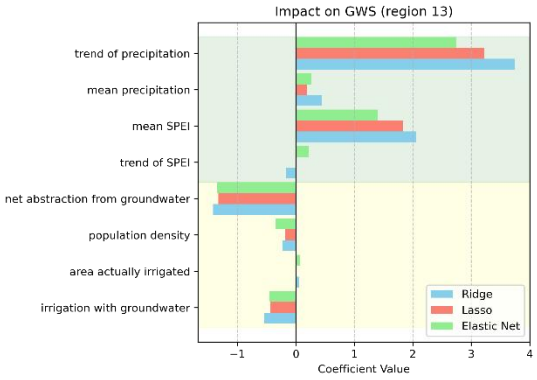
Impact on GWS (region 13)
trend of precipitation
mean precipitation
mean SPEI
trend of SPEI
net abstraction from groundwater
population density
area actually irrigated
irrigation with groundwater
Ridge
Lasso
Elastic Net
−1 0 1 2 3 4
Coefficient Value

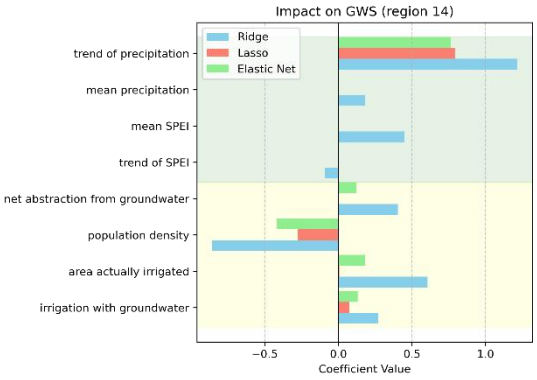
Impact on GWS (region 14)
trend of precipitation
mean precipitation
mean SPEI
trend of SPEI
net abstraction from groundwater
population density
area actually irrigated
irrigation with groundwater
Ridge
Lasso
Elastic Net
−0.5 0.0 0.5 1.0
Coefficient Value

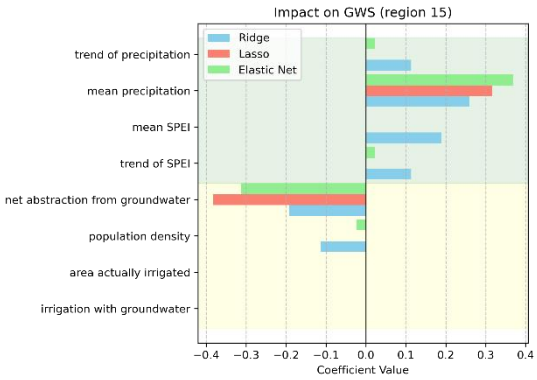
Impact on GWS (region 15)
trend of precipitation
mean precipitation
mean SPEI
trend of SPEI
net abstraction from groundwater
population density
area actually irrigated
irrigation with groundwater
Ridge
Lasso
Elastic Net
−0.4 −0.3 −0.2 −0.1 0.0 0.1 0.2 0.3 0.4
Coefficient Value

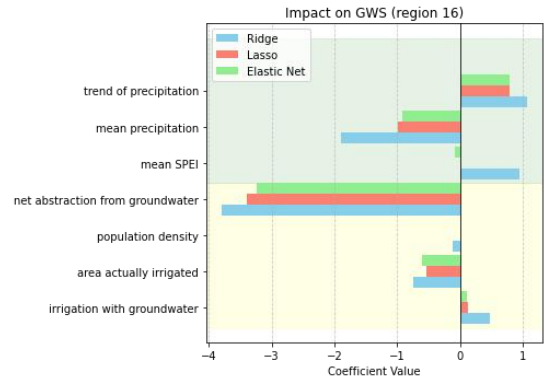
Impact on GWS (region 16)
trend of precipitation
mean precipitation
mean SPEI
net abstraction from groundwater
population density
area actually irrigated
irrigation with groundwater
Ridge
Lasso
Elastic Net
−4 −3 −2 −1 0 1
Coefficient Value

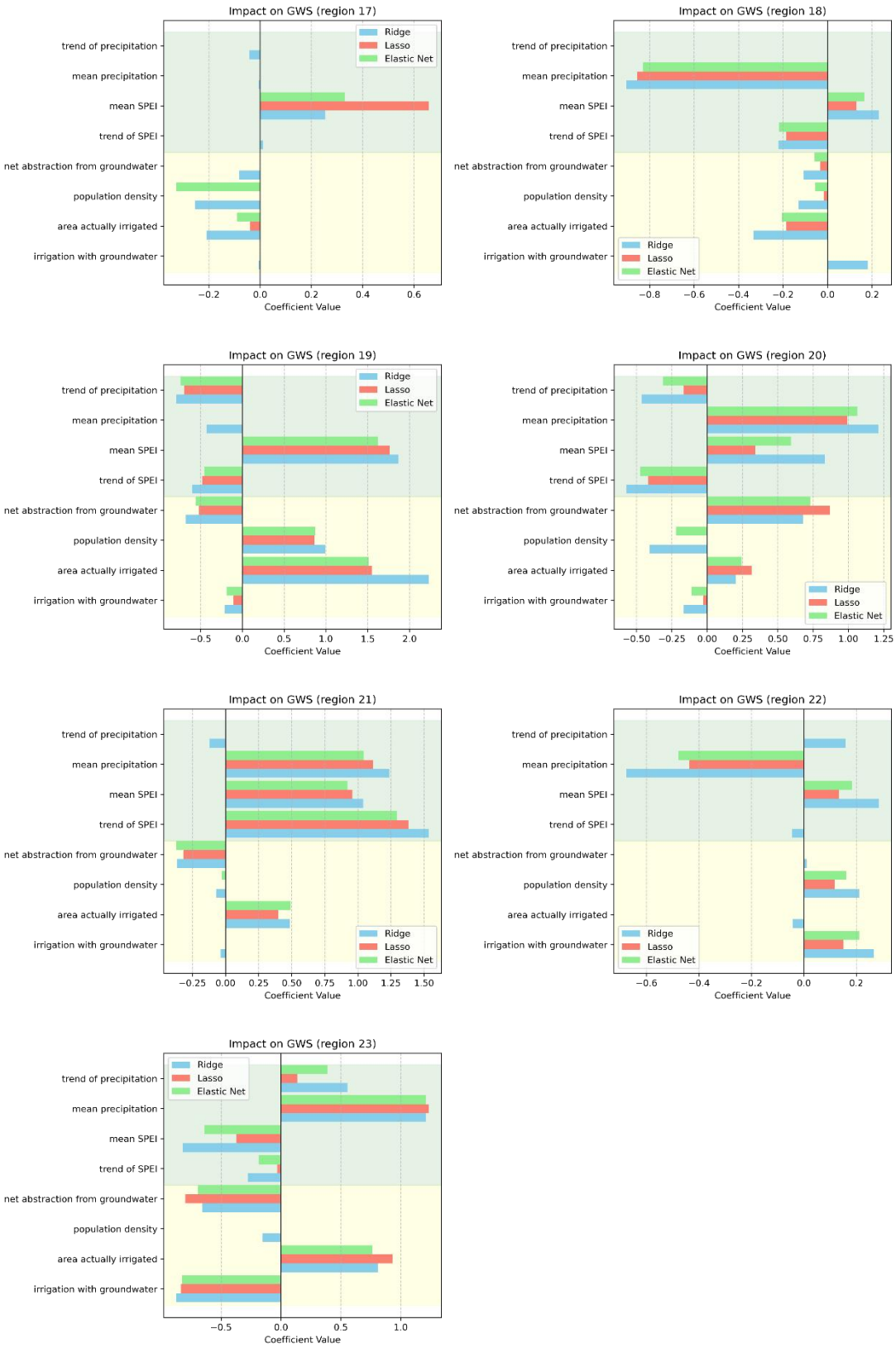

Fig. 2-13 The histogram illustrates the results of Ridge, Lasso, and Elastic Net regression analyses for groundwater storage (GWS) changes across 23 selected regions. In this chart, higher absolute values

indicate a stronger influence of each factor on GWS. Green shading in the histogram represents the impact of climatic factors on GWS, while yellow shading denotes the influence of human factors.

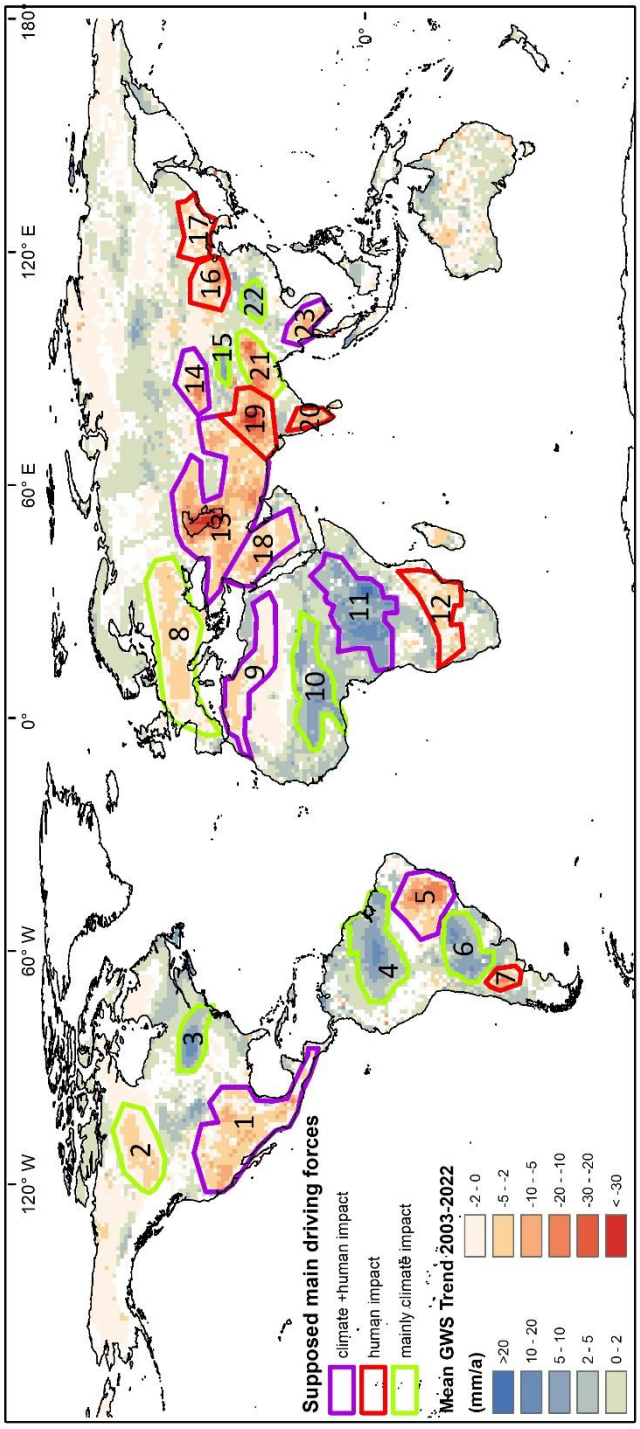

Fig. 2-14 The annotated map shows the 23 selected regions where significant changes in global groundwater storage occurred from 2003 to 2022, along with the supposed main driving forces behind these changes

North America

A historically severe drought that began in 2011-2014 (Griffin & Anchukaitis 2014) and has persisted to the present in Western America (region 1), centered in southern California and extends into Mexico. This drought period is characterized by a low mean Standardized Precipitation Evapotranspiration Index (SPEI) and a downward trend in SPEI values, indicating continuous aridification (Alam et al. 2021). This has resulted in a mean groundwater storage (GWS) decline at a rate of -3 mm/a and an increased groundwater demand, with net abstraction reaching a maximum of 177 mm/a. Approximately 50% of the surface area is agricultural, with 30% of this region irrigated using groundwater and 268 million people. Consequently, the decline in groundwater levels is due to a combination of drought and agricultural water demands that exceed renewable water resources.

From 2003 to 2022, overall precipitation has been slightly decreasing, leading to an average GWS decline of -1.9 mm/a in Central Canada (region 2). This loss of water aligns with a recent study concluding that Canada's subarctic lakes are vulnerable to drying when snow cover declines (Bouchard et al. 2013). Moreover, there is hardly any abstraction from groundwater connected to irrigation. Therefore, the changes are supposed to be climate-related.

The increasing precipitation trend in the Eastern United States (region 3) has led to a significant rise in groundwater storage (Rateb et al. 2020), with an average increase of 5.4 mm/a and a maximum increase of 16.4 mm/a. In this region, 38% of the land is used for irrigation, mostly relying on groundwater. However, the increase in groundwater levels due to the wetter climate persists despite the extensive use of groundwater for irrigation.

South America

Despite the decreasing trend in precipitation and significant deforestation in the Amazon (region 4) over the past few decades (Lin et al. 2016), the region still receives an average annual rainfall of 2362 mm, making it one of the most precipitation-rich areas globally. During these two decades, GWS in central and western Brazil and its neighboring areas increased at an average rate of 4.7 mm/a, with a maximum increase of 14.1 mm/a. This trend is attributed to changes of the Amazon water cycle, which has been significantly

altered by changes in climate, land cover (especially deforestation, as supported also by a negative trend in the LAI), sea surface temperature and precipitation patterns since the 1980's (Heerspink et al. 2020; Satizábal-Alarcón et al. 2024).

Eastern Brazil (region 5) has recently experienced a severe drought (Lima et al. 2022), characterized by a significant decrease in the SPEI values and reduced precipitation. This phenomenon is likely associated with a strong El Niño event (Santos et al. 2021). In fact, 2015 was the driest year in the past 37 years (Marengo et al. 2017). Consequently, GWS over the past 20 years has decreased by 5.2 mm/a, with a maximum decline of 17.9 mm/a. This region's challenges result from a combination of human impacts and severe drought. Agriculture occupies 88% of the area, with most of it dependent on rainfed agriculture. Groundwater storage has shown significant increases over the past two decades in southern Brazil and adjacent regions in Paraguay (region 6). On average, GWS has increased by 5 mm/a, with a maximum increase of 12.3 mm/a. Despite a decreasing trend in precipitation, the SPEI values indicate a gradual shift towards a drought climate.

Groundwater storage in Central Argentina (region 7) had previously been declining at a rate of -3.5 mm/a, with the maximum decline reaching -11.4 mm/a. Vegetation in central Argentina is sparse, with a mean Leaf Area Index (LAI) of only 0.33%. A multi-year drought that began in 2009 has persisted to the present (Müller et al. 2014). Regression results indicate that the primary driver of groundwater storage decline in this region is irrigation.

Europe

An analysis of the mean annual trends over the study period reveals a slight decrease in GWS in many European countries, with an average value of -1.9 mm/a for Central Europe (region 8). The maximum annual net abstraction from groundwater reached 244 mm/a, which supports 16% of agricultural activities and 443 million people. Concurrently, extreme drought events over the past 20 years (e.g., 2003, 2011-2013, 2015-2016) (Ionita et al. 2021; Van Lanen et al. 2016) have also influenced the distribution of groundwater reserves. That is depicted also in negative trend of the SPEI in parts of the region, e.g. northern Germany. The results clearly indicate medium-term groundwater stress in most European countries (Xanke & Liesch 2022).

Africa

During the study period, a severe drought occurred in Northern Africa (region 9) (Spinoni et al. 2019), closely aligning with areas experiencing groundwater depletion. The region exhibited a weak negative trend with an average decrease of -1.6 mm/a. Sparse abstraction regions are concentrated in densely populated areas, with the highest abstraction from groundwater at 140 mm/a, supporting 6% of irrigation from groundwater and 48 million people. Therefore, the primary cause of groundwater depletion is attributed to meteorological drought and abstraction from groundwater.

Groundwater storage in the tropical climate of Western Africa (region 10) has been increasing at an average rate of 4.9 mm/year. The maximum groundwater abstraction of 22 mm/a supports a population of 199 million people and a small amount of agricultural land. Additionally, the relatively abundant mean annual precipitation (1374 mm/year) and the construction of dams (Scanlon et al. 2022; Zarfl et al. 2015) may contribute to the accumulation of groundwater storage. In addition, land-use change has also been noted as an important driver of groundwater storage trends (Yira et al. 2016).

The groundwater level in Nile headwaters (region 11) has experienced the largest increase globally, with a maximum groundwater storage (GWS) rise of 28.2 mm/a and mean rise of 6.9 mm/a. Despite a large population of 270 million, the maximum abstraction amount is only 3.27 mm/a. This suggests that increased precipitation (positive Precipitation trend of 0.2 mm/a and wetter climate) is the primary driver of GWS variations. Additionally, the management of large lakes and dam construction (Ahmed et al. 2014) in the northern part of the region could also contribute to these changes (Kebede et al. 2017).

The negative trend along the southeastern coast of Africa (region 12) has resulted in an average groundwater storage decline of -2.1 mm/a. This event was associated with a pronounced north–south dipole pattern of positive or negative rainfall and water balance anomalies, typical of the El Niño–Southern Oscillation (ENSO) teleconnection to the region (Kolusu et al. 2019; Scanlon et al. 2022).

Asia

The demise of the Aral Sea and Caspian Sea (region 13) has been extensively documented in numerous studies (Qadir et al. 2009; Hu et al. 2022). Our estimates indicate a mean groundwater storage (GWS) depletion rate of -5.8 mm/year, with a maximum recorded rate of -40.4 mm/year. This area represents the second-largest groundwater depletion region globally, characterized by both its vast expanse and significant depth of the groundwater depression. The primary climate type in this region is arid, with desert precipitation. Concurrently, the area experiences a high abstraction rate, reaching up to 102 mm/a to support approximately 369 million people. Precipitation in this region is minimal and continues to decrease (as depicted by a negative P trend), contributing to worsening drought conditions. Approximately 22% of the land is equipped for irrigation, with 13% of the irrigation relying on groundwater. Therefore, the decline in groundwater levels is attributed to both climate impact and human activity.

During the study period, the groundwater storage in Northwestern China (region 14) decreased by 3 mm/a, with a maximum decrease of 14.7 mm/a. This decline may be related to ice melt from the Tien Shan mountains (Jacob et al. 2012). In this region, 20% of the area consists of arable land that primarily relies on rainfed agriculture. The annual average precipitation is low (195mm/a), and the trend in precipitation is also declining, with a low leaf area index (LAI). Over the past 20 years, the SPEI Index has shown a drought trend towards.

The majority of lakes in the Tibetan Plateau (region 15) have increased in water level and extent during the 2000s due to a combination of elevated precipitation rates and increased glacier-melt flows, which are difficult to disentangle (Zhang et al. 2013). Over the past 20 years, groundwater has been rising at a mean rate of 5.5 mm/a. There is no abstraction for agricultural irrigation in this region, thus the rise in GWS can be attributed to climate.

Numerous studies indicate a gradual GWS decline in the North China Plain (region 16) (e.g. Gong et al. 2018; Su et al. 2021). This region supports a large population of 209 million, with an average annual groundwater abstraction rate of 290 mm/a. The region surrounding Beijing heavily relies on extensive agriculture, which constitutes 44% of the area. A significant portion of the water used for agriculture (30%) comes from groundwater. The

observed trend of groundwater depletion is primarily driven by excessive groundwater exploitation, a human-induced phenomenon likely to persist until groundwater scarcity or regulatory measures curtail consumption rates.

61% of Northeast China (region 17) covered by agriculture, 36% of irrigation comes from groundwater. The net abstraction from groundwater reaches a maximum of 69 mm/a, primarily supporting 137 million people and intense irrigation. During the GRACE period under consideration, the estimated mean rate of groundwater storage change was -1.7mm/a, with a maximum of -5 mm/a. During this period, an increase in precipitation and a general wetting trend were observed. All available evidence suggests that the negative groundwater storage (GWS) trend is attributable to intensive agriculture and a high population density (Sun et al. 2022).

Decreasing water storage in the Arabian Peninsula (region 18) has been quantified using GRACE in previous studies (Joodaki et al. 2014; Voss et al. 2013). Over the past 20 years, most of the Arabian Peninsula has shown an increasing trend of aridity. The average groundwater storage (GWS) in this region is -2.9 mm/year, while precipitation, characteristic of a desert climate, averages 114 mm/year. Groundwater abstraction reaches a maximum of 169 mm/year, thus by far exceeding recharge rates and being not sustainable. This decline in groundwater storage is attributed to minimal rainfall and extensive groundwater extraction.

Over the past 20 years, Northern India (region 19) has experienced the most severe groundwater depletion globally (Asoka et al. 2017; Bhanja & Mukherjee 2019). Despite an upward trend in precipitation and wetting trend in SPEI values, the substantial groundwater depletion trend persists. The average groundwater storage (GWS) in this region has decreased by -9.9 mm/a, with a maximum decline of -54.8 mm/a. The contribution of Himalayan glacier mass loss to this regional trend is minor (Tiwari et al. 2009; Rodell et al. 2018). Agriculture occupies 60% of the area, with 37% of irrigation relying on groundwater. Annual net abstraction from groundwater has reached 252 mm/a, exceeding the recharge rate, to support 566 million people and irrigation.

The groundwater storage in India exhibit distinct regional trends: a significant decline in the north, a rise in the central part, and a decreasing trend in Southern India (region 20). In the

study by Asoka et al. (2017), southern India showed an increasing trend from 2002 to 2013. However, over the 20-year period from 2003 to 2022, groundwater storage (GWS) has exhibited a sharp decline, with an average decrease of -4.8 mm/a and a maximum decrease of -11.7 mm/a. In this region, groundwater abstraction reaches a maximum of 174 mm/a, with 58% of the area relying on groundwater for irrigation, supporting 194 million population. The primary factors contributing to the groundwater decline include intensive agriculture (Salmon et al. 2015), significant groundwater extraction, and high population density, all of which result in excessive groundwater withdrawal.

Approximately half of the South Asia (region 21) is devoted to irrigation. The region's highest net abstraction from groundwater is 238 mm/a, supporting irrigation agriculture and exceeding 478 million population and persistent groundwater withdrawal has led to a downward trend in groundwater levels. Despite the area's relatively abundant annual rainfall of approximately 1200 mm and its generally humid climate, the groundwater decline persists. The primary driver of this trend is the excessive water extraction driven by intensive agricultural activities and population density. The fact that extractions already exceed recharge during years of normal precipitation indicates a concerning outlook for groundwater availability during future drought (Aadhar & Mishra 2017).

Despite the dominance of rainfed agriculture (71%) in Eastern Central China (region 22), groundwater storage has, on average, increased by 3.6 mm/a, with a maximum annual increase of 5.4 mm. This region also exhibits the largest positive trend in global precipitation, and the gradually increasing Standardized Precipitation Evapotranspiration Index (SPEI) may contribute to increased groundwater storage. Additionally, it is noteworthy that the construction and filling of the Three Gorges Dam (Yang & Lu 2014) have significantly contributed to the increase in groundwater storage (Chao et al. 2020; Yin et al. 2021).

In Mainland Southeast Asia (region 23), 50% of the area is dedicated to agriculture, yet the water source for irrigation is rarely from groundwater. Overall, the region experiences abundant rainfall, averaging 1847 mm/a, with a rising precipitation trend at the rate of 2.12 mm/a over the past 20 years. Despite this, the mean groundwater storage (GWS) has the mean negative trend of -3.3 mm/a, with a maximum decline of -9.7 mm/a. This decline may

be associated with climatic factors, such as the El Niño-Southern Oscillation (ENSO) (Sulaiman et al. 2023; Le et al. 2021) and intensity irrigation.

2.4 Conclusion

Groundwater is a critical component of land surface processes, playing a vital role in water and energy cycles. Moreover, it is an important source of drinking water supply and for agricultural irrigation. Thus, groundwater resources worldwide are impacted by climate change and human activities. This study utilized GRACE and ERA5-Land data to investigate groundwater storage variability from 2003 to 2022 at a 1° spatial resolution. GRACE data has revealed significant changes in global groundwater resources, allowing quantification at regional scales despite the limitations of sparse measurements and restrictive data-access policies.

Over the past two decades, groundwater storage has exhibited spatial heterogeneity, with most depletion occurring within the Earth's mid-latitudes. With a 95% confidence level, approximately 81 % of global regions, excluding ice melt regions, have shown significant alterations in groundwater storage. Among these regions, 48 % have observed a decline in groundwater levels, while 52 % have recorded an increase. Approximately 3.4 billion people live in areas where groundwater has significantly declined over the past 20 years. Hotspots of groundwater storage (GWS) depletion, with significant declining trends (>20 mm/year), have been identified in northern India, eastern Brazil, and areas surrounding the Caspian Sea. These changes indicate a future where already limited groundwater resources will become increasingly valuable.

Spatial analysis revealed that the most significant groundwater declines occurred in arid and semi-arid regions, particularly where the aridity index (AI) ranges from 0.1 to 0.5, peaking at 0.1 to 0.2. These regions, characterized by sparse vegetation and fragile ecosystems, are experiencing declining groundwater storage. In contrast, groundwater storage is increasing in humid regions (AI≥ 0.8). This disparity may lead to a more uneven distribution of groundwater.

Contrary to common belief, although there is a correlation between precipitation and groundwater storage (Thomas & Famiglietti 2019; Russo & Lall 2017), changes in precipitation do often not directly affect groundwater storage. Compared to precipitation, changes in the Standardized Precipitation-Evapotranspiration Index (SPEI) have a more significant spatial impact on groundwater storage, i.e. evapotranspiration and thus temperature play a vital role. While climate variability contributes to changes in water storage, human activities, particularly irrigation and excessive groundwater abstraction, are the major drivers of groundwater storage decline (Russo & Lall 2017). Among human activities, agricultural activities have a more significant impact on groundwater storage than population density. This may be due to the high demand for groundwater abstraction for agricultural irrigation, which is likely distributed in less populated areas (Chen et al. 2016). In contrast, groundwater use related to high population density, such as for drinking water, requires less groundwater. There are two main causes of groundwater rise: wetter climate conditions and dam construction. Reservoirs created by dam construction have led to significant groundwater rise in many regions, such as the Nile headwaters (Kebede et al. 2017), and Eastern Central China (Chao et al. 2020).

GRACE data transcends national borders and data confidentiality policies, enabling the study of terrestrial water storage (TWS) and groundwater storage (GWS) at global scale. Long-term monitoring with GRACE is essential for understanding large-scale groundwater storage trends. For instance, southern India showed an increasing trend in groundwater storage from 2002 to 2013 (Asoka et al. 2017), but it has since declined due to intensive agriculture and unreasonable abstraction from groundwater. Thus, continuous dynamic monitoring is crucial for developing effective groundwater management policies. Awareness of groundwater storage trends (Fig. 2-1) is the first step toward addressing the challenges through improved groundwater use efficiency and water management policies. Governments and planners in regions experiencing groundwater depletion can develop sustainable groundwater discharge and water conservation plans based on this information, promoting the sustainable use of freshwater resources.

Chapter 3
3 Karst and land use change

Reproduced from: Zhang, J., Liesch, T., Chen, Z., & Goldscheider, N. (2023). Global analysis of land-use changes in karst areas and the implications for water resources. Hydrogeology Journal, 31(5), 1197-1208.

Abstract

Karst areas contain valuable groundwater resources and high biodiversity, but are particularly vulnerable to climate change and human impacts. Land-use change is the cause and consequence of global environmental change. The releases of the Climate Change Initiative-Land Cover (CCI-LC) and World Karst Aquifer Map (WOKAM) datasets have made it possible to explore global land-use changes in karst areas. This paper firstly analyses the global karst land use distribution in 2020, as well as the land use transition characteristics between 1992 and 2020. Then, two indicators, proportion of land-use change and dominant type of land-use change, are proposed to identify the spatial characteristics of land-use change in global karst areas. Finally, three examples of land-use change in karst areas are analyzed in detail. Land-use types and proportions of the global karst areas from large to small are as follows: forest (31.78%), bare area (27.58%), cropland (19.02%), grassland (10.87%), shrubland (7.21%), wetland (1.67%), ice and snow (1.16%) and urban (0.71%). The total area of global karst land-use change is 1.30 million km², about 4.85% of global karst surface. The land-use change trend of global karst is dominated by afforestation, supplemented by scattered urbanization and agricultural reclamation. The tropical climate has a higher intensity of land-use change. Regions of agricultural reclamation are highly consistent with the population density. These results reflect the impact of human activities and climate change on land-use changes in global karst areas, and serve as a basis for further research and planning of land resource management.

3.1 Introduction

Land-use change is an important component (Foley et al. 2005; Turner et al. 2013) and one of the key drivers (Ward et al. 2000) of global environmental change, and it is the result of a combination of driving factors under the human-land relationship (Liu et al. 2003; Meyfroidt et al. 2013). At the same time, land use also has a close relationship to population migration and economic conditions (DeFries, 2013). Thus, the assessment of land-use changes is important for the effective planning and management of resources. In recent decades, large scale anthropogenic land-use changes have led to profound changes in the water cycle and has significantly affected the water resources and ecosystem, which in turn has caused changes in groundwater quality and quantity (Grimm et al. 2008; Winkler et al. 2021).

Karst aquifers make important contributions to the water supply of many regions, cities and countries; about 678 million people or 9.2% of the world's population rely on freshwater from karst aquifers (Stevanovic 2019). While karst aquifers are essential for water supply, karst areas provide a variety of habitats for many species, including numerous rare and endemic plant and animal species (Goldscheider 2019). At the same time, the karst groundwater system is closely related to the external surface where there can be rapid transformation, so karst aquifers are particularly vulnerable to land-use change and difficult to manage (Nguyet & Goldscheider 2006; Parise et al. 2015; Panagopoulos & Giannika 2022). With the development of the economy and the expansion of population, human behavior, such as the expansion of cropland, will gradually increase the stress on karst aquifers in terms of groundwater quality and quantity (Hartmann et al. 2014), for example, the pressure on groundwater quantity caused by the intensification of agriculture and the pressure on groundwater quality caused by the application of pesticides and fertilizers (Foley et al. 2011). At the same time, urbanization is a strong trend of economic development. This trend will inevitably lead to the expansion of urban land use and the growth of urban population. In the process of urbanization, these changes in land use and landscape patterns are the most obvious changes in the karst surface area (Lambin et al. 2001).

Numerous institutions have released global land-use data products that are inconsistent in scale and classification (Grekousis et al. 2015), e.g., the International Geosphere-Biosphere

Programme's Data and Information System land-use cover (IGBP DISCover; Loveland et al. 2000), Global Land Cover 2000 (GLC2000; Bartholome & Belward 2005), Moderate Resolution Imaging Spectroradiometer LAND-COVER (LC) dataset (MCD12; Friedl et al. 2010), GLOBCOVER and Global Map-Global LC dataset (GLCNMO; Tateishi et al. 2011), GlobalLand 30 (Chen et al. 2015). These global land-use products by different institutions are limited by inconsistencies in resolution, time scale and classification systems, making it challenging to compare and combine the data. Difficulties in accurately assessing the impacts of land-use changes and making decisions about land and resource management can result from a lack of clear understanding of trends and patterns (Fuchs et al. 2013; Winkler et al. 2021). To resolve these issues, it is crucial for institutions to adopt a standardized approach to land-use data collection and analysis, using consistent scales and classification systems.

The World Karst Aquifer Map (WOKAM) was completed in 2017, providing a comprehensive description of the global distribution of karst features (Chen et al. 2017b). This release of data offers valuable insights into the distribution of karst aquifers across the world. Moreover, since most of the global karst areas are discontinuous regions (Chen et al. 2017a), land use analysis in karst regions requires a high resolution relative to global class datasets. The European Space Agency (ESA) released the Climate Change Initiative – Land Cover dataset (CCI-LC; Bontemps et al. 2013) of global land use with a resolution of 300 m and multi-year time series. The CCI-LC dataset allow one to derive absolute areas and areal changes between land uses (Li et al. 2018, Liu et al. 2018).

Most previous studies on karst water resources have only considered land-use change at the catchment scale (Sonter et al. 2014; Misra & Balaji, 2015; Chen et al. 2021). It is essential to quantify and understand the spatiotemporal dynamics of global karst land-use change. Such assessment could provide more comprehensive data for global karst change analysis, and contribute to the awareness of ecological or environmental change by quantifying global karst land-use change characteristics, allowing for a better understanding of global karst land-use change.

This study aims to quantify the spatiotemporal dynamics of land use change in karst regions at a global scale based on various global geographical information systems (GIS) datasets. It represents the first attempt to combine CCI-LC data and WOKAM data from 1992 to 2020 to identify and quantify the distribution patterns and land-use changes in global karst regions (Goldscheider et al. 2020). The research content of this article is as follows:

(1) Summary of the general situation of land use distribution in global karst areas.

(2) For each land use type, analysis of the area changes between 1992 and 2020 and quantification of the global land-use transition.

(3) Identification of the spatiotemporal dynamics of global karst land-use change.

3.2 Materials and methods

This project was undertaken using ArcGIS Desktop by ESRI (version 10.8), the coordinate system is Robinson projection, longitude of central meridian 11°E, spheroid WGS84. The legends, values and areas mentioned in this paper refer to land use on global karst.

3.2.1 Data source and reclassification system

The European Space Agency released the year-by-year global land use dataset from 1992 to 2015 (Bontemps et al. 2013; Defourny et al. 2017). Since 2016, the Copernicus Climate Change Service (C3S) has released land cover data for 2016-2020, which are consistent with the global map series produced from 1992-2015 (Defourny et al. 2021). This dataset is the longest global land-use dataset in time series and is ideal for exploring large-scale land-use changes. The accuracy of this database is 74.1% (Defourny et al. 2017).

The CCI-LC legend contains 36 land cover classes. These categories are defined using the Land Cover Classification System (LCCS) developed by FAO (Di Gregorio, 2005). This work reclassified the CCI-LC types to general types for clarity in analysis, referring to a general classification system (Gong et al. 2013). The original 36 classification and reclassification criteria are shown in Table 3-1.

Table 3-1 Correspondence between new land categories used for the change detection and the LCCS legend used in the CCI-LC classes.

Reclassification		**LCCS legend and its code number used in ESA-CCI LC maps**	
Cropland	Rainfed cropland	10, 11, 12	Rainfed cropland
	Irrigated cropland	20	Irrigated cropland
	Mixed cropland	30	Mosaic cropland (>50%) / natural vegetation (tree, shrub, herbaceous cover) (<50%)
		40	Mosaic natural vegetation (tree, shrub, herbaceous cover) (>50%) / cropland (< 50%)
Forest	Broadleaved forest	50	Tree cover, broadleaved, evergreen, closed to open (>15%)
		60, 61, 62	Tree cover, broadleaved, deciduous, closed to open (> 15%)
	Needle-leaved forest	70, 71, 72	Tree cover, needle-leaved, evergreen, closed to open (> 15%)
		80, 81, 82	Tree cover, needle-leaved, deciduous, closed to open (> 15%)
	Mixed forest	90	Tree cover, mixed leaf type (broadleaved and needle-leaved)
		100	Mosaic tree and shrub (>50%) / herbaceous cover (< 50%)
Grassland	Grassland	110	Mosaic herbaceous cover (>50%) / tree and shrub (<50%)
		130	Grassland
Wetland	Wetland	160	Tree cover, flooded, fresh or brackish water
		170	Tree cover, flooded, saline water
		180	Shrub or herbaceous cover, flooded, fresh-saline or brackish water
Urban	Urban	190	Urban areas
Shrubland	Shrubland	120, 121, 122	Shrubland
Bare area	Bare area (partly with sparse vegetation)	140	Lichens and mosses
		150,152,153,	Sparse vegetation (tree, shrub, herbaceous cover) (<15%)

		200,201,202	Bare areas
Water	Water	210	Water bodies
Ice	Ice and snow	220	Permanent snow and ice (stable)

3.2.2 Spatial change characterization

Land use transition analysis can describe the quantitative information of land-use changes, but this analysis cannot analyze the spatial information of land-use changes. Given the fine resolution of CCI-LC, the land use analysis at the world level will become too fragmented to capture variation characteristics. This work aggregates the original 300-m resolution into 10 km × 10 km cells (Li et al. 2018; Nowosad et al. 2019). This scale provides high resolution, enough to include meaningful feature analysis within each cell.

Each 10 km × 10 km grid contains multiple small grids of 300 m × 300 m. Here, the 'Statistics' function of ArcGIS software is used to calculate the changed area and the most dominant type of land use change in each 10 km × 10 km grid. This paper proposes the ratio of the area of land-use change to the grid area of 10 km x 10 km, that is, the intensity of land-use change of each cell (Aldwaik & Pontius 2012). The calculation method is as follows:

$$\text{Proportion of land use change} = \frac{\text{Land use change area}}{\text{One cell size}} \times 100\% \quad (1)$$

Land-use change over time is measured by the difference in land use between the initial and final time (Nowosad et al. 2019). This work aims to explore the land-use change over the longest available period of time in the ESA dataset, that is, the 1992 and 2020 maps as the first- and last-time steps. The map was eventually classified into 5 levels, with percent change indicating the intensity of land-use change. A percentage above 30% is classified as a "high change", a percentage between 15% and 30% is classified as a "moderate high change", and a percentage between 5% and 15% is classified as a "moderate change".

3.3 Results and discussion

3.3.1 Global karst land-use distribution map in 2020

The CCI-LC map in 2020 (reclassified according to Table 3-1) is combined with the WOKAM global karst area distribution map, as shown in Fig. 3-1.

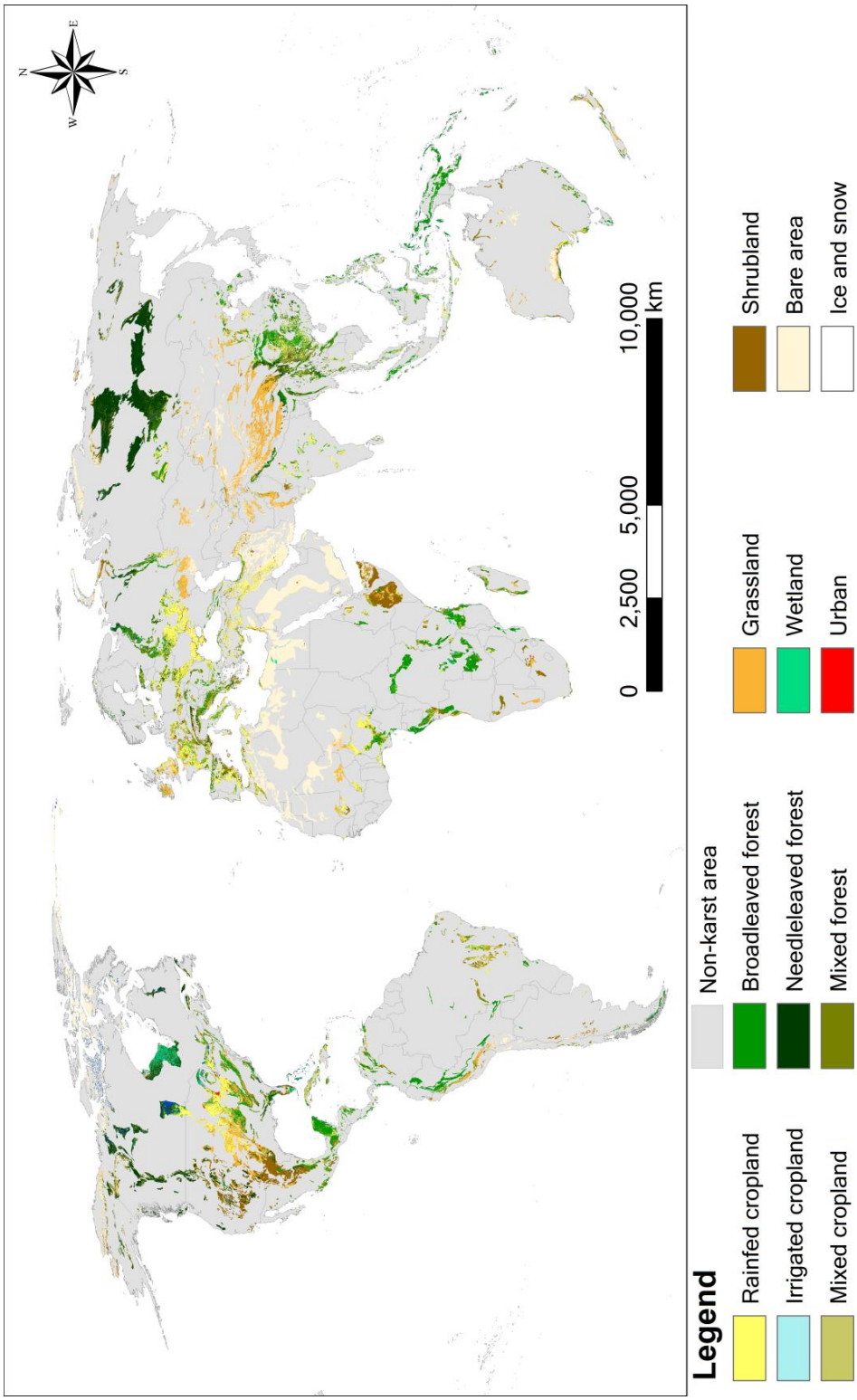

Fig. 3-1 Spatial patterns of global karst area land use in 2020, at 300 m spatial resolution. Data source: Global karst distribution data from WOKAM (Chen et al. 2017a), Land use data from CCI-LC 2020 version (Defourny et al. 2021).

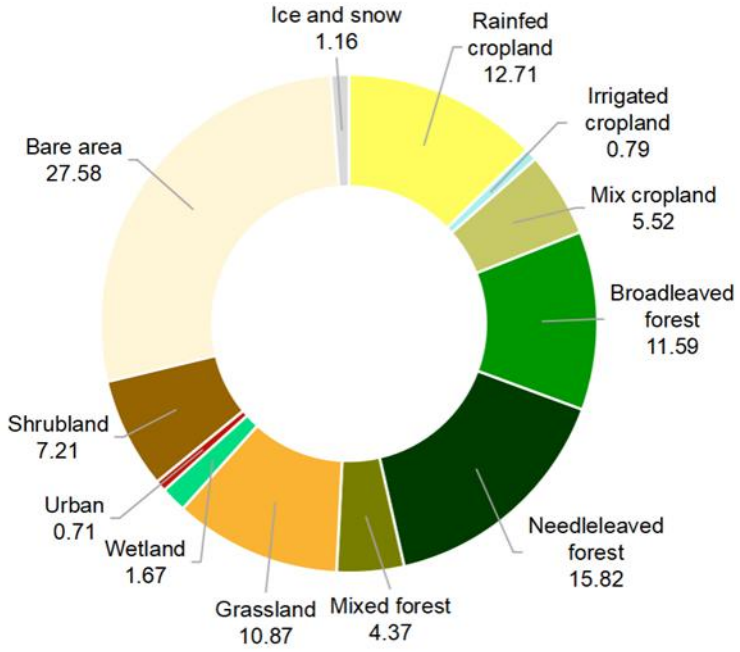

Fig. 3-2 Pie chart of 2020 global karst area land use (unit: %)

Fig. 3-1 and Fig. 3-2 show the global karst land-use distribution map and proportion of each land-use type in 2020, respectively. About 8.54 million km^2 (31.78 %) of the karst area is forest, which is also the land use type with the largest proportion of global karst areas. Broadleaved forest is about 3.12 million km^2, accounting for 11.59%. Most are located in tropical climate zones, which are mainly determined by climatic conditions (high temperature and precipitation). These regions occur in Southeast Asia, Latin America and Central Africa. The area of needle-leaved forest is 4.25 million km^2 (15.82%), mainly distributed in the cold climate regions distributed in northern Russia and Canada, where the population density is very low (less than 20 person/km^2). About 7.41 million km^2 (27.58%) of the global karst area are bare land, and the most widespread bare land is distributed in the Arabian Peninsula and North Africa. Most of these areas have arid climate, where there are high temperatures combined with less rain. About 1.94 million km^2 (7.21%) are shrubland, which are distributed with bare land in the arid climate zone. Shrubs were suitable for

revegetation in harsh karst areas because of high tolerance to severe drought compared to trees (Liu et al. 2011). Around 5.11 million km^2 (19.02%) of karst land is covered with cropland. Cropland is mainly distributed in the temperate climate areas, which is relatively warm with high precipitation amounts and seasonality. Rainfed cropland is mainly distributed in Europe, the eastern United States and other regions, with an area of about 3.42 million km^2 (12.71%). Irrigated cropland is about 0.21 million km^2 (0.79%). Although the area of irrigated cropland is relatively small, it represents managed landscapes with the highest agricultural inputs (Václavík et al. 2013). Concentrated irrigated agricultural areas are in regions such as China, Egypt and India. Grassland (10.87%) has less precipitation and is distributed in the central United States and Central Asia. The urban area is about 0.19 million km^2, accounting for about 0.71%. Urban areas are scattered throughout the world, with a high density of population.

3.3.2 Global change patterns

Land use area change

The results of analysis of the area change of each land use type over the 29-year period, from 1992 to 2020, are shown in Fig. 3-3 (numbers are in 10^3 km^2). Before 2000, the total amount of cropland increased, and then decreased year by year until 2017, followed by a minor increase from 2017 until 2018 and a stable period until 2020. Cropland referred to in the figure is the sum of rainfed cropland, irrigated cropland and mixed cropland. Globally, cropland area has been maintained at 5.11 million km^2, and 2/3 of the area is rainfed cropland. About half of the forests are needle-leaved forests, and after 2017 the area of needle-leaved forests has decreased sharply, accompanied by mixed forests that have been increasing over time. Such a sharp decline may be due to the classification of remote sensing data; some areas were classified as needle-leaved before 2017, and then classified as mixed forest. But overall, forest is on the rise. The bare area shows a shrinking trend of 0.09 million km^2, about the size of Portugal. In contrast, the urban area increases gradually during the 28 years from 1992 to 2020, with an increase of 0.10 million km^2, which is about the size of the country of Iceland.

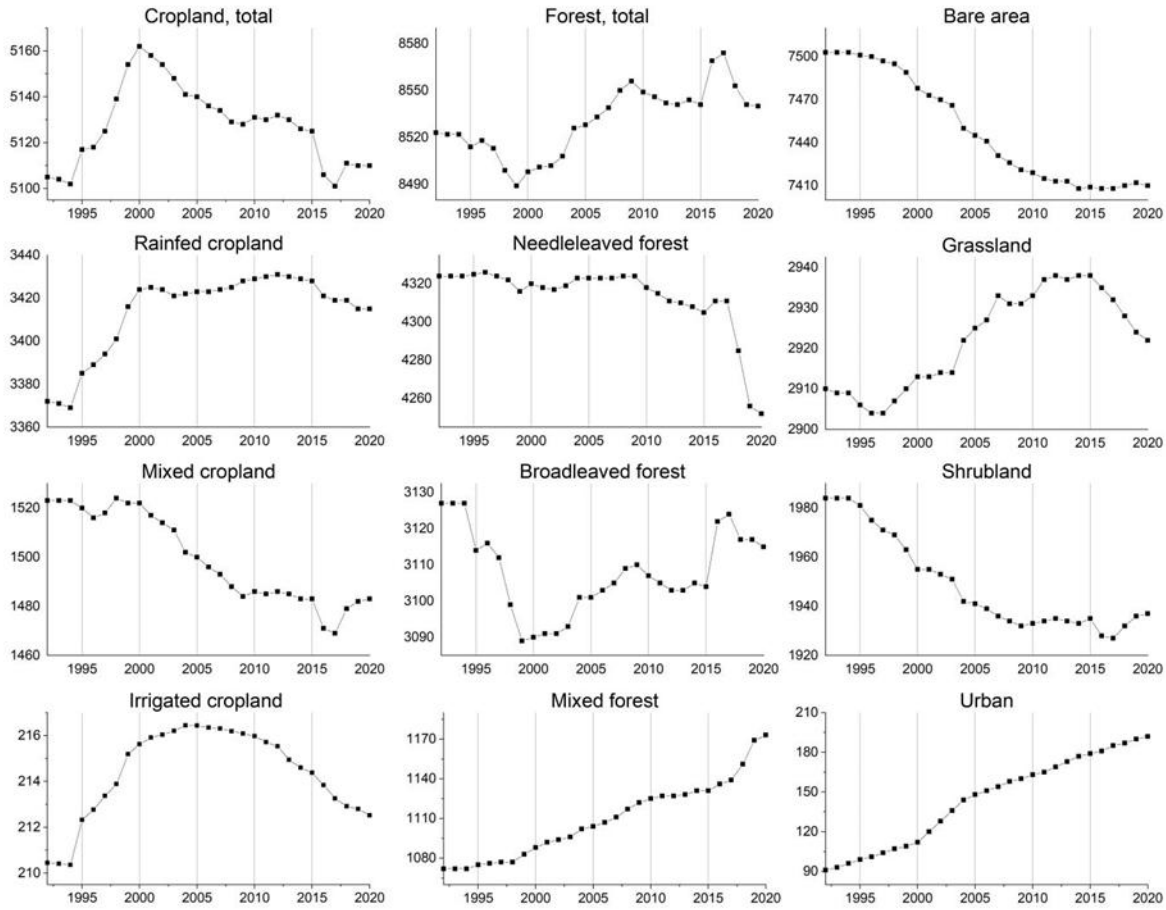

Fig. 3-3 Land-use area change in global karst regions from 1992 to 2020 (unit: 1,000 km^2)

Land use transition

Fig. 3-4 illustrates land-use transition processes quantitatively between different types of global karst areas from 1992 to 2020. Net change shows the difference in area of land use between 1992 and 2020, shown in Table 3-2. Except for the category of snow and ice, all other land use types experienced varying degrees of change in global karst area. Permanent snow and ice remained constant over the 29-year period (0.31 million km^2), mainly distributed in northern Canada and the Tibetan Plateau. This conclusion is different from that of Li et.al (2019), and this may be due to different databases or data accuracy.

The total global karst area that experience land-use changes from 1992 to 2020 is 1.30 million km², which means that almost 4.85% of the global karst surface has changed. Overall, the most frequent land-use changes occurred between cropland and forest; the largest

land-use change types were 'cropland to forest' and 'forest to cropland' with 0.20 million km^2 and 0.18 million km^2 respectively, accounting for 29.39% of all land-use changes on karst.

The total area of forest expansion is 17,400 km^2, with forest gains mainly coming from the annual growth of mixed forest (an increase of 0.10 million km^2). For broadleaved forest, the main gross loss was to mixed cropland and rainfed cropland amounting to 0.08 million and 0.04 million km^2, respectively. For needle-leaved forest, the main loss was to shrubland (0.05 million km^2), mixed forest (0.04 million km^2) and mixed cropland (0.02 million km^2).

Urbanization has received considerable attention due to economic development and dense population (Kalnay & Cai 2003). Globally, the area of change in urban areas is relatively small compared to other land-use changes. Urban area has been increased by 0.10 million km^2, accounting for 7.73% of the gross total global land-use change. The net increase in urban area mainly comes from conversion of cropland and grassland, amounting to 0.07 million km^2 and 0.01 million km^2, respectively. Cropland loss was mainly to forest and urban area. In addition to turning cropland to forest, urban encroachment on cropland is also a key cause of cropland loss (Winfield 1973). This indicates that the urban expansion caused by anthropogenic land usage from 1992 to 2020 was significant in the global karst regions.

Grassland also had an obvious transition to bare land; the loss of bare land cover was mainly to grassland (0.10 million km^2), rainfed cropland (0.03 million km^2) and needle-leaved forest (0.02 million km^2). The gain of bare area was mainly coming from grassland (0.06 million km^2) and needle-leaved forest (0.02 million km^2). Despite a gross bare area gain of 0.09 million km^2, the larger gross loss (1.85 million km^2) results in a net loss of 0.09 million km^2. This shows that grassland restoration is discernible in the karst area.

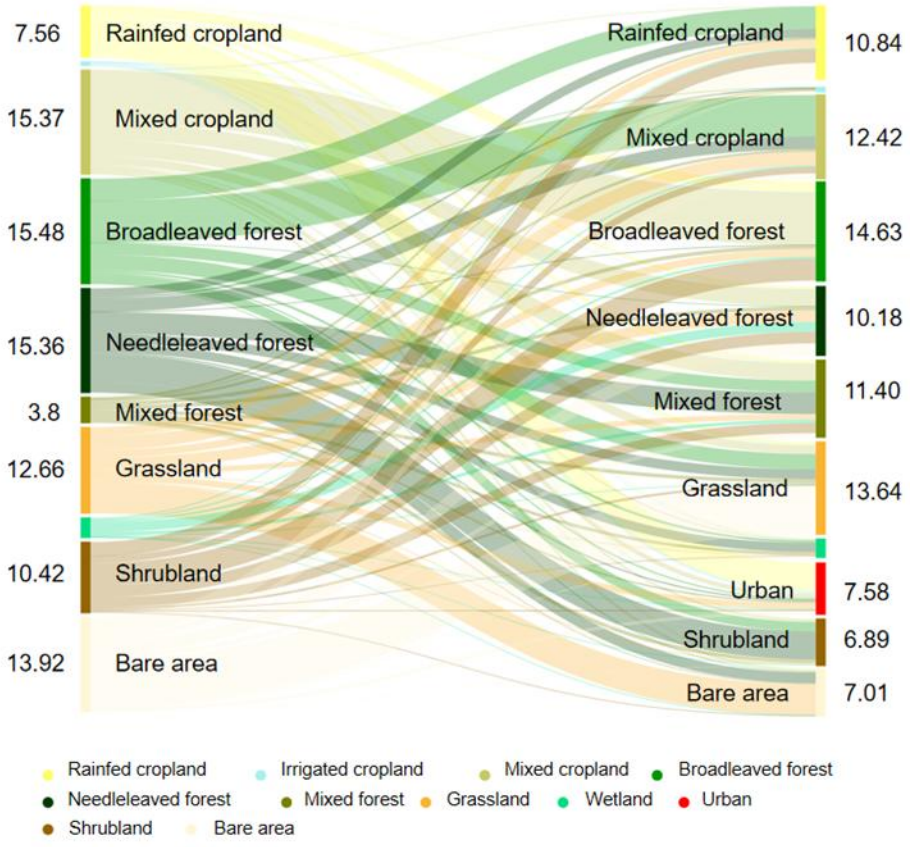

Fig. 3-4 Transition of global karst land-use-change area from 1992 to 2020 (unit: %)

Table 3-2 Net change of different land-use types (unit: $10^3 km^2$)

Land use type	Net change
Rainfed cropland	43.41
Irrigated cropland	2.07
Mixed cropland	-40.37
Broadleaved forest	-11.87
Needle-leaved forest	-72.08
Mixed forest	101.35
Grassland	12.46
Wetland	-2.78
Urban	101.31
Shrubland	-47.11
Bare area	-92.94

3.3.3 Spatial land-use change identification

Intensity of land-use change

In order to identify the spatial distribution of land-use change characteristics, the proportion of land-use change within each grid cell is calculated here according to Eq (1). The spatial pattern of the proportion of land-use change in the global karst area is shown in Fig. 3-5. 38.49% of the grid is 'no change', mainly distributed in northern North America, northern Africa and the Arabian Peninsula. The areas with more than 15% land-use change are mainly distributed in regions such as eastern North America, Central Europe and Southeast Asia, accounting for 9.92% of all karst areas. Areas with more than 30% land-use changes are distributed in Central America, Central Africa and South Asia, accounting for 2.70% of the total karst proportion. The tropical climate has a higher proportion of land-use change, and most of the regions with land-use change proportion of more than 30% are within this climate region.

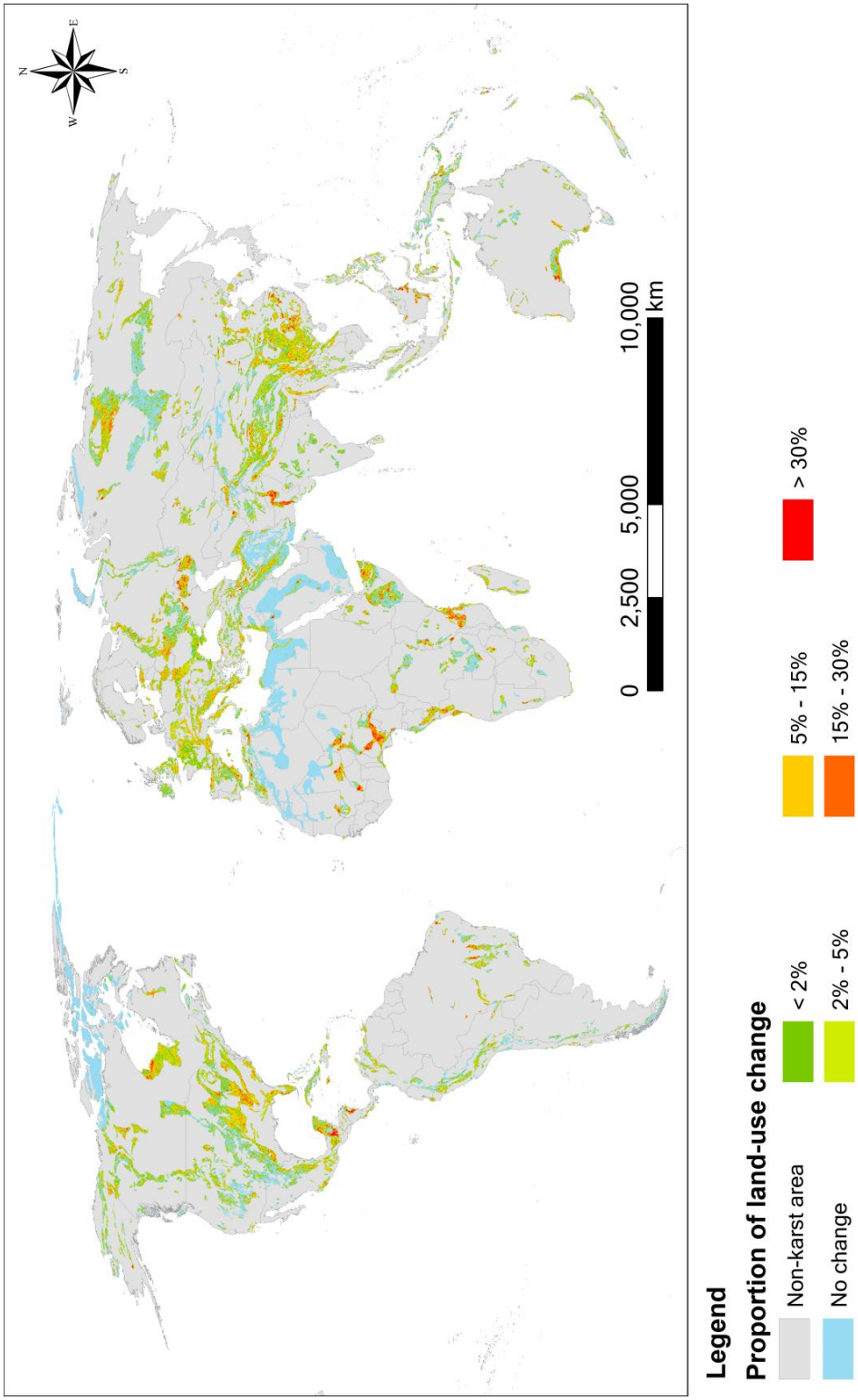

Fig. 3-5 Proportion of land-use change area in the 10 km × 10 km cells

Spatial distribution of the dominant type of land-use change

A variety of land-use change types occur in the global karst region from 1992 to 2020 within one cell Fig. 3-6 shows the distribution of the dominant type of land-use change. Land-use change usually has a high degree of spatial heterogeneity, which indicates that land-use change is related to local climatic factors and land use planning, etc. (Liu et al. 2018).

Contrary to the prevailing view of global forest area decline, afforestation is the most common type of land-use change in global karst areas (Song et al. 2018), mainly distributed in North America, the east and west coasts of Africa, and southwest China. These shifts are related to changes in factors such as the 'Returning Farmland to Forest' program supported by local governments (Liu et al. 2015) or economically beneficial tree planting (Laikre et al. 2010; Hansen et al. 2013). Afforestation will improve the vegetation cover and decreased the loss of water and soil due to agricultural practices. This situation implies a greening trend due to a more suitable environment or increased precipitation in some areas (Song et al. 2018; Zhu et al. 2016).

Over the past few decades, agricultural reclamation areas have existed due to the expansion of cropland areas driven by growing populations (Tilman et al. 2011). Regions that contain significant cropland expansion are Southeast Asia, Central Asia, and Central North America, as well as sporadic locations such as Latin America and Africa. Agricultural reclamation regions are highly consistent with the population density in karst regions (Goldscheider et al. 2020). In northern Africa, bare area and shrubland encompassing several regions have been transformed into cropland expansion. In comparison, the southern region of Africa is mostly characterized by a conversion of forest into cropland.

The urbanization process leads to a range of environment-related issues (Lambin et al. 2001; Brown & Vivas 2005), including soil erosion, desertification, and water scarcity, etc. (Wang & Fang, 2011). Urban expansion has occurred mainly in Central and Eastern Europe, the eastern regions of the USA, and sporadically in eastern China and the Arabian Peninsula. The most important land-use change involved in urban expansion is from rainfed cropland around the city.

Intense human activities have resulted in the karst rocky desertification landscape with extensive exposed bedrock, severe soil loss, shallow soil layers, and discontinuous soil coverage (Chen et al. 2021). The main desertification areas of global karst areas are in Tibetan Plateau, eastern North America and Central Russia. Among them, the karst areas in North America are dominated by the transformation from forest into shrubland, while in Tibet and Russia, grassland is mainly degraded into bare area.

Detailed analyses of land-use change in three sample areas

The karst regions of south-central Europe, eastern North America and southwest China are the three major karst concentrations in the world (Yuan, 1999). In this study, locations with a large proportion of land-use change in the global karst concentration area are selected as samples: in the eastern United States (A), southeastern Spain (B) and central south China (C). A location map of the selected sample areas, and the corresponding proportions of land-use change and the dominant type of land-use change maps, are shown in Fig. 3-7.

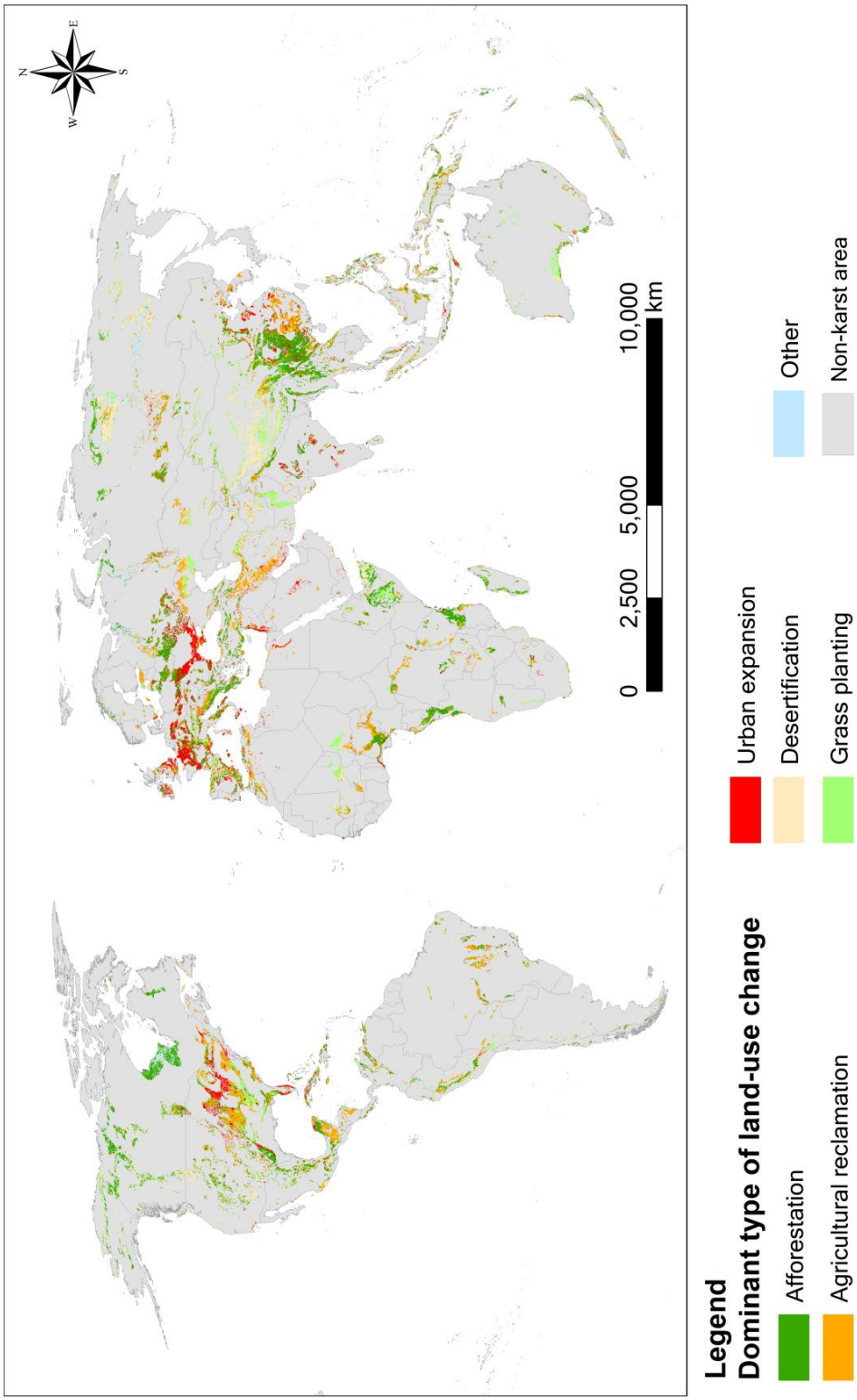

Fig. 3-6 The dominant type of land-use change in the 10 km × 10 km cell

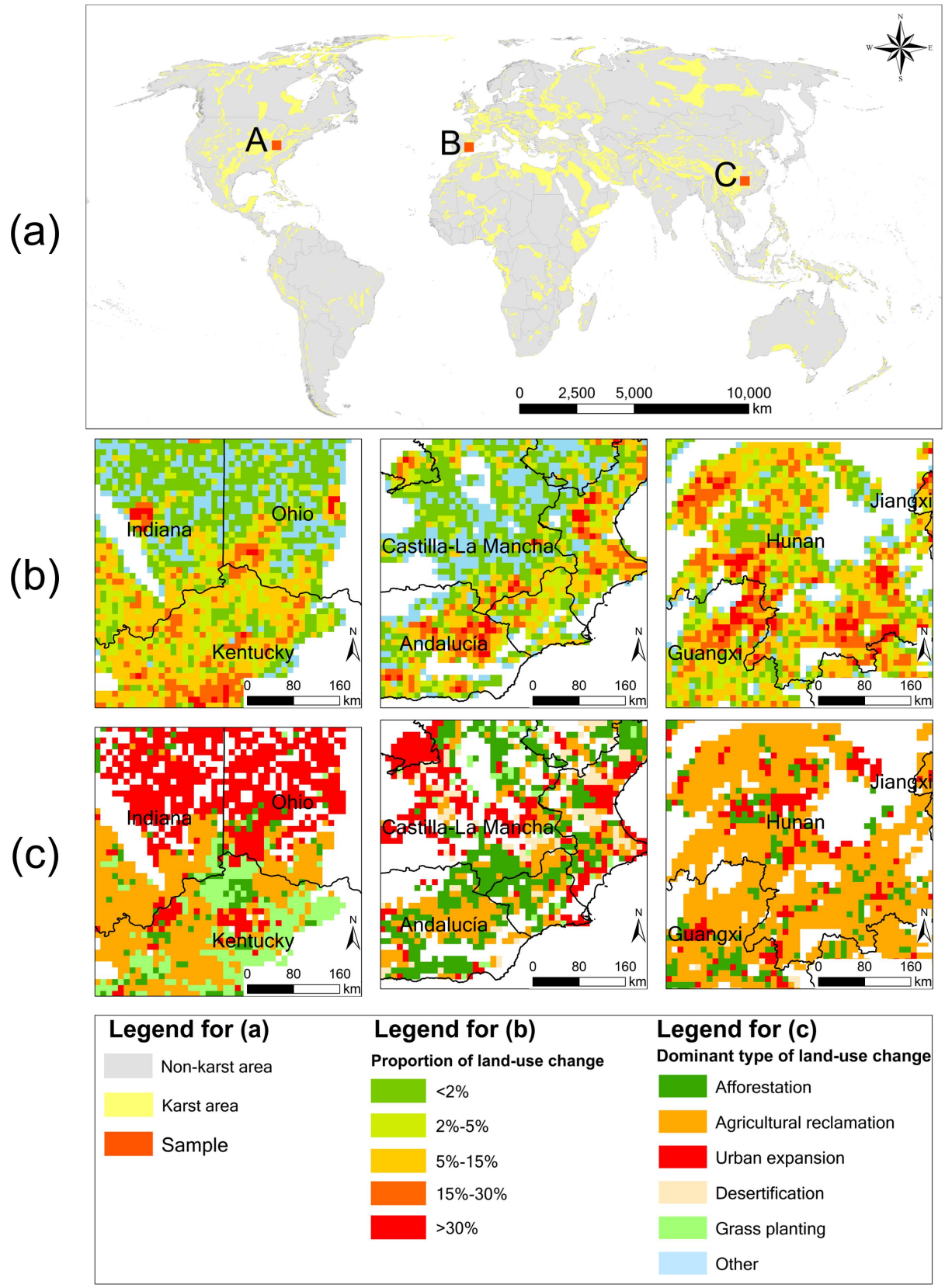

Fig. 3-7 Land-use changes between 1992 and 2020 for three karst areas: eastern United States (*A*), southeastern Spain (*B*), and central south China (*C*), showing (**a**) Global karst distribution map and sample sites, (**b**) Proportion of land-use change, and (**c)** Dominant type of land-use change.

Sample area A is in the Eastern United States. The USA is the second largest karst water consumer, where approximately 50 million people (Stevanovic 2019) are supplied with drinking water from karst. Sample area A is located in the eastern United States, on the borders of Kentucky, Indiana and Ohio, most of which rely on karst groundwater. The map shows an area within the state of Indiana where the proportion of land-use change exceeds 30%. The dominant type of land-use change is cropland to urban, indicating that urban expansion is significant in Indiana and Ohio (Lawler et al. 2014). Large-scale urban expansion will lead to the depletion of natural vegetation within protected areas (Martinuzzi et al. 2015). The area south of the sample shows not only urban expansion, but also forest deforestation and agricultural reclamation.

Sample area B is located in southeastern Spain, Valencia and its northern regions. The main land-use change type is intense afforestation and agricultural reclamation, with urbanization around the cities. In the central and southern part, this area of agriculture is dense rainfed cropland, and the main land use is bare area. Trends in land-use change also include the expansion of irrigated crop systems (Serra et al. 2014). Urban expansion in the northern part mainly comes from urban encroachment on cropland. The gradual conversion of traditional agriculture into forestry or intensive farming has been driven by agricultural and socio-economic policies (Hewitt & Escobar 2011).

Sample area C is located in central south China, which has a large continuous distribution of ecologically fragile karst areas (Jiang et al. 2014; Bai et al. 2013). At the same time, there are vegetation degradation and rocky desertification in the karst region of South China (Liao et al. 2018). Sample area C shows the highest proportion of land-use change among the three samples. The most common type of land-use change is forest to cropland, and there is also a shrubland to cropland type of change. Land policy has promoted cropland expansion (Peng et al. 2011), which is associated with dense population in the southwestern karst areas of China. Agriculture in the region is dominated by irrigated cropland and mixed cropland which will lead to erosion in karst areas (Liu et al. 2014).

3.4 Conclusion

This paper represents the first attempt to combine two global datasets for analysis and comparison. The study utilized CCI-LC data and WOKAM data from 1992 to 2020 to identify and quantify land-use changes and distribution patterns in global karst areas. The availability of these datasets describing the global karst distribution and land use change has enabled the first quantification of land use change in karst regions at a global scale. The main findings and conclusions can be summarized as follows:

In 2020, around 8.54 million km^2 (31.78 %) of the global karst areas are forest, about half of which is needle-leaved forest. About 5.11 million km^2 (19.02%) of karst areas are covered with cropland, which can be further divided into rainfed cropland (12.71%), irrigated cropland (0.79%) and mixed cropland (5.52%). Bare area and grassland accounted for 27.58% and 10.87%, respectively. The urban area is 0.19 million km^2 (0.71%).

The area of land-use changes in global karst areas from 1992 to 2020 is 1.30 million km^2, which means that almost 4.85% of the global karst surface has changed. Most of the changes occurred in the conversion between forest and cropland, accounting for 29.39% of all land-use changes on karst. The net increase of urban area is 0.1 million km^2, with most of the expansion coming from rainfed cropland. In contrast, the bare area and shrubland have been shrinking by about 0.09 million km^2 and 0.05 million km^2, respectively.

This paper proposes two indicators – land-use change proportion and dominant type of land-use change – in 10 km × 10 km cells to identify the characteristics of land-use change in karst regions. The areas with more than 15% land-use change are mainly distributed in eastern North America, Central Europe and Southeast Asia, accounting for 9.92% of all karst areas. The tropical climate regions have a higher proportion of land-use change. In addition, when exploring the characteristics of land-use change in global karst areas, it is found that the land-use change is dominated by forest expansion, accompanied by sporadic urbanization and agricultural reclamation. These agricultural reclamation regions are highly consistent with higher population density, mainly concentrated in China, Europe and North America.

These results reflect the current status and distribution of global karst land use, showing land use transition over the last 29 years. Continuous satellite observation will provide a basis of evidence for understanding land use and its change at global scale. Human activities

and climate change directly or indirectly affected land use. Traces of land-use change by human activities have been found in large areas of every continent. It is necessary to pay continuous attention to the impact of karst land use on karst groundwater resources.

Chapter 4

4 Conclusions and outlook

4.1 Conclusions

The core focus of this thesis is to examine the impact of environmental changes on groundwater at a global scale. The study integrates the analysis of global groundwater storage trends and land-use changes in karst regions to understand the spatiotemporal dynamics of these critical environmental factors and their driving mechanisms. The research utilizes datasets such as CCI-LC, WOKAM, GRACE, ERA5, meteorological data, and human activity data to develop a global-scale methodology for analyzing groundwater and environmental changes. The findings of this study contribute to the development of sustainable water resource and land use management strategies, particularly in vulnerable karst regions and other areas undergoing significant environmental changes. Moreover, this research enhances our understanding of global groundwater dynamics and provides a scientific basis for the assessment, availability, and management of global groundwater resources.

The study first estimates global groundwater storage using data from the GRACE gravity satellite and ERA5 datasets over past two decades. It integrates additional data, including precipitation, aridity index, drought conditions, irrigation, and groundwater abstraction, to understand and analyze the response of global groundwater storage to climate change and human activities. Recognizing the variability in hydrological processes and the intensity of human activities across different regions, the study further conducts an in-depth analysis of 23 regions that have experienced significant changes in groundwater storage over the past 20 years. This paper identifies the "driving forces" behind groundwater storage changes in each region, providing scientific evidence and effective references for localized water resource management.

The paper examines the current status and distribution of land use in global karst regions using the CCI-LC and WOKAM datasets. It provides a comprehensive analysis of land use patterns and transitions from 1992 to 2020, offering a quantitative assessment of changes in these areas. The study employs two key indicators—the proportion of land-use change and

the dominant type of land-use change—to identify the spatial characteristics of these changes. Additionally, it presents detailed case studies of three karst regions experiencing significant land use change, exploring the specific instances and mechanisms driving these changes.

To provide a conclusive summary of the findings of this thesis, the following section briefly addresses the research questions in Chapter 1.6:

RQ 1: How is the global groundwater storage trends over the past 20 years? Where are the major regions with significant groundwater storage decline? How many people live in areas experiencing with groundwater storage decline?

- Over the past two decades, groundwater storage has exhibited spatial heterogeneity, with most depletion occurring within the Earth's mid-latitudes. With a 95% confidence level, approximately 81.15% of global regions, excluding ice melt regions, have shown significant alterations in groundwater storage. Among these regions, 48.37% have observed a decline in groundwater levels, while 51.63% have recorded an increase.
- Hotspots of groundwater storage (GWS) depletion, with significant declining trends (>20 mm/a), have been identified in northern India, eastern Brazil, and areas surrounding the Caspian Sea. These changes indicate a future where already limited groundwater resources will become increasingly valuable.
- Approximately 3.4 billion people live in areas where groundwater has significantly declined over the past 20 years.

RQ 2: Which meteorological factors and human factors most significantly impact changes on groundwater storage?

- Spatial analysis revealed that the most significant groundwater declines occurred in arid and semi-arid regions, particularly where the aridity index (AI) ranges from 0.1 to 0.5, peaking at 0.1 to 0.2. Groundwater storage is increasing in humid regions (AI > 0.8). This disparity may lead to a more uneven distribution of groundwater.
- The study finds that changes in the Standardized Precipitation-Evapotranspiration Index (SPEI), rather than precipitation, exert a more significant impact on

groundwater storage trends. This highlights the crucial role of evapotranspiration and temperature in influencing groundwater dynamics.

- Furthermore, human activities, especially agricultural irrigation and excessive groundwater abstraction, are identified as major drivers of groundwater depletion. Compared to other factors, population density has a relatively smaller impact on groundwater storage.

RQ 3: In regions with significant changes in global groundwater storage over the past 20 years, what are the specific characteristic observed? How is the human activity and climate change in these regions? What are the driving forces behind the changes in groundwater storage?

- Based on the spatiotemporal characteristics of global groundwater storage changes from 2003 to 2022, the study examines 23 regions that have experienced significant changes in groundwater storage during this period. By integrating hydrometeorological and human activity data, the study comprehensively analyzes the driving factors of groundwater storage changes.
- The decline in groundwater storage can be attributed to various factors, such as intensive irrigation, prolonged droughts, unreasonable discharge and the ENSO cycles, etc. In contrast, increases in groundwater levels are associated with wetter climate conditions and the construction of dams, which create reservoirs that significantly affect local groundwater storage.

RQ 4: What is the current status of land use in global karst regions?

- In 2020, around 8.54 million km^2 (31.78 %) of the global karst areas are forest, about half of which is needle-leaved forest. About 5.11 million km^2 (19.02%) of karst areas are covered with cropland, which can be further divided into rainfed cropland (12.71%), irrigated cropland (0.79%) and mixed cropland (5.52%). Bare area and grassland accounted for 27.58% and 10.87%, respectively. The urban area is 0.19 million km^2 (0.71%).

RQ 5: What are the patterns of land-use area changes and land-use transitions in global karst regions from 1992 to 2020? What are the characteristics of these land-use changes?

- Over the 29-year period from 1992 to 2020, approximately 1.30 million km² of global karst areas underwent land-use changes, amounting to 4.85% of the total karst surface. The most significant land-use transitions occurred between forests and croplands, contributing to 29.39% of all changes, while urban expansion predominantly encroached upon rainfed croplands. Interestingly, the study found a net reduction in bare areas and shrublands, reflecting a trend towards increased vegetation coverage.

RQ 6: **In high land-use intensity areas within global karst regions, what are the causes of these changes? and what is their spatial distribution?**

- Two novel indicators were introduced—land-use change proportion and the dominant type of land-use change within 10×10 km grids—to characterize the spatial patterns of land-use changes in karst regions. Areas experiencing more than 15% land-use change are primarily located in eastern North America, Central Europe, and Southeast Asia, regions also noted for higher population densities and intensive agricultural practices.
- The land-use change trend of global karst is dominated by afforestation, supplemented by scattered urbanization and agricultural reclamation. The tropical climate has a higher intensity of land-use changes. Regions of agricultural reclamation are highly consistent with the population density.

In conclusion, this research offers a critical understanding of the current state and trends of land-use changes in karst areas and groundwater storage globally. The insights gained from this study are crucial for developing informed strategies to manage these vital resources sustainably in the face of ongoing environmental and climatic changes. This continuous monitoring is essential for formulating effective groundwater management policies, especially in regions experiencing severe change.

4.2 Outlook

During the research process, several new issues were identified that warrant further investigation:

1. **Impact of Land Use Change on Groundwater Storage**

While Chapter 2 of this study examines the effects of climate change and human activities on groundwater storage, it does not address the impact of land-use changes. Land-use changes, such as urbanization, agricultural expansion, and vegetation alteration, will directly affect groundwater recharge by influencing the infiltration capacity of precipitation. These changes can impact groundwater recharge rates, groundwater storage, and plant transpiration. Therefore, future research should focus on a more in-depth exploration of the effects of land use changes on groundwater storage.

2. **Improving Remote Sensing Accuracy for Groundwater Monitoring**
   Remote sensing technology has become a well-established method for monitoring groundwater changes. This study's analysis of groundwater storage change and land-use changes is based on advancements in remote sensing technology. As the temporal span of remote sensing data continues to increase and spatial resolution improves, more accurate and reliable results will be achieved. However, despite the success of remote sensing satellites in global groundwater monitoring, discrepancies still exist when compared to ground-based station data. Future research should develop models that account for these discrepancies to enhance the accuracy and performance of groundwater estimates from remote sensing data.
3. **Application of Artificial Neural Networks to Enhance GRACE Satellite Data**
   Although the GRACE satellite effectively reflects changes in groundwater storage under the combined effects of human activities and climate change. With the rapid development of Artificial Neural Network (ANN) technology, its application across various disciplines has increased significantly. Future research could build on the findings of this study by employing ANN methods and incorporating a variety of meteorological and human activity data. This approach aims to optimize the use of GRACE satellite data for studying global groundwater storage changes.

By addressing these issues, future studies can contribute to a more comprehensive understanding of groundwater dynamics in the context of environmental and anthropogenic changes.

Declaration of authorship

Study 1 (Chapter 2)

Citation: Zhang, J., Liesch, T., & Goldscheider, N. Impacts of climate change and human activities on global groundwater storage from 2003-2022. Submitted

Declaration of authorship: JZ & TL conceptualized the study, all authors contributed to the methodology. JZ & TL developed the software code. TL and NG supervised the work. JZ analyzed and mapped the data, wrote the manuscript. The manuscript was reviewed and edited by all authors.

Study 2 (Chapter 3)

Hydrogeology Journal
https://doi.org/10.1007/s10040-023-02650-5

PAPER

Global analysis of land-use changes in karst areas and the implications for water resources

Jiawen Zhang[1] · Tanja Liesch[1] · Zhao Chen[2] · Nico Goldscheider[1]

Received: 29 September 2022 / Accepted: 26 May 2023

Abstract
Karst areas contain valuable groundwater resources and high biodiversity, but are particularly vulnerable to climate change and human impacts. Land-use change is the cause and consequence of global environmental change. The releases of the Climate Change Initiative-Land Cover (CCI-LC) and World Karst Aquifer Map (WOKAM) datasets have made it possible to explore global land-use changes in karst areas. This paper firstly analyses the global karst land-use distribution in 2020, as well as the land-use transition characteristics between 1992 and 2020. Then, two indicators, proportion of land-use change and dominant type of land-use change, are proposed to identify the spatial characteristics of land-use change in global karst areas. Finally, three examples of land-use change in karst areas are analyzed in detail. Land-use types and proportions of the global karst areas from large to small are as follows: forest (31.78%), bare area (27.58%), cropland (19.02%), grassland (10.87%), shrubland (7.21%), wetland (1.67%), ice and snow (1.16%) and urban (0.71%). The total area of global karst land-use change is 1.30 million km², about 4.85% of global karst surface. The land-use change trend of global karst is dominated by afforestation, supplemented by scattered urbanization and agricultural reclamation. The tropical climate has a higher intensity of land-use change. Regions of agricultural reclamation are highly consistent with the population density. These results reflect the impact of human activities and climate change on land-use changes in global karst areas, and serve as a basis for further research and planning of land resource management.

Keywords Karst · Global mapping · Land-use change · Satellite imagery · Anthropogenic use

Introduction

Land-use change is an important component (Foley et al. 2005; Turner et al. 2013) and one of the key drivers (Ward et al. 2000) of global environmental change, and it is the result of a combination of driving factors under the human-land relationship (Liu et al. 2003; Meyfroidt et al. 2013). At the same time, land use also has a close relationship to population migration and economic conditions (DeFries 2013); thus, the assessment of land-use changes is important for the effective planning and management of resources. In recent decades, large-scale anthropogenic land-use changes have led to profound changes in the water cycle and have significantly affected the water resources and ecosystem, which in turn have caused changes in groundwater quality and quantity (Grimm et al. 2008; Winkler et al. 2021).

Karst aquifers make important contributions to the water supply of many regions, cities and countries; about 678 million people or 9.2% of the world's population rely on freshwater from karst aquifers (Stevanović 2019). While karst aquifers are essential for water supply, karst areas provide a variety of habitats for many species, including numerous rare and endemic plant and animal species (Goldscheider 2019). At the same time, the karst groundwater system is closely related to the external surface where there can be rapid transformation, so karst aquifers are particularly vulnerable to land-use change and difficult to manage (Ngayet and Goldscheider 2006; Parise et al. 2015; Panagopoulos and Giannika 2022). With the development of the economy and the expansion of population, human behavior, such as the expansion of

✉ Jiawen Zhang
jiawen.zhang@kit.edu
✉ Nico Goldscheider
nico.goldscheider@kit.edu
[1] Institute of Applied Geosciences, Division of Hydrogeology, Karlsruhe Institute of Technology (KIT), Kaiserstr. 12, 76131 Karlsruhe, Germany
[2] Institute of Groundwater Management, Technical University of Dresden, 01062 Dresden, Germany

Published online: 23 June 2023

Springer

Citation: Zhang, J., Liesch, T., Chen, Z., & Goldscheider, N. (2023). Global analysis of land-use changes in karst areas and the implications for water resources. Hydrogeology Journal, 31(5), 1197-1208.

Declaration of authorship: JZ & NG conceptualized the study, all authors contributed to the methodology. NG and TL supervised the work. JZ analyzed and mapped the data, wrote the manuscript. The manuscript was reviewed and edited by all authors.

References

Aadhar, S., & Mishra, V. (2017). High-resolution near real-time drought monitoring in South Asia. Scientific Data, 4(1), 1-14.

Abbott, B. W., Bishop, K., Zarnetske, J. P., Minaudo, C., Chapin III, F. S., Krause, S., ... & Pinay, G. (2019). Human domination of the global water cycle absent from depictions and perceptions. Nature Geoscience, 12(7), 533-540.

Ahmed, M., Sultan, M., Wahr, J., & Yan, E. (2014). The use of GRACE data to monitor natural and anthropogenic induced variations in water availability across Africa. Earth-Science Reviews, 136, 289-300.

Alam, S., Gebremichael, M., Ban, Z., Scanlon, B. R., Senay, G., & Lettenmaier, D. P. (2021). Post-Drought Groundwater Storage Recovery in California's Central Valley. Water Resources Research, 57(10), e2021WR030352.

Aldwaik, S. Z., & Pontius Jr, R. G. (2012). Intensity analysis to unify measurements of size and stationarity of land changes by interval, category, and transition. Landscape and urban planning, 106(1), 103-114.

Amanambu, A. C., Obarein, O. A., Mossa, J., Li, L., Ayeni, S. S., Balogun, O., Oyebamiji, A., Ochege F. U., & Ochege, F. U. (2020). Groundwater system and climate change: Present status and future considerations. Journal of Hydrology, 589, 125163.

Anghileri, D., Botter, M., Castelletti, A., Weigt, H., & Burlando, P. (2018). A comparative assessment of the impact of climate change and energy policies on Alpine hydropower. Water Resources Research, 54(11), 9144-9161.

Anyah, R. O., Forootan, E., Awange, J. L., & Khaki, M. (2018). Understanding linkages between global climate indices and terrestrial water storage changes over Africa using GRACE products. Science of the Total Environment, 635, 1405-1416.

Asoka, A., Gleeson, T., Wada, Y., & Mishra, V. (2017). Relative contribution of monsoon precipitation and pumping to changes in groundwater storage in India. Nature Geoscience, 10(2), 109-117.

Azadi, H., Keramati, P., Taheri, F., Rafiaani, P., Teklemariam, D., Gebrehiwot, K., ... & Witlox, F. (2018). Agricultural land conversion: Reviewing drought impacts and coping strategies. International Journal of Disaster Risk Reduction, 31, 184-195.

Bai, M., Mo, X., Liu, S., & Hu, S. (2019). Contributions of climate change and vegetation greening to evapotranspiration trend in a typical hilly-gully basin on the Loess Plateau, China. Science of the Total Environment, 657, 325-339.

Bai, X. Y., Wang, S. J., & Xiong, K. N. (2013). Assessing spatial-temporal evolution processes of karst rocky desertification land: indications for restoration strategies. Land Degradation & Development, 24(1), 47-56.

Barichivich, J., Osborn, T. J., Harris, I., van der Schrier, G., & Jones, P. D. (2022). Monitoring global drought using the self-calibrating Palmer Drought Severity Index [in "State of the Climate in 2021"]. Bull. Amer. Meteor. Soc., 103 (8), S31–S33, (https://doi.org/10.1175/BAMS-D-22-0092.1).

Bartholome, E., & Belward, A. S. (2005). GLC2000: a new approach to global land cover mapping from Earth observation data. International Journal of Remote Sensing, 26(9), 1959-1977.

Beguería, S., Vicente Serrano, S. M., Reig-Gracia, F., & Latorre Garcés, B. (2023). SPEIbase v. 2.9 [Dataset].

Bhanja, S. N., & Mukherjee, A. (2019). In situ and satellite-based estimates of usable groundwater storage across India: Implications for drinking water supply and food security. Advances in Water Resources, 126, 15-23.

Bhanja, S. N., Mukherjee, A., & Rodell, M. (2020). Groundwater storage change detection from in situ and GRACE-based estimates in major river basins across India. Hydrological Sciences Journal, 65(4), 650-659.

Bhanja, S. N., Mukherjee, A., Saha, D., Velicogna, I., & Famiglietti, J. S. (2016). Validation of GRACE based groundwater storage anomaly using in-situ groundwater level measurements in India. Journal of Hydrology, 543, 729-738.

Biazin, B., & Sterk, G. (2013). Drought vulnerability drives land-use and land cover changes in the Rift Valley dry lands of Ethiopia. Agriculture, ecosystems & environment, 164, 100-113.

Bontemps, S., Defourny, P., Radoux, J., Van Bogaert, E., Lamarche, C., Achard, F., ... & Arino, O. (2013, September). Consistent global land cover maps for climate modelling communities: current achievements of the ESA's land cover CCI. In Proceedings of the ESA living planet symposium, Edimburgh (Vol. 13, pp. 9-13).

Bouchard, F., Turner, K. W., MacDonald, L. A., Deakin, C., White, H., Farquharson, N., Medeiros A. S., Wolfe B. B., Hall R. I., Pienitz R., & Edwards, T. W. D. (2013). Vulnerability of shallow subarctic lakes to evaporate and desiccate when snowmelt runoff is low. Geophysical Research Letters, 40(23), 6112-6117.

Brauman, K. A., Richter, B. D., Postel, S., Malsy, M., & Flörke, M. (2016). Water depletion: An improved metric for incorporating seasonal and dry-year water scarcity into water risk assessments. Elementa, 4, 000083.

Brown, M. T., & Vivas, M. B. (2005). Landscape development intensity index. Environmental monitoring and assessment, 101, 289-309.

Chao, N., Chen, G., Li, J., Xiang, L., Wang, Z., & Tian, K. (2020). Groundwater storage change in the Jinsha River Basin from GRACE, hydrologic models, and in situ data. Groundwater, 58(5), 735-748.

Chao, N., Jin, T., Cai, Z., Chen, G., Liu, X., Wang, Z., & Yeh, P. J. F. (2021). Estimation of component contributions to total terrestrial water storage change in the Yangtze river basin. Journal of Hydrology, 595, 125661.

Chaudhary, A., & Mooers, A. O. (2018). Terrestrial vertebrate biodiversity loss under future global land use change scenarios. Sustainability, 10(8), 2764.

Chen, F., Wang, S., Bai, X., Liu, F., Zhou, D., Tian, Y., ... & Yang, Y. (2021). Assessing spatial-temporal evolution processes and driving forces of karst rocky desertification. Geocarto International, 36(3), 262-280.

Chen, J. L., Wilson, C. R., & Tapley, B. D. (2010). The 2009 exceptional Amazon flood and interannual terrestrial water storage change observed by GRACE. Water Resources Research, 46(12).

Chen, J., Chen, J., Liao, A., Cao, X., Chen, L., Chen, X., ... & Mills, J. (2015). Global land cover mapping at 30 m resolution: A POK-based operational approach. ISPRS Journal of Photogrammetry and Remote Sensing, 103, 7-27.

Chen, J., Famigliett, J. S., Scanlon, B. R., & Rodell, M. (2016). Groundwater storage changes: present status from GRACE observations. Remote sensing and water resources, 207-227.

Chen, W., Zhang, X., & Huang, Y. (2021). Spatial and temporal changes in ecosystem service values in karst areas in southwestern China based on land use changes. Environmental Science and Pollution Research, 28(33), 45724-45738.

Chen, Z., Auler, A. S., Bakalowicz, M., Drew, D., Griger, F., Hartmann, J., ... & Goldscheider, N. (2017). The World Karst Aquifer Mapping project: concept, mapping procedure and map of Europe. Hydrogeology Journal, 25(3), 771.

Chen, Z., Goldscheider, N., Auler, A., & Bakalowicz, M. (2017). World Karst Aquifer Map (WHYMAP WOKAM).

Chiu, C. C., Château, P. A., Lin, H. J., & Chang, Y. C. (2019). Modeling the impacts of coastal land use changes on regional carbon balance in the Chiku coastal zone, Taiwan. Land use policy, 87, 104079.

Collow, T. W., Robock, A., Basara, J. B., & Illston, B. G. (2012). Evaluation of SMOS retrievals of soil moisture over the central United States with currently available in situ observations. Journal of Geophysical Research: Atmospheres, 117(D9).

Condon, L. E., Atchley, A. L., & Maxwell, R. M. (2020). Evapotranspiration depletes groundwater under warming over the contiguous United States. Nature communications, 11(1), 873.

Connor, R., & Miletto, M. (2022). The United Nations World Water Development Report 2022: groundwater: making the invisible visible; executive summary.

Cuthbert, M. O., Taylor, R. G., Favreau, G., Todd, M. C., Shamsudduha, M., Villholth, K. G., ... & Kukuric, N. (2019). Observed controls on resilience of groundwater to climate variability in sub-Saharan Africa. Nature, 572(7768), 230-234.

Dai, A. (2013). Increasing drought under global warming in observations and models. Nature climate change, 3(1), 52-58.

Dai, Q., Peng, X., Yang, Z., & Zhao, L. (2017). Runoff and erosion processes on bare slopes in the Karst Rocky Desertification Area. Catena, 152, 218-226.

Defourny, P., Bontemps, S., Lamarche, C., Brockmann, C., Boettcher, M., Wevers, J., Kirches, G. (2017). Land Cover CCI: Product User Guide Version 2.0. Available at: http://maps.elie.ucl.ac.be/CCI/viewer/.

Defourny, P., Lamarche, C., Marissiaux, Q., Brockmann, C., Boettcher, M., & Kirches, G. (2021). Product user guide and specification ICDR land cover 2016–2020. ECMWF: Reading, UK, 37.

DeFries, R. (2013). Why forest monitoring matters for people and the planet. Global forest monitoring from Earth observation, 1-14.

Di Gregorio, A. (2005). Land cover classification system: classification concepts and user manual: LCCS (Vol. 2). Food & Agriculture Org..

Döll, P., Müller Schmied, H., Schuh, C., Portmann, F. T., & Eicker, A. (2014). Global-scale assessment of groundwater depletion and related groundwater abstractions: Combining hydrological modeling with information from well observations and GRACE satellites. Water Resources Research, 50(7), 5698-5720.

Dong, N., Liu, Z., Luo, M., Fang, C., & Lin, H. (2019). The effects of anthropogenic land use changes on climate in China driven by global socioeconomic and emission scenarios. Earth's Future, 7(7), 784-804.

Duveiller, G., Hooker, J., & Cescatti, A. (2018). The mark of vegetation change on Earth's surface energy balance. Nature communications, 9(1), 679.

Eicker, A., Forootan, E., Springer, A., Longuevergne, L., & Kusche, J. (2016). Does GRACE see the terrestrial water cycle "intensifying"?. Journal of Geophysical Research: Atmospheres, 121(2), 733-745.

Eitelberg, D. A., van Vliet, J., Doelman, J. C., Stehfest, E., & Verburg, P. H. (2016). Demand for biodiversity protection and carbon storage as drivers of global land change scenarios. Global Environmental Change, 40, 101-111.

Famiglietti, J. S. (2014). The global groundwater crisis. Nature climate change, 4(11), 945-948.

Famiglietti, J. S., Lo, M., Ho, S. L., Bethune, J., Anderson, K. J., Syed, T. H., ... & Rodell, M. (2011). Satellites measure recent rates of groundwater depletion in California's Central Valley. Geophysical Research Letters, 38(3).

Famiglietti, J. S., Lo, M., Ho, S. L., Bethune, J., Anderson, K. J., Syed, T. H., Swenson, S. C., de Linage, C. R., and Rodell, M. (2011). Satellites measure recent rates of groundwater depletion in California's Central Valley. Geophysical Research Letters 38

Fan, X., Duan, Q., Shen, C., Wu, Y., & Xing, C. (2020). Global surface air temperatures in CMIP6: Historical performance and future changes. Environmental Research Letters, 15(10), 104056.

Fan, Y., Li, H., & Miguez-Macho, G. (2013). Global patterns of groundwater table depth. Science, 339(6122), 940-943.

Feng, S., & Fan, F. (2021). Impervious surface extraction based on different methods from multiple spatial resolution images: a comprehensive comparison. International Journal of Digital Earth, 14(9), 1148-1174.

Feng, W., Wang, C. Q., Mu, D. P., Zhong, M., Zhong, Y. L., and Xu, H. Z. (2017). Groundwater storage variations in the North China Plain from GRACE with spatial constraints. Chinese Journal of Geophysics-Chinese Edition 60, 1630-1642.

Feng, W., Zhong, M., Lemoine, J. M., Biancale, R., Hsu, H. T., and Xia, J. (2013). Evaluation of groundwater depletion in North China using the Gravity Recovery and Climate Experiment (GRACE) data and ground-based measurements. Water Resources Research 49, 2110-2118.

Foley, J. A., DeFries, R., Asner, G. P., Barford, C., Bonan, G., Carpenter, S. R., ... & Snyder, P. K. (2005). Global consequences of land use. science, 309(5734), 570-574.

Foley, J. A., Ramankutty, N., Brauman, K. A., Cassidy, E. S., Gerber, J. S., Johnston, M., ... & Zaks, D. P. (2011). Solutions for a cultivated planet. Nature, 478(7369), 337-342.

Friedl, M. A., Sulla-Menashe, D., Tan, B., Schneider, A., Ramankutty, N., Sibley, A., & Huang, X. (2010). MODIS Collection 5 global land cover: Algorithm refinements and characterization of new datasets. Remote sensing of Environment, 114(1), 168-182.

Fu, T., Chen, H., & Wang, K. (2016). Structure and water storage capacity of a small karst aquifer based on stream discharge in southwest China. Journal of Hydrology, 534, 50-62.

Fuchs, R., Herold, M., Verburg, P. H., & Clevers, J. G. (2013). A high-resolution and harmonized model approach for reconstructing and analysing historic land changes in Europe. Biogeosciences, 10(3), 1543-1559.

Gao, S., Hao, W., Fan, Y., Li, F., & Wang, J. (2023). A Multi-Source GRACE Fusion Solution via Uncertainty Quantification of GRACE-Derived Terrestrial Water Storage (TWS) Change. Journal of Geophysical Research: Solid Earth, 128(11), e2023JB026908.

Gao, X., Sun, M., Luan, Q., Zhao, X., Wang, J., He, G., & Zhao, Y. (2020). The spatial and temporal evolution of the actual evapotranspiration based on the remote sensing method in the Loess Plateau. Science of the Total Environment, 708, 135111.

García-García, D., Ummenhofer, C. C., & Zlotnicki, V. (2011). Australian water mass variations from GRACE data linked to Indo-Pacific climate variability. Remote Sensing of Environment, 115(9), 2175-2183.

Gates, J. B., Scanlon, B. R., Mu, X., & Zhang, L. (2011). Impacts of soil conservation on groundwater recharge in the semi-arid Loess Plateau, China. Hydrogeology Journal, 4(19), 865-875.

Gebrelibanos, T., & Assen, M. (2015). Land use/land cover dynamics and their driving forces in the Hirmi watershed and its adjacent agro-ecosystem, highlands of Northern Ethiopia. Journal of Land Use Science, 10(1), 81-94.

Getirana, A., Kumar, S., Girotto, M., & Rodell, M. (2017). Rivers and floodplains as key components of global terrestrial water storage variability. Geophysical Research Letters, 44(20), 10-359.

Gleeson, T., Wada, Y., Bierkens, M. F., & Van Beek, L. P. (2012). Water balance of global aquifers revealed by groundwater footprint. Nature, 488(7410), 197-200.

Goldscheider, N. (2019). A holistic approach to groundwater protection and ecosystem services in karst terrains. Carbonates and Evaporites, 34(4), 1241-1249.

Goldscheider, N., Chen, Z., Auler, A. S., Bakalowicz, M., Broda, S., Drew, D., ... & Veni, G. (2020). Global distribution of carbonate rocks and karst water resources. Hydrogeology Journal, 28, 1661-1677.

Gong, H., Pan, Y., Zheng, L., Li, X., Zhu, L., Zhang, C., ... & Zhou, C. (2018). Long-term groundwater storage changes and land subsidence development in the North China Plain (1971–2015). Hydrogeology Journal, 26(5), 1417-1427.

Gong, P., Wang, J., Yu, L., Zhao, Y., Zhao, Y., Liang, L., ... & Chen, J. (2013). Finer resolution observation and monitoring of global land cover: First mapping results with Landsat TM and ETM+ data. International journal of remote sensing, 34(7), 2607-2654.

Green, T. R., Taniguchi, M., Kooi, H., Gurdak, J. J., Allen, D. M., Hiscock, K. M., ... & Aureli, A. (2011). Beneath the surface of global change: Impacts of climate change on groundwater. Journal of Hydrology, 405(3-4), 532-560.

Grekousis, G., Mountrakis, G., & Kavouras, M. (2015). An overview of 21 global and 43 regional land-cover mapping products. International Journal of Remote Sensing, 36(21), 5309-5335.

Griffin, D., & Anchukaitis, K. J. (2014). How unusual is the 2012–2014 California drought?. Geophysical Research Letters, 41(24), 9017-9023.

Grimm, N. B., Faeth, S. H., Golubiewski, N. E., Redman, C. L., Wu, J., Bai, X., & Briggs, J. M. (2008). Global change and the ecology of cities. science, 319(5864), 756-760.

Guida-Johnson, B., & Zuleta, G. A. (2013). Land-use land-cover change and ecosystem loss in the Espinal ecoregion, Argentina. Agriculture, ecosystems & environment, 181, 31-40.

Gutiérrez, F., Parise, M., De Waele, J., & Jourde, H. (2014). A review on natural and human-induced geohazards and impacts in karst. Earth-Science Reviews, 138, 61-88.

Han, Z., Huang, S., Huang, Q., Leng, G., Wang, H., He, L., ... & Li, P. (2019). Assessing GRACE-based terrestrial water storage anomalies dynamics at multi-timescales and their correlations with teleconnection factors in Yunnan Province, China. Journal of Hydrology, 574, 836-850.

Hansen, M. C., Potapov, P. V., Moore, R., Hancher, M., Turubanova, S. A., Tyukavina, A., ... & Townshend, J. R. (2013). High-resolution global maps of 21st-century forest cover change. science, 342(6160), 850-853.

Harris, I., Osborn, T. J., Jones, P., & Lister, D. (2020). Version 4 of the CRU TS monthly high-resolution gridded multivariate climate dataset. Scientific Data, 7(1), 109.

Hartmann, A., Goldscheider, N., Wagener, T., Lange, J., & Weiler, M. (2014). Karst water resources in a changing world: Review of hydrological modeling approaches. Reviews of Geophysics, 52(3), 218-242.

Hartmann, J., & Moosdorf, N. (2012). The new global lithological map database GLiM: A representation of rock properties at the Earth surface. Geochemistry, Geophysics, Geosystems, 13(12).

Heerspink, B. P., Kendall, A. D., Coe, M. T., & Hyndman, D. W. (2020). Trends in streamflow, evapotranspiration, and groundwater storage across the Amazon Basin linked to changing precipitation and land cover. Journal of Hydrology: Regional Studies, 32, 100755.

Herbert, C., & Döll, P. (2019). Global assessment of current and future groundwater stress with a focus on transboundary aquifers. Water Resources Research, 55(6), 4760-4784.

Herrera-Pantoja, M., & Hiscock, K. M. (2008). The effects of climate change on potential groundwater recharge in Great Britain. Hydrological Processes: An International Journal, 22(1), 73-86.

Hewitt, R., & Escobar, F. (2011). The territorial dynamics of fast-growing regions: Unsustainable land use change and future policy challenges in Madrid, Spain. Applied Geography, 31(2), 650-667.

Hibbert, A. R. (1969). Water yield changes after converting a forested catchment to grass. Water Resources Research, 5(3), 634-640.

Hirsch, A. L., Guillod, B. P., Seneviratne, S. I., Beyerle, U., Boysen, L. R., Brovkin, V., ... & Wilson, S. (2018). Biogeophysical impacts of land-use change on climate extremes in low-emission scenarios: results from HAPPI-Land. Earth's future, 6(3), 396-409.

Hirsch, R. M., Slack, J. R., & Smith, R. A. (1982). Techniques of trend analysis for monthly water quality data. Water Resources Research, 18(1), 107-121.

Hollingsworth, E. (2009). Karst Regions of the World: Populating Global Karst Datasets and Generating Maps to Advance the Understanding of Karst Occurrence and Protection of Karst Species and Habitats Worldwide. MSc Thesis, Fayetteville, AK: University of Arkansas.

Hong, C., Burney, J. A., Pongratz, J., Nabel, J. E., Mueller, N. D., Jackson, R. B., & Davis, S. J. (2021). Global and regional drivers of land-use emissions in 1961–2017. Nature, 589(7843), 554-561.

Hu, K., Awange, J. L., Forootan, E., Goncalves, R. M., & Fleming, K. (2017). Hydrogeological characterisation of groundwater over Brazil using remotely sensed and model products. Science of the Total Environment, 599, 372-386.

Hu, Z., Chen, X., Zhou, Q., Yin, G., & Liu, J. (2022). Dynamical variations of the terrestrial water cycle components and the influences of the climate factors over the Aral Sea Basin through multiple datasets. Journal of Hydrology, 604, 127270.

Ionita, M., Dima, M., Nagavciuc, V., Scholz, P., & Lohmann, G. (2021). Past megadroughts in central Europe were longer, more severe and less warm than modern droughts. Communications Earth & Environment, 2(1), 61.

IPCC Climate Change. (2013). The physical science basis. Contribution of working group I to the fifth assessment report of the intergovernmental panel on climate change, 1535.

IPCC, 2021: Climate Change 2021: The Physical Science Basis. Contribution of Working Group I to the Sixth Assessment Report of the Intergovernmental Panel on Climate Change [Masson-Delmotte, V., P. Zhai, A. Pirani, S.L. Connors, C. Péan, S. Berger, N. Caud, Y. Chen, L. Goldfarb, M.I. Gomis, M. Huang, K. Leitzell, E. Lonnoy, J.B.R. Matthews, T.K. Maycock, T. Waterfield, O. Yelekçi, R. Yu, and B. Zhou (eds.)]. Cambridge University Press, Cambridge, United Kingdom and New York, NY, USA, 2391 pp. doi:10.1017/9781009157896.

Jacob, T., Wahr, J., Pfeffer, W. T., & Swenson, S. (2012). Recent contributions of glaciers and ice caps to sea level rise. Nature, 482(7386), 514-518.

Jasechko, S., & Perrone, D. (2021). Global groundwater wells at risk of running dry. Science, 372(6540), 418-421.

Jasechko, S., Seybold, H., Perrone, D., Fan, Y., Shamsudduha, M., Taylor, R. G., ... & Kirchner, J. W. (2024). Rapid groundwater decline and some cases of recovery in aquifers globally. Nature, 625(7996), 715-721.

Jiang, Z., Lian, Y., & Qin, X. (2014). Rocky desertification in Southwest China: Impacts, causes, and restoration. Earth-Science Reviews, 132, 1-12.

Joodaki, G., Wahr, J., & Swenson, S. (2014). Estimating the human contribution to groundwater depletion in the Middle East, from GRACE data, land surface models, and well observations. Water Resources Research, 50(3), 2679-2692.

Kalnay, E., & Cai, M. (2003). Impact of urbanization and land-use change on climate. Nature, 423(6939), 528-531.

Kang, Z., Chen, J., Yuan, D., He, S., Li, Y., Chang, Y., ... & Zhang, Q. (2020). Promotion function of forest vegetation on the water & carbon coupling cycle in karst critical zone: Insights from karst groundwater systems in south China. Journal of Hydrology, 590, 125246.

Katpatal, Y. B., Rishma, C., & Singh, C. K. (2018). Sensitivity of the Gravity Recovery and Climate Experiment (GRACE) to the complexity of aquifer systems for monitoring of groundwater. Hydrogeology Journal, 26(3).

Kebede, S., Abdalla, O., Sefelnasr, A., Tindimugaya, C., & Mustafa, O. (2017). Interaction of surface water and groundwater in the Nile River basin: isotopic and piezometric evidence. Hydrogeology Journal, 25(3), 707.

Keenan, T. F., & Riley, W. J. (2018). Greening of the land surface in the world's cold regions consistent with recent warming. Nature Climate Change, 8(9), 825-828.

Kiptala, J. K., Mohamed, Y., Mul, M. L., & Van der Zaag, P. (2013). Mapping evapotranspiration trends using MODIS and SEBAL model in a data scarce and heterogeneous landscape in Eastern Africa. Water resources research, 49(12), 8495-8510.

Kolusu, S. R., Shamsudduha, M., Todd, M. C., Taylor, R. G., Seddon, D., Kashaigili, J. J., ... & MacLeod, D. A. (2019). The El Niño event of 2015–2016: climate anomalies and their impact on groundwater resources in East and Southern Africa. Hydrology and Earth System Sciences, 23(3), 1751-1762.

Laikre, L., Schwartz, M. K., Waples, R. S., & Ryman, N. (2010). Compromising genetic diversity in the wild: unmonitored large-scale release of plants and animals. Trends in ecology & evolution, 25(9), 520-529.

Lambin, E. F., Geist, H., & Rindfuss, R. R. (2006). Introduction: local processes with global impacts. In Land-use and land-cover change: Local processes and global impacts (pp. 1-8). Berlin, Heidelberg: Springer Berlin Heidelberg.

Lambin, E. F., Turner, B. L., Geist, H. J., Agbola, S. B., Angelsen, A., Bruce, J. W., ... & Xu, J. (2001). The causes of land-use and land-cover change: moving beyond the myths. Global environmental change, 11(4), 261-269.

Lang, Y., Song, W., & Deng, X. (2018). Projected land use changes impacts on water yields in the karst mountain areas of China. Physics and Chemistry of the Earth, Parts A/B/C, 104, 66-75.

Lawler, J. J., Lewis, D. J., Nelson, E., Plantinga, A. J., Polasky, S., Withey, J. C., ... & Radeloff, V. C. (2014). Projected land-use change impacts on ecosystem services in the United States. Proceedings of the National Academy of Sciences, 111(20), 7492-7497.

Le, T., Ha, K. J., & Bae, D. H. (2021). Projected response of global runoff to El Niño-Southern oscillation. Environmental Research Letters, 16(8), 084037.

LeGrand, H. E. (1973). Hydrological and Ecological Problems of Karst Regions: Hydrological actions on limestone regions cause distinctive ecological problems. Science, 179(4076), 859-864.

Leh, M., Bajwa, S., & Chaubey, I. (2013). Impact of land use change on erosion risk: an integrated remote sensing, geographic information system and modeling methodology. Land Degradation & Development, 24(5), 409-421.

Li, B., & Rodell, M. (2015). Evaluation of a model-based groundwater drought indicator in the conterminous US. Journal of Hydrology, 526, 78-88.

Li, B., Rodell, M., Kumar, S., Beaudoing, H. K., Getirana, A., Zaitchik, B. F., ... & Bettadpur, S. (2019). Global GRACE data assimilation for groundwater and drought monitoring: Advances and challenges. Water Resources Research, 55(9), 7564-7586.

Li, W., Bao, L., Yao, G., Wang, F., Guo, Q., Zhu, J., ... & Lu, S. (2024). The analysis on groundwater storage variations from GRACE/GRACE-FO in recent 20 years driven by influencing factors and prediction in Shandong Province, China. Scientific Reports, 14(1), 5819.

Li, W., MacBean, N., Ciais, P., Defourny, P., Lamarche, C., Bontemps, S., ... & Peng, S. (2018). Gross and net land cover changes in the main plant functional types derived from the annual ESA CCI land cover maps (1992–2015). Earth System Science Data, 10(1), 219-234.

Li, Y. B., Shao, J. A., Yang, H., & Bai, X. Y. (2009). The relations between land use and karst rocky desertification in a typical karst area, China. Environmental Geology, 57, 621-627.

Li, Y. J., Ding, Y. J., Shangguan, D. H., & Wang, R. J. (2019). Regional differences in global glacier retreat from 1980 to 2015. Advances in Climate Change Research, 10(4), 203-213.

Li, Z., Gao, P., & Lu, H. (2019). Dynamic changes of groundwater storage and flows in a disturbed alpine peatland under variable climatic conditions. Journal of Hydrology, 575, 557-568.

Liao, C., Yue, Y., Wang, K., Fensholt, R., Tong, X., & Brandt, M. (2018). Ecological restoration enhances ecosystem health in the karst regions of southwest China. Ecological Indicators, 90, 416-425.

Liesch, T., & Ohmer, M. (2016). Comparison of GRACE data and groundwater levels for the assessment of groundwater depletion in Jordan. Hydrogeology Journal, 24(6), 1547.

Lima, F. V., Gonçalves, R. M., Montecino, H. D., Carvalho, R. A., & Mutti, P. R. (2022). Multi-sensor geodetic observations for drought characterization in the Northeast Atlantic Eastern Hydrographic Region, Brazil. Science of The Total Environment, 846, 157426.

Lin, Y. H., Lo, M. H., & Chou, C. (2016). Potential negative effects of groundwater dynamics on dry season convection in the Amazon River basin. Climate Dynamics, 46, 1001-1013.

Liu, C. C., Liu, Y. G., Guo, K., Li, G. Q., Zheng, Y. R., Yu, L. F., & Yang, R. (2011). Comparative ecophysiological responses to drought of two shrub and four tree species from karst habitats of southwestern China. Trees, 25, 537-549.

Liu, J., Liu, M., Zhuang, D., Zhang, Z., & Deng, X. (2003). Study on spatial pattern of land-use change in China during 1995–2000. Science in China Series D: Earth Sciences, 46, 373-384.

Liu, L., Xu, X., Liu, J., Chen, X., & Ning, J. (2015). Impact of farmland changes on production potential in China during 1990–2010. Journal of Geographical Sciences, 25, 19-34.

Liu, X., Yu, L., Si, Y., Zhang, C., Lu, H., Yu, C., & Gong, P. (2018). Identifying patterns and hotspots of global land cover transitions using the ESA CCI Land Cover dataset. Remote Sensing Letters, 9(10), 972-981.

Liu, Y., Huang, X., Yang, H., & Zhong, T. (2014). Environmental effects of land-use/cover change caused by urbanization and policies in Southwest China Karst area–A case study of Guiyang. Habitat International, 44, 339-348.

López-Carr, D., Davis, J., Jankowska, M. M., Grant, L., López-Carr, A. C., & Clark, M. (2012). Space versus place in complex human–natural systems: Spatial and multi-level models of tropical land use and cover change (LUCC) in Guatemala. Ecological modelling, 229, 64-75.

Loveland, T. R., Reed, B. C., Brown, J. F., Ohlen, D. O., Zhu, Z., Yang, L. W. M. J., & Merchant, J. W. (2000). Development of a global land cover characteristics database and IGBP DISCover from 1 km AVHRR data. International journal of remote sensing, 21(6-7), 1303-1330.

Mansour, S., Al-Belushi, M., & Al-Awadhi, T. (2020). Monitoring land use and land cover changes in the mountainous cities of Oman using GIS and CA-Markov modelling techniques. Land use policy, 91, 104414.

Marengo, J. A., Torres, R. R., & Alves, L. M. (2017). Drought in Northeast Brazil—past, present, and future. Theoretical and Applied Climatology, 129, 1189-1200.

Martens, B., Miralles, D.G., Lievens, H., van der Schalie, R., de Jeu, R.A.M., Fernández-Prieto, D., Beck, H.E., Dorigo, W.A., and Verhoest, N.E.C. (2017). GLEAM v3: satellite-based land evaporation and root-zone soil moisture. Geoscientific Model Development, 10, 1903–1925, doi: 10.5194/gmd-10-1903-2017.

Martinuzzi, S., Radeloff, V. C., Joppa, L. N., Hamilton, C. M., Helmers, D. P., Plantinga, A. J., & Lewis, D. J. (2015). Scenarios of future land use change around United States' protected areas. Biological Conservation, 184, 446-455.

Matasov, V., Prishchepov, A. V., Jepsen, M. R., & Müller, D. (2019). Spatial determinants and underlying drivers of land-use transitions in European Russia from 1770 to 2010. Journal of Land Use Science, 14(4-6), 362-377.

Mekonnen, M. M., & Hoekstra, A. Y. (2016). Four billion people facing severe water scarcity. Science advances, 2(2), e1500323.

Meyfroidt, P., Lambin, E. F., Erb, K. H., & Hertel, T. W. (2013). Globalization of land use: distant drivers of land change and geographic displacement of land use. Current Opinion in Environmental Sustainability, 5(5), 438-444.

Middleton, N., & Thomas, D. (1997). World Atlas of Desertification, 2nd edn, Arnold E (ed). UNEP, Hodder Headline plc.: London.

Miralles, D.G., Holmes, T.R.H., de Jeu, R.A.M., Gash, J.H., Meesters, A.G.C.A., Dolman, A.J. (2011). Global land-surface evaporation estimated from satellite-based observations. Hydrology and Earth System Sciences, 15, 453–469, doi: 10.5194/hess-15-453-2011.

Misra, A., & Balaji, R. A. (2015). A study on the shoreline changes and Land-use/land-cover along the South Gujarat coastline. Procedia Engineering, 116, 381-389.

Monroe, A. P., Aldridge, C. L., O'Donnell, M. S., Manier, D. J., Homer, C. G., & Anderson, P. J. (2020). Using remote sensing products to predict recovery of vegetation across space and time following energy development. Ecological Indicators, 110, 105872.

Morris, B. L., Lawrence, A. R., Chilton, P. J. C., Adams, B., Calow, R. C., & Klinck, B. A. (2003). Groundwater and its susceptibility to degradation: a global assessment of the problem and options for management.

Müller Schmied, H., Cáceres, D., Eisner, S., Flörke, M., Herbert, C., Niemann, C., Peiris, T., A., Popat, E., Portmann, F., T., Reinecke, R., Shadkam, S., Trautmann, T., & Döll, P. (2021). The global water resources and use model WaterGAP v2. 2d: Model description and evaluation. Geoscientific Model Development, 14(2), 1037-1079.

Muñoz Sabater, J. (2019). ERA5-Land monthly averaged data from 1981 to present. Copernicus Climate Change Service (C3S) Climate Data Store (CDS). https://doi.org/10.24381/cds.68d2bb3

Muñoz Sabater, J. (2021). ERA5-Land monthly averaged data from 1950 to 1980. Copernicus Climate Change Service (C3S) Climate Data Store (CDS). https://doi.org/10.24381/cds.68d2bb3

Myneni, R., Knyazikhin, Y., Park, T. (2021). MODIS/Terra Leaf Area Index/FPAR 8-Day L4 Global 500m SIN Grid V061 [Data set]. NASA EOSDIS Land Processes Distributed Active Archive Center. Accessed 2023-11-28 from https://doi.org/10.5067/MODIS/MOD15A2H.061

Newman, M. E., McLaren, K. P., & Wilson, B. S. (2014). Long-term socio-economic and spatial pattern drivers of land cover change in a Caribbean tropical moist forest, the Cockpit Country, Jamaica. Agriculture, Ecosystems & Environment, 186, 185-200.

Nguyen, T., Novak, R., Xiao, L., & Lee, J. (2021). Dataset distillation with infinitely wide convolutional networks. Advances in Neural Information Processing Systems, 34, 5186-5198.

Nguyet, V. T. M., & Goldscheider, N. (2006). A simplified methodology for mapping groundwater vulnerability and contamination risk, and its first application in a tropical karst area, Vietnam. Hydrogeology Journal, 14, 1666-1675.

Nowosad, J., Stepinski, T. F., & Netzel, P. (2019). Global assessment and mapping of changes in mesoscale landscapes: 1992–2015. International Journal of Applied Earth Observation and Geoinformation, 78, 332-340.

Ohmer, M., Liesch, T., & Goldscheider, N. (2019). On the optimal spatial design for groundwater level monitoring networks. Water Resources Research, 55(11), 9454-9473.

O'Loughlin, F. E., Neal, J., Yamazaki, D., & Bates, P. D. (2016). ICESat-derived inland water surface spot heights. Water Resources Research, 52(4), 3276-3284.

Padrón, R. S., Gudmundsson, L., Decharme, B., Ducharne, A., Lawrence, D. M., Mao, J., Krinner, G., Kim, H., Seneviratne, S. I. (2020). Observed changes in dry-season water availability attributed to human-induced climate change. Nature Geoscience, 13(7), 477-481.

Panagiotou, C. F., Kyriakidis, P., & Tziritis, E. (2022). Application of geostatistical methods to groundwater salinization problems: A review. Journal of Hydrology, 615, 128566.

Panagopoulos, A., & Giannika, V. (2022). Comparative techno-economic and environmental analysis of minimal liquid discharge (MLD) and zero liquid discharge (ZLD) desalination systems for

seawater brine treatment and valorization. Sustainable Energy Technologies and Assessments, 53, 102477.

Parise, M., Closson, D., Gutiérrez, F., & Stevanović, Z. (2015). Anticipating and managing engineering problems in the complex karst environment. Environmental Earth Sciences, 74, 7823-7835.

Peng, J., Xu, Y. Q., Cai, Y. L., & Xiao, H. L. (2011). The role of policies in land use/cover change since the 1970s in ecologically fragile karst areas of Southwest China: A case study on the Maotiaohe watershed. Environmental Science & Policy, 14(4), 408-418.

Perez-Valdivia, C., Sauchyn, D., & Vanstone, J. (2012). Groundwater levels and teleconnection patterns in the Canadian Prairies. Water Resources Research, 48(7).

Phillips, T. J., & Gleckler, P. J. (2006). Evaluation of continental precipitation in 20th century climate simulations: The utility of multimodel statistics. Water Resources Research, 42(3).

Pragnaditya, M., Abhijit, M., Bhanja, S. N., Kumar, R. R., Sudeshna, S., & Anwar, Z. (2021). Machine-learning-based regional-scale groundwater level prediction using GRACE. Hydrogeology Journal, 29(3), 1027-1042.

Prestele, R., Arneth, A., Bondeau, A., de Noblet-Ducoudré, N., Pugh, T. A., Sitch, S., ... & Verburg, P. H. (2017). Current challenges of implementing anthropogenic land-use and land-cover change in models contributing to climate change assessments. Earth System Dynamics, 8(2), 369-386.

Qadir, M., Noble, A. D., Qureshi, A. S., Gupta, R. K., Yuldashev, T., & Karimov, A. (2009). Salt-induced land and water degradation in the Aral Sea basin: A challenge to sustainable agriculture in Central Asia. In Natural Resources Forum (Vol. 33, No. 2, pp. 134-149). Oxford, UK: Blackwell Publishing Ltd.

Qi, W., Liu, J., & Chen, D. (2018). Evaluations and improvements of GLDAS2. 0 and GLDAS2. 1 forcing data's applicability for basin scale hydrological simulations in the Tibetan Plateau. Journal of Geophysical Research: Atmospheres, 123(23), 13-128.

Rangzan, K., Kabolizadeh, M., Karimi, D., & Zareie, S. (2019). Supervised cross-fusion method: a new triplet approach to fuse thermal, radar, and optical satellite data for land use classification. Environmental monitoring and assessment, 191, 1-12.

Rateb, A., Scanlon, B. R., Pool, D. R., Sun, A., Zhang, Z., Chen, J., ... & Zell, W. (2020). Comparison of groundwater storage changes from GRACE satellites with monitoring and modeling of major US aquifers. Water Resources Research, 56(12), e2020WR027556.

Ravbar, N., & Šebela, S. (2015). The effectiveness of protection policies and legislative framework with special regard to karst landscapes: insights from Slovenia. Environmental Science & Policy, 51, 106-116.

Richey, A. S., Thomas, B. F., Lo, M. H., Famiglietti, J. S., Swenson, S., & Rodell, M. (2015). Uncertainty in global groundwater storage estimates in a T otal G roundwater S tress framework. Water resources research, 51(7), 5198-5216.

Richey, A. S., Thomas, B. F., Lo, M. H., Reager, J. T., Famiglietti, J. S., Voss, K., ... & Rodell, M. (2015). Quantifying renewable groundwater stress with GRACE. Water resources research, 51(7), 5217-5238.

Ridler, M. E., Madsen, H., Stisen, S., Bircher, S., & Fensholt, R. (2014). Assimilation of SMOS-derived soil moisture in a fully integrated hydrological and soil-vegetation-atmosphere transfer model in Western Denmark. Water Resources Research, 50(11), 8962-8981.

Rocha, M., Searcy, C., & Karapetrovic, S. (2007). Integrating sustainable development into existing management systems. Total quality management & business excellence, 18(1-2), 83-92.

Rodell, M., & Famiglietti, J. S. (1999). Detectability of variations in continental water storage from satellite observations of the time dependent gravity field. Water resources research, 35(9), 2705-2723.

Rodell, M., Famiglietti, J. S., Wiese, D. N., Reager, J. T., Beaudoing, H. K., Landerer, F. W., & Lo, M. H. (2018). Emerging trends in global freshwater availability. Nature, 557(7707), 651-659.

Rodell, M., Velicogna, I., & Famiglietti, J. S. (2009). Satellite-based estimates of groundwater depletion in India. Nature, 460(7258), 999-1002.

Rogan, J., & Chen, D. (2004). Remote sensing technology for mapping and monitoring land-cover and land-use change. Progress in planning, 61(4), 301-325.

Rohde, M. M., Albano, C. M., Huggins, X., Klausmeyer, K. R., Morton, C., Sharman, A., ... & Stella, J. C. (2024). Groundwater-dependent ecosystem map exposes global dryland protection needs. Nature, 632(8023), 101-107.

Russo, T. A., & Lall, U. (2017). Depletion and response of deep groundwater to climate-induced pumping variability. Nature Geoscience, 10(2), 105-108.

Sahin, V., & Hall, M. J. (1996). The effects of afforestation and deforestation on water yields. Journal of hydrology, 178(1-4), 293-309.

Salmon, J. M., Friedl, M. A., Frolking, S., Wisser, D., & Douglas, E. M. (2015). Global rain-fed, irrigated, and paddy croplands: A new high resolution map derived from remote sensing, crop inventories and climate data. International Journal of Applied Earth Observation and Geoinformation, 38, 321-334.

Samaniego, L., Thober, S., Kumar, R., Wanders, N., Rakovec, O., Pan, M., ... & Marx, A. (2018). Anthropogenic warming exacerbates European soil moisture droughts. Nature Climate Change, 8(5), 421-426.

Santos, E. B., de Freitas, E. D., Rafee, S. A. A., Fujita, T., Rudke, A. P., Martins, L. D., ... & Martins, J. A. (2021). Spatio-temporal variability of wet and drought events in the Paraná River basin—Brazil and its association with the El Niño—Southern oscillation phenomenon. Int. J. Climatol, 41, 4879-4897.

Satizábal-Alarcón, D. A., Suhogusoff, A., & Ferrari, L. C. (2024). Characterization of groundwater storage changes in the Amazon River Basin based on downscaling of GRACE/GRACE-FO data with machine learning models. Science of The Total Environment, 912, 168958.

Save, H. (2020) CSR GRACE and GRACE-FO RL06 Mascon Solutions v02. https://doi.org/10.15781/cgq9-nh24

Save, H., Bettadpur, S., & Tapley, B. D. (2016). High-resolution CSR GRACE RL05 mascons. Journal of Geophysical Research: Solid Earth, 121(10), 7547-7569.

Scanlon, B. R., Fakhreddine, S., Rateb, A., de Graaf, I., Famiglietti, J., Gleeson, T., ... & Zheng, C. (2023). Global water resources and the role of groundwater in a resilient water future. Nature Reviews Earth & Environment, 4(2), 87-101.

Scanlon, B. R., Rateb, A., Anyamba, A., Kebede, S., MacDonald, A. M., Shamsudduha, M., Small, J., Sun A., Taylor, R. G. & Xie, H. (2022). Linkages between GRACE water storage, hydrologic extremes, and climate teleconnections in major African aquifers. Environmental Research Letters, 17(1), 014046.

Scanlon, B. R., Zhang, Z., Save, H., Sun, A. Y., Müller Schmied, H., Van Beek, L. P., ... & Bierkens, M. F. (2018). Global models underestimate large decadal declining and rising water storage trends relative to GRACE satellite data. Proceedings of the National Academy of Sciences, 115(6), E1080-E1089.

Schweizer, P. E., & Matlack, G. R. (2014). Factors driving land use change and forest distribution on the coastal plain of Mississippi, USA. Landscape and Urban Planning, 121, 55-64.

Sen, P. K. (1968). Estimates of the regression coefficient based on Kendall's tau. Journal of the American statistical association, 63(324), 1379-1389.

Serra, P., Vera, A., Tulla, A. F., & Salvati, L. (2014). Beyond urban–rural dichotomy: Exploring socioeconomic and land-use processes of change in Spain (1991–2011). Applied Geography, 55, 71-81.

Setegn, S. G., Rayner, D., Melesse, A. M., Dargahi, B., & Srinivasan, R. (2011). Impact of climate change on the hydroclimatology of Lake Tana Basin, Ethiopia. Water Resources Research, 47(4).

Shamsudduha, M., & Taylor, R. G. (2020). Groundwater storage dynamics in the world's large aquifer systems from GRACE: uncertainty and role of extreme precipitation. Earth System Dynamics, 11(3), 755-774.

Shen, M., Chen, J., Zhuan, M., Chen, H., Xu, C. Y., & Xiong, L. (2018). Estimating uncertainty and its temporal variation related to global climate models in quantifying climate change impacts on hydrology. Journal of Hydrology, 556, 10-24.

Shukla, P. R., Skeg, J., Buendia, E. C., Masson-Delmotte, V., Pörtner, H. O., Roberts, D. C., ... & Malley, J. (2019). Climate Change and Land: an IPCC special report on climate change, desertification, land degradation, sustainable land management, food security, and greenhouse gas fluxes in terrestrial ecosystems.

Siebert, S., Burke, J., Faures, J. M., Frenken, K., Hoogeveen, J., Döll, P., & Portmann, F. T. (2010). Groundwater use for irrigation–a global inventory. Hydrology and earth system sciences, 14(10), 1863-1880.

Siebert, S., Henrich, V., Frenken, K., & Burke, J. (2013). Update of the digital global map of irrigation areas to version 5. Rheinische Friedrich-Wilhelms-Universität, Bonn, Germany and Food and Agriculture Organization of the United Nations, Rome, Italy, 10(2.1), 2660-6728.

Sinha, D., Syed, T. H., & Reager, J. T. (2019). Utilizing combined deviations of precipitation and GRACE-based terrestrial water storage as a metric for drought characterization: A case study over major Indian river basins. Journal of hydrology, 572, 294-307.

Song, X. P., Hansen, M. C., Stehman, S. V., Potapov, P. V., Tyukavina, A., Vermote, E. F., & Townshend, J. R. (2018). Global land change from 1982 to 2016. Nature, 560(7720), 639-643.

Sonter, L. J., Moran, C. J., Barrett, D. J., & Soares-Filho, B. S. (2014). Processes of land use change in mining regions. Journal of Cleaner Production, 84, 494-501.

Spinoni, J., Barbosa, P., De Jager, A., McCormick, N., Naumann, G., Vogt, J. V., ... & Mazzeschi, M. (2019). A new global database of meteorological drought events from 1951 to 2016. Journal of Hydrology: Regional Studies, 22, 100593.

Stevanović, Z. (2019). Karst waters in potable water supply: a global scale overview. Environmental Earth Sciences, 78(23), 662.

Su, G., Wu, Y., Zhan, W., Zheng, Z., Chang, L., & Wang, J. (2021). Spatiotemporal evolution characteristics of land subsidence caused by groundwater depletion in the North China plain during the past six decades. Journal of hydrology, 600, 126678.

Sulaiman, A., Osaki, M., Takahashi, H., Yamanaka, M. D., Susanto, R. D., Shimada, S., ... & Tsuji, N. (2023). Peatland groundwater level in the Indonesian maritime continent as an alert for El Niño and moderate positive Indian Ocean dipole events. Scientific Reports, 13(1), 939.

Sun, Q., Xu, C., Gao, X., Lu, C., Cao, B., Guo, H., ... & He, X. (2022). Response of groundwater to different water resource allocation patterns in the Sanjiang Plain, Northeast China. Journal of Hydrology: Regional Studies, 42, 101156.

Sy, S., & Quesada, B. (2020). Anthropogenic land cover change impact on climate extremes during the 21st century. Environmental Research Letters, 15(3), 034002.

Syed, T. H., Famiglietti, J. S., Rodell, M., Chen, J., & Wilson, C. R. (2008). Analysis of terrestrial water storage changes from GRACE and GLDAS. Water Resources Research, 44(2).

Tabari, H. (2020). Climate change impact on flood and extreme precipitation increases with water availability. Scientific reports, 10(1), 13768.

Tao, F., Chen, Y., & Fu, B. (2020). Impacts of climate and vegetation leaf area index changes on global terrestrial water storage from 2002 to 2016. Science of the Total Environment, 724, 138298.

Tateishi, R., Uriyangqai, B., Al-Bilbisi, H., Ghar, M. A., Tsend-Ayush, J., Kobayashi, T., ... & Sato, H. P. (2011). Production of global land cover data–GLCNMO. International Journal of Digital Earth, 4(1), 22-49.

Taylor, R. G., Scanlon, B., Döll, P., Rodell, M., Van Beek, R., Wada, Y., ... & Treidel, H. (2013). Ground water and climate change. Nature climate change, 3(4), 322-329.

Thomas, B. F., & Famiglietti, J. S. (2019). Identifying climate-induced groundwater depletion in GRACE observations. Scientific reports, 9(1), 4124.

Thomas, B. F., Caineta, J., & Nanteza, J. (2017). Global assessment of groundwater sustainability based on storage anomalies. Geophysical Research Letters, 44(22), 11-445.

Tilman, D., Balzer, C., Hill, J., & Befort, B. L. (2011). Global food demand and the sustainable intensification of agriculture. Proceedings of the national academy of sciences, 108(50), 20260-20264.

Tiwari, V. M., Wahr, J., & Swenson, S. (2009). Dwindling groundwater resources in northern India, from satellite gravity observations. Geophysical Research Letters, 36(18).

Tomaszkiewicz, M., Abou Najm, M., & El-Fadel, M. (2014). Development of a groundwater quality index for seawater intrusion in coastal aquifers. Environmental Modelling & Software, 57, 13-26.

Turner, B. L., Janetos, A. C., Verbug, P. H., & Murray, A. T. (2013). Land system architecture: Using land systems to adapt and mitigate global environmental change (No. PNNL-SA-93482). Pacific Northwest National Lab.(PNNL), Richland, WA (United States).

Václavík, T., Lautenbach, S., Kuemmerle, T., & Seppelt, R. (2013). Mapping global land system archetypes. Global Environmental Change, 23(6), 1637-1647.

Valjavec, M. B., Zorn, M., & Čarni, A. (2018). Bioindication of human-induced soil degradation in enclosed karst depressions (dolines) using Ellenberg indicator values (Classical Karst, Slovenia). Science of the Total Environment, 640, 117-126.

Van Lanen, H. A., Laaha, G., Kingston, D. G., Gauster, T., Ionita, M., Vidal, J. P., ... & Van Loon, A. F. (2016). Hydrology needed to manage droughts: the 2015 European case. Hydrological Processes, 30(17), 3097-3104.

Van Loon, A. F. (2015). Hydrological drought explained. Wiley Interdisciplinary Reviews: Water, 2(4), 359-392.

Veldkamp, T. I. E., Wada, Y., Aerts, J. C. J. H., Döll, P., Gosling, S. N., Liu, J., ... & Ward, P. J. (2017). Water scarcity hotspots travel downstream due to human interventions in the 20th and 21st century. Nature communications, 8(1), 15697.

Velicogna, I., Sutterley, T. C., & Van Den Broeke, M. R. (2014). Regional acceleration in ice mass loss from Greenland and Antarctica using GRACE time-variable gravity data. Geophysical Research Letters, 41(22), 8130-8137.

Vicente-Serrano, S. M., Beguería, S., & López-Moreno, J. I. (2010). A multiscalar drought index sensitive to global warming: the standardized precipitation evapotranspiration index. Journal of climate, 23(7), 1696-1718.

Vicente-Serrano, S. M., Quiring, S. M., Peña-Gallardo, M., Yuan, S., & Domínguez-Castro, F. (2020). A review of environmental droughts: Increased risk under global warming?. Earth-Science Reviews, 201, 102953.

Voss, K. A., Famiglietti, J. S., Lo, M., De Linage, C., Rodell, M., & Swenson, S. C. (2013). Groundwater depletion in the Middle East from GRACE with implications for transboundary water management in the Tigris-Euphrates-Western Iran region. Water resources research, 49(2), 904-914.

Wada, Y., Van Beek, L. P., Van Kempen, C. M., Reckman, J. W., Vasak, S., & Bierkens, M. F. (2010). Global depletion of groundwater resources. Geophysical research letters, 37(20).

Wada, Y., Wisser, D., & Bierkens, M. F. (2014). Global modeling of withdrawal, allocation and consumptive use of surface water and groundwater resources. Earth System Dynamics, 5(1), 15-40.

Wang, J., & Fang, C. (2011). Growth of urban construction land: Progress and prospect. Progress in Geography, 30(11), 1440-1448.

Wang, L., & Zhang, Y. (2024). Filling GRACE data gap using an innovative transformer-based deep learning approach. Remote Sensing of Environment, 315, 114465.

Wang, S. J., Liu, Q. M., & Zhang, D. F. (2004). Karst rocky desertification in southwestern China: geomorphology, landuse, impact and rehabilitation. Land degradation & development, 15(2), 115-121.

Wang, W., Zhu, Y., Xu, R., & Liu, J. (2015). Drought severity change in China during 1961–2012 indicated by SPI and SPEI. Natural Hazards, 75, 2437-2451.

Ward, D., Phinn, S. R., & Murray, A. T. (2000). Monitoring growth in rapidly urbanizing areas using remotely sensed data. The Professional Geographer, 52(3), 371-386.

Williams, A. P., Cook, E. R., Smerdon, J. E., Cook, B. I., Abatzoglou, J. T., Bolles, K., ... & Livneh, B. (2020). Large contribution from anthropogenic warming to an emerging North American megadrought. Science, 368(6488), 314-318.

Winfield, D. (1973). Function minimization by interpolation in a data table. IMA Journal of Applied Mathematics, 12(3), 339-347.

Winkler, K., Fuchs, R., Rounsevell, M., & Herold, M. (2021). Global land use changes are four times greater than previously estimated. Nature communications, 12(1), 2501.

WorldPop (www.worldpop.org - School of Geography and Environmental Science, University of Southampton; Department of Geography and Geosciences, University of Louisville; Departement de Geographie, Universite de Namur) and Center for International Earth Science Information Network (CIESIN), Columbia University (2018). Global High Resolution Population Denominators Project - Funded by The Bill and Melinda Gates Foundation (OPP1134076). https://dx.doi.org/10.5258/SOTON/WP00647

Xanke, J., & Liesch, T. (2022). Quantification and possible causes of declining groundwater resources in the Euro-Mediterranean region from 2003 to 2020. Hydrogeology Journal, 30(2), 379-400.

Yang, X., & Lu, X. X. (2014). Drastic change in China's lakes and reservoirs over the past decades. Scientific Reports, 4(1), 1-6.

Yin, W., Zhang, G., Han, S. C., Yeo, I. Y., & Zhang, M. (2022). Improving the resolution of GRACE-based water storage estimates based on machine learning downscaling schemes. Journal of Hydrology, 613, 128447.

Yin, Z., Xu, Y., Zhu, X., Zhao, J., Yang, Y., & Li, J. (2021). Variations of groundwater storage in different basins of China over recent decades. Journal of Hydrology, 598, 126282.

Yira, Y., Diekkrüger, B., Steup, G., & Bossa, A. Y. (2016). Modeling land use change impacts on water resources in a tropical West African catchment (Dano, Burkina Faso). Journal of Hydrology, 537, 187-199.

Yuan, D. (1999). Progress in the study on karst processes and carbon cycle. Advances in Earth Science, 14(5), 425.

Zarfl, C., Lumsdon, A. E., Berlekamp, J., Tydecks, L., & Tockner, K. (2015). A global boom in hydropower dam construction. Aquatic Sciences, 77, 161-170.

Zhang, M., & Yuan, X. (2020). Crucial role of natural processes in detecting human influence on evapotranspiration by multisource data analysis. Journal of Hydrology, 580, 124350.

Zhang, T. Y., & Jin, S. G. (2013). Estimate of glacial isostatic adjustment uplift rate in the Tibetan Plateau from GRACE and GIA models. Journal of Geodynamics, 72, 59-66.

Zhao, S., Pereira, P., Wu, X., Zhou, J., Cao, J., & Zhang, W. (2020). Global karst vegetation regime and its response to climate change and human activities. Ecological Indicators, 113, 106208.

Zhu, Z., Piao, S., Myneni, R. B., Huang, M., Zeng, Z., Canadell, J. G., ... & Zeng, N. (2016). Greening of the Earth and its drivers. Nature climate change, 6(8), 791-795.

Zou, M., Kang, S., Niu, J., & Lu, H. (2020). Untangling the effects of future climate change and human activity on evapotranspiration in the Heihe agricultural region, Northwest China. Journal of Hydrology, 585, 124323.